APPLICATION OF SEMIDEFINITE OPTIMIZATION TECHNIQUES TO PROBLEMS IN ELECTRIC POWER SYSTEMS

By

Daniel K. Molzahn

A dissertation submitted in partial fulfillment of
the requirements for the degree of

Doctor of Philosophy
(Electrical Engineering)

at the
UNIVERSITY OF WISCONSIN–MADISON
2013

Date of final oral examination: August 9, 2013

The dissertation is approved by the following members of the Final Oral Committee:

Bernard C. Lesieutre, Professor, Electrical and Computer Engineering
Christopher L. DeMarco, Professor, Electrical and Computer Engineering
Thomas M. Jahns, Professor, Electrical and Computer Engineering
Giri Venkataramanan, Professor, Electrical and Computer Engineering
Michael C. Ferris, Professor, Computer Sciences
Stephen J. Wright, Professor, Computer Sciences
Ian A. Hiskens, Professor, Electrical Engineering and Computer Science

To my parents, David and Debra Molzahn.

ACKNOWLEDGMENTS

I would like to express my deep gratitude to the many people who have helped me complete my undergraduate and graduate educations. I am very grateful to my advisor, Dr. Bernard Leiseutre. His guidance, thoughtfulness, and dedication was a constant source of support and inspiration. The depth and breath of his knowledge showed me the importance of drawing on ideas from a variety of areas to solve practical and challenging problems. I will forever remain indebted for his tutelage.

I am also very grateful for the assistance and advice provided by my doctoral committee. Dr. Christopher DeMarco's guidance in numerous projects and his assistance in the publishing process have been invaluable. Dr. Thomas Jahns and Dr. Giri Venkataramanan inspired me to pursue a research career in electric power. I am fortunate for their instruction in power electronics and electric machines. I also greatly benefited from Dr. Michael Ferris' and Dr. Stephen Wright's vast knowledge of optimization theory and practice. Drawing on this knowledge has been essential to my dissertation research. Going back to my introductory circuits class, Dr. Ian Hiskens has been a valuable mentor. I very much look forward to working with him during my postdoctoral work at the University of Michigan.

There have been many other professors who guided me throughout my undergraduate and graduate educations. Dr. Ian Dobson's instruction in systems theory has provided me with a strong foundation for power systems research. I am grateful to Dr. William Hitchon for providing a research opportunity during my undergraduate education. I could not have asked for a better power engineering teacher than Dr. Donald Novotny. His ability to impart the fundamentals of power engineering is second to none. I am also inspired by the research acumen and leadership of Dr. Robert Lorenz. I further thank Dr. David Anderson for his encouragement.

I also appreciate the advice and teaching of many professors in the La Follette School of Public Affairs. I would especially like to thank Dr. Carolyn Heinrich for her support and teaching of quantitative policy analysis, Dr. Gregory Nemet for his guidance in the Energy Analysis and Policy program, and Dr. Susan Yackee for her instructional excellence in several policy courses.

I am also thankful for the friendship and advice of many current and former graduate students at the University of Wisconsin–Madison. These include Adam Bechle, Vikas Dawar, Alex Borden, Daniel Chéverez-González, Dan Schwarting, Chaitanya Baone, Mike Schlindwein, Steve Almquist, Heng Chen, Rafael Viloria, Honghao Zheng, Kanishka Kumar, Hillary Brown, Sowmya Acharya, JongMin Lim, Fatou Thiam, Nishant Meta, Aditya Shastri, Rahul Srinivasan, Tyler Giles, Corey Singletary, Scott Williams, Jesse Holzer, Zev Friedman, Yanchao Liu, and Taedong Kim.

My undergraduate studies in power engineering also benefited from many fellow students. Some of these many colleagues include John Losee, Hughes Wike, James Quigley, Jesse Zellmer, Adria Corcoran, Kate Katrana, and Matt Barbian.

Many primary and secondary teachers laid the foundation for my collegiate successes. I am greatly indebted to Mr. Jack Batten, who I can confidently say without exaggeration is among the world's best and most inspiring teachers. Some of the many other influential educators include Mr. Jarrod Valley, Mr. Dave Haller, Mr. Donald Schwedrsky, Mr. Mike Wittig, Mr. Jason Baudhuin, Mrs. Andi Erickson, Mrs. Theresa Williams, and Mrs. Jeanne Craanen.

I would like to express my deepest gratitude for the support and love of my family. Growing up in a family of teachers and engineers is a great privilege. I can never thank my parents and grandparents enough for their encouragement and love. Individual attention from my stay-at-home mother, Debra Molzahn, an expert in early childhood education, was an enormous advantage. I am also grateful for the love and encouragement of my grandmother, Arlene Molzahn, whose support and teaching was instrumental to my education. As a third-generation power engineer, I am proud to follow in the footsteps of my grandfather, Kenneth Molzahn, and father, David Molzahn. My father's power engineering background and his encouragement for learning math, science, and writing provided a strong foundation for educational success. My grandfather's love and encouragement was a constant source of support throughout my education. He is fondly remembered and

greatly missed. I am also fortunate for the love of my grandfather, Leo Koslowski. Although he passed away early in my childhood, he helped set me on a path for success. I am further thankful for the camaraderie and support of my brothers, Nicholas and Michael, who are also studying engineering at the University of Wisconsin–Madison. I also thank my father and mother in-laws, Bob and Cindy Simon, for their support throughout my graduate education. Finally, I greatly appreciate the companionship and patience of my fiancée, Norma-Jean Simon. Her support throughout my graduate studies was essential to my success.

I gratefully acknowledge the support of the National Science Foundation Graduate Research Fellowship, the University of Wisconsin–Madison Department of Electrical and Computer Engineering Fellowship, the Grainger Power Engineering Award, research assistantships funded by grants from the Department of Energy and the Federal Energy Regulatory Commission, and a teaching assistantship from the University of Wisconsin–Madison.

TABLE OF CONTENTS

Page

Page

Page

LIST OF TABLES

Table Page

LIST OF FIGURES

Figure Page

ABSTRACT

Motivated by the potential for improvements in electric power system economics and reliability, this dissertation investigates applications of a semidefinite programming relaxation of the power flow equations, which model the steady-state relationship between power injections and voltages in a power system. In contrast to other optimal power flow solution techniques, semidefinite program solvers can reliably find a global optimum in polynomial time when the semidefinite relaxation is "tight" (i.e., the solution has zero relaxation gap). Semidefinite relaxations have been applied to a variety of computationally difficult problems in many fields. The power systems literature details limited success in applying semidefinite programming to the optimal power flow (OPF) problem, which minimizes operating cost under engineering and network constraints. Semidefinite programming holds significant promise for application to other power systems problems.

This dissertation first investigates power system economics using a semidefinite relaxation of the OPF problem. In contrast to claims in the literature, this dissertation shows that the semidefinite relaxation may fail to give a physically meaningful solution (i.e., the solution has non-zero relaxation gap) for some practical problems. This dissertation also provides computational and modeling advances required for solving large-scale, realistic OPF problems. Modeling advances include allowing multiple generators at the same bus; parallel transmission lines and transformers; and an approximate method for modeling constant impedance, constant current, constant power (ZIP) loads. Existing methods exploit system sparsity to speed computation using matrix completion techniques that decompose the large positive semidefinite matrix constraint into constraints on many smaller matrices. Computational advances include modifying the matrix decomposition

techniques for further reductions in solver times, extending the applicability of an existing decomposition, and a method for obtaining an optimal voltage profile from a solution to a decomposed semidefinite program. This dissertation also provides a sufficient condition test for global optimality of a candidate OPF solution obtained by any method.

This dissertation next provides techniques for improving power system reliability. The first reliability-related research develops a sufficient condition under which the power flow equations have no solution. This sufficient condition is evaluated using a feasible semidefinite optimization problem. The objective employed in this optimization problem yields a measure of distance (in a parameter set) to the power flow solvability boundary. This distance is closely related to quantities that previous authors have proposed as voltage stability margins. A typical margin is expressed in terms of the parameters of system loading (injected powers); this dissertation additionally introduces a new margin in terms of the parameters of regulated bus voltages. This dissertation considers generators modeled as ideal voltage sources and generators with reactive power limits, which require either mixed-integer semidefinite programming or sum of squares programming formulations.

Also related to power system reliability is the problem of finding multiple solutions to the power flow equations. Power systems typically operate at a high-voltage, stable power flow solution; however, other solutions are used for stability calculations. Existing literature claims that a continuation-based algorithm can reliably find all power flow solutions. This claim is demonstrated to be incorrect with a small counterexample system. Thus, no computationally tractable algorithms exist for reliably finding all power flow solutions. Methods for calculating multiple power flow solutions therefore deserve further research. This dissertation describes a method for finding multiple power flow solutions using semidefinite programming. Results suggest the method's promise for identifying large numbers of power flow solutions.

Although the semidefinite relaxation of the power flow equations is often "tight," non-zero relaxation gap solutions can occur. This dissertation investigates examples of non-zero relaxation gap solutions to semidefinite formulations for the optimal power flow problem, for the power flow insolvability condition, and for determining multiple solutions to the power flow equations.

Chapter 1

Introduction

1.1 Motivation

The National Academy of Engineering has classified widespread electrification as one of the greatest engineering achievements of the 20^{th} century [1]. Electric power systems are closely connected to most aspects of modern society so that electric service interruptions are extremely burdensome and expensive; a 2006 study esimated that the national annual cost of power interruptions is $79 billion dollars [2]. Improving electric system reliability is therefore a major research emphasis. Ensuring reliable electric service and preventing blackouts requires grid operators to supply consumers' load demands while remaining within both physical and engineering constraints of the network and connected facilities. As for many engineering systems, operating in a secure region far from potential failure points (i.e., operation with sufficient stability margins) is desired for maintaining reliability. This is particularly important in electric power systems due to the inherent uncertainty resulting from, for instance, uncontrollable customer load demands, uncertain system parameters, and the potential for unexpected outages of generation and transmission facilities. Failure to maintain sufficient stability margins may result in uncontrolled operation, potentially leading to voltage collapse and wide-scale blackouts, as occurred in the August 2003 blackout that affected 50 million people in the Eastern United States and had estimated cost between $4 billion and $10 billion [3, 4].

In addition to reliability, economic operation of electric power systems is a major concern of power system engineers. With the large size of the power system industry in the United States (as one measure of industry size, electric industry revenues in the United States were $369 billion in

2010 [5]), improvements in power system economics have the potential for significant impacts. Many aspects of electric power systems are optimized to reduce costs. This dissertation discusses research into the "optimal power flow" problem of minimizing generation cost while satisfying physical network constraints and engineering limits.

The power flow equations are at the heart of many of the tools used by power system engineers to maintain reliable, economically operated power systems. These equations model the non-linear relationship between voltages and active and reactive power injections in a power system. The power flow equations are typically solved using iterative numerical techniques for systems of non-linear equations, such as the Newton-Raphson and Gauss-Seidel methods. The power flow equations inform important aspects of reliable and economic power system operation, including voltage stability margins, dynamic stability assessments, and power transfer limitations.

There has recently been significant research emphasis on a semidefinite programming relaxation of the power flow equations [6, 7]. Semidefinite programming is a convex optimization technique that minimizes a linear objective function while constraining a matrix to be positive semidefinite (i.e., all eigenvalues are constrained to be non-negative). Solution techniques for semidefinite programs guarantee global optimality in polynomial time, which cannot generally be achieved with traditional algorithms used in power flow problems. When the semidefinite relaxation is "tight" (i.e., zero relaxation gap exists between solutions to the classical problem and the semidefinite relaxation), an optimal solution can be recovered. Conversely, when the semidefinite relaxation is not "tight" (i.e., the solution has non-zero relaxation gap), the solution from the semidefinite program provides a lower bound on the optimal objective value but does not provide a feasible solution to the original problem.

Using the semidefinite programming relaxation of the power flow equations, this dissertation details advances that help enable reliable and economic operation of electric power systems. Regarding reliability, this dissertation investigates both static voltage stability margins through sufficient conditions for which the power flow equations do not admit a solution and the calculation of multiple solutions to the power flow equations, which are used in dynamic stability assessments. Regarding economic operation, the power flow equations model the physical network constraints

inherent to the optimal power flow problem, which is used to minimize system operating costs. This dissertation investigates a semidefinite programming relaxation of the optimal power flow problem and provides modeling and computational advances necessary for application to large-scale electric power systems. Before presenting these contributions in later chapters, this introduction provides background on the power flow equations, the optimal power flow problem, and semidefinite programming.

1.2 The Power Flow Equations

The power flow equations describe the sinusoidal steady-state equilibrium of a power network, and hence are formulated in terms of complex "phasor" representation of circuit quantities (see, for example, Chapter 9 of [8]). The underlying voltage-to-current relationships of the network are linear, but the nature of equipment in a power system is such that injected/demanded complex power at a bus is typically specified, rather than current. The relation of interest is between the active and reactive power injected at each bus and the complex voltages at each bus, and hence the associated equations are non-linear. Using polar representation for complex voltages and rectangular "active/reactive" representation of complex power, the power balance equations at bus i are given by

$$P_i = V_i \sum_{k=1}^{n} V_k \left(\mathbf{G}_{ik} \cos\left(\delta_i - \delta_k\right) + \mathbf{B}_{ik} \sin\left(\delta_i - \delta_k\right) \right) \tag{1.1a}$$

$$Q_i = V_i \sum_{k=1}^{n} V_k \left(\mathbf{G}_{ik} \sin\left(\delta_i - \delta_k\right) - \mathbf{B}_{ik} \cos\left(\delta_i - \delta_k\right) \right) \tag{1.1b}$$

where P_i and Q_i are the active and reactive power injections, respectively, at bus i, V_i and δ_i are the voltage magnitude and phase angle, respectively, at bus i, $\mathbf{Y} = \mathbf{G} + j\mathbf{B}$ is the network admittance matrix (see [9] for details on the network admittance matrix), and n is the number of buses in the system. This dissertation considers a single synchronously connected power system; the analyses described herein can be repeatedly applied to each connected component of power systems with multiple islands.

To represent typical behavior of equipment in a power system, each bus is classified as PQ, PV, or slack according to the constraints imposed at that bus. PQ buses, which typically correspond to loads, treat P_i and Q_i as specified quantities, and enforce the active power (1.1a) and reactive power (1.1b) equations at that bus. PV buses, which typically correspond to generators, specify a known voltage magnitude V_i and active power injection P_i, and enforce only the active power equation (1.1a). The associated reactive power Q_i may be computed as an "output quantity," via (1.1b). Finally, a single slack bus is selected, with specified V_i and δ_i (typically chosen to be 0°). The active power P_i and reactive power Q_i at the slack bus are determined from (1.1a) and (1.1b); network-wide conservation of complex power is thereby satisfied.

One generator model is an ideal voltage source capable of maintaining fixed bus voltage magnitude regardless of the reactive power output. More detailed models consider generators' reactive power limits. If a generator's reactive power output is between the upper and lower limits, the generator maintains a constant voltage magnitude at the bus (i.e., the bus behaves like a PV bus). If a generator's reactive power output reaches its upper limit, the reactive power output is fixed at the upper limit and the bus voltage magnitude is allowed to decrease (i.e., the bus behaves like a PQ bus with reactive power injection determined by the upper limit). If the generator's reactive power

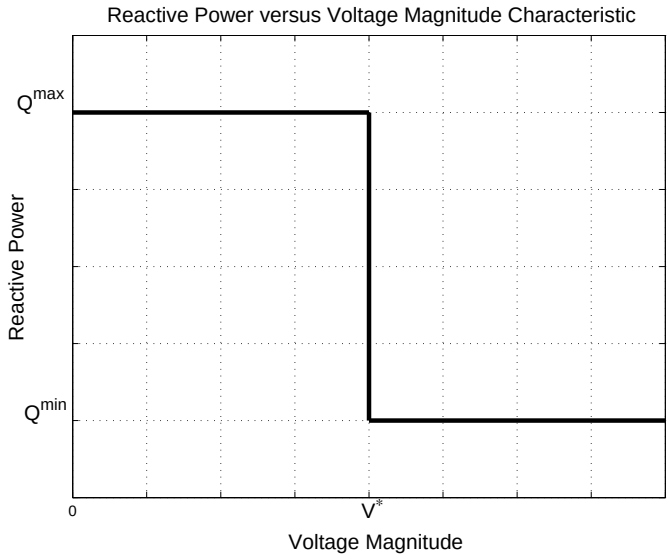

Figure 1.1 Reactive Power versus Voltage Magnitude Characteristic

output reaches its lower limit, the reactive power output is fixed at the lower limit and the voltage magnitude is allowed to increase (i.e., the bus behaves like a PQ bus with reactive power injection determined by the lower limit). Figure 1.1 shows the reactive power versus voltage characteristic for this generator model with a voltage setpoint of V^*, lower reactive power limit of Q^{min}, and upper reactive power limit of Q^{max}.

The power flow equations can also be written in terms of rectangular voltage components V_d and V_q. Formulation in rectangular voltage coordinates reveals the coupled-quadratic form of these equations. See [10] for a review of the power flow equations in rectangular voltage coordinates.

$$P_i = V_{di} \sum_{k=1}^{n} \left(\mathbf{G}_{ik} V_{dk} - \mathbf{B}_{ik} V_{qk} \right) + V_{qi} \sum_{k=1}^{n} \left(\mathbf{B}_{ik} V_{dk} + \mathbf{G}_{ik} V_{qk} \right) \tag{1.2a}$$

$$Q_i = V_{di} \sum_{k=1}^{n} \left(-\mathbf{B}_{ik} V_{dk} - \mathbf{G}_{ik} V_{qk} \right) + V_{qi} \sum_{k=1}^{n} \left(\mathbf{G}_{ik} V_{dk} - \mathbf{B}_{ik} V_{qk} \right) \tag{1.2b}$$

The rectangular voltage components must additionally satisfy the voltage magnitude equation.

$$V_i^2 = V_{di}^2 + V_{qi}^2 \tag{1.2c}$$

The non-linear power flow equations require iterative numerical solution techniques, such as Gauss-Seidel or, most commonly, Newton-Raphson [9], whose convergence performances are dependent on an initial guess of the solution voltage magnitudes and angles. These techniques are only locally convergent; they do not generally converge to a particular solution from an arbitrary initial guess [11]. A initial guess consisting of a "flat start" voltage profile with uniform voltage magnitudes and zero phase angles can often be used to find a solution for "typical" parameters. However, it is important to recognize that as parameters move outside of routine operating ranges the behavior of the power flow equations can be highly complex, resulting in convergence failure for these solution techniques.

The properties of the Newton-Raphson iteration guarantee (under suitable differentiability assumptions) convergence to a solution for an initial condition selected in a sufficiently small neighborhood around that solution [12]. However, when a selected initial condition (or some limited

set of multiple initial conditions) fails to yield convergence, the user of a Newton-Raphson-based software package is left with an indeterminate outcome: does the specified problem have no solution, or has the initial condition(s) simply failed to fall within the attractive set of a solution that does exist? Since the existence of a power flow solution is necessary for power system stability, conditions regarding power flow solution existence are powerful tools for power system reliability.

Conditions to guarantee existence of solutions to the power flow equations have therefore been an active topic of study. For example, [13] and [14] describe sufficient conditions for power flow solution existence. However, as sufficient conditions, these are often conservative: a solution may exist for a much larger range of operating points than satisfy the sufficient conditions. Other work on sufficient conditions for power flow solvability includes [15], which focuses on the decoupled (active power-voltage angle, reactive power-voltage magnitude) power flow model. Reference [16] describes a modified Newton-Raphson iteration tailored to the type of ill-conditioning that can appear in power systems problems. While convergence to a solution may be judged a constructive sufficient condition to demonstrate solvability, such approaches do not escape the fundamental limitations of a locally convergent iteration. In more recent work, [17] provides two necessary conditions for saddle-node bifurcation based on lines reaching their static transfer stability limits; however, this work does not yet provide a test for power flow solvability.

A measure of the distance to the solvability boundary (the set of operating points where a solution exists, but small perturbations may result in insolvability of the power flow equations [18]) is desirable to ensure that power systems are operated with security margins. If a solution does not exist for a specified set of power injections, a measure of the distance to the solvability boundary indicates how close the power flow equations are to having a solution. If a power flow solution exists, desired margins indicate distances to solution non-existence at the solvability boundary. Existing work in this area uses a Newton-Raphson optimal multiplier approach [19] to find the voltage profile that yields the closest power injections to those specified [20, 21]. The method described in [20, 21] forms a non-convex optimization problem, solved by an iterative algorithm that may yield only a locally optimal solution, dependent on an initial condition. In particular, the method of [20, 21] is only guaranteed to find a locally optimal voltage profile, yielding the power

injections closest (in a Euclidean norm) to those specified. Moreover, the approach of [20, 21] as presented does not seek to obtain security margins for solvable sets of power injections (though one might postulate modifications of its algorithm that could do so). For solvable sets of power injections, iterative techniques for finding load margins comprised of the locally optimal minimum distance to the power flow solvability boundary are detailed in references [22] and [23]. An algorithm that combines continuation and non-linear optimization techniques to either solve the power flow equations, when possible, or calculate a measure of power flow insolvability is presented in reference [24]. Reference [25] describes an optimization problem that applies interior point methods to minimize the load shedding necessary to obtain solvable power flow equations. The minimum amount of load shedding is used as a measure of power flow insolvability. Investigating the worst-case load shedding necessary for power flow solvability is also discussed in references [26] and [27]. Reference [28] summarizes and compares some of these power flow insolvability measures.

Ideal voltage sources with no limits on reactive power output often serve as simple generator models. The work in Chapter 4 proposes a power flow insolvability condition and voltage stability margins without consideration of reactive power limited generators. However, reactive power limits are relevant to practical power flow solvability since non-existence of power flow solutions may result from limit-induced bifurcations [29–31]. In common industry practice, static voltage stability margins are determined using repeated power flow calculations to find the "nose point" of a power versus voltage ("P-V") curve. Closely related methods trace this curve while monitoring "reactive margins" on generators (i.e., the margin between a generator's reactive power output at a given operating point and its maximum reactive output). Descriptions of relevant industry standards are found in such works as [32–34]. Chapter 5 proposes sufficient conditions for power flow insolvability and voltage stability margins with consideration of reactive power limited generators.

In addition to the potential for solution non-existence, it is also well recognized that the power flow equations may have a very large number of solutions; for example, the work of [35] establishes cases for which the number of solutions grows faster than polynomial with respect to network size. Although power systems are typically operated at a high-voltage, stable solution, other power

flow solutions, particularly those exhibiting low-voltage magnitude, are important to power system stability assessment and bifurcation analysis [36–40].

One very direct approach to finding multiple power flow solutions simply initializes a Newton-Raphson iteration over a range of carefully selected candidate initial conditions. Each solution has a set of initial conditions that converges to that solution in a Newton-Raphson iteration. Characterization of Newton-Raphson regions of attraction was the subject of [41], which demonstrated cases for which the boundaries of these attractive sets were factual in nature. Thus, Newton-Raphson-based techniques do not guarantee obtaining all power flow solutions.

In another approach, Salam et al. [42] apply the homotophy method of Chow et al. [43] to the power flow problem. This method reliably finds all solutions, but has a computational complexity that grows exponentially with system size. It is computationally intractable for large systems.

Ma and Thorp published a continuation-based algorithm that they claimed would reliably find all solutions to the power flow equations [44, 45]. Since the computational complexity of this algorithm scales with the number of actual rather than possible solutions, it is computationally tractable for large systems. A similar algorithm claims to find all Type-1 power flow solutions in [46]. Type-1 solutions are those where the Jacobian of the power flow equations has a single eigenvalue with positive real part. Type-1 solutions are closely related to voltage instability [47].

A recent critique of the Ma and Thorp continuation-based algorithm revealed a flaw in the associated proof of completeness (i.e., the claim that the algorithm can reliably find all solutions) [48]. In Chapter 6, this dissertation presents a counterexample to the claim of completeness. Thus, one may fairly characterize the state of the art as lacking a computationally tractable algorithm to compute all power flow solutions. Chapter 6 proposes a semidefinite programming formulation for finding multiple power flow solutions.

1.3 The Optimal Power Flow Problem

The power flow equations enable engineers to determine the voltage magnitudes and angles for a given dispatch (set of generator active power injections and voltage magnitudes and load active and reactive power demands). This dispatch must be specified as an input to the power flow

equations. Determining an appropriate dispatch requires solution of the optimal power flow (OPF) problem. The OPF problem seeks decision variable values that yield an optimal operating point for an electric power system in terms of a specified objective function, subject to both network equality constraints (i.e., the power flow equations) and engineering inequality constraints (e.g., limits on voltage magnitudes, active and reactive power generations, and flows on transmission lines and transformers). Total generation cost is typically chosen as the objective function, although other objective functions, such as reducing network losses, are also possible.

The OPF problem is non-convex due to the non-linear power flow equations [49] and is, in general, NP-hard [7]. Non-convexity of the OPF problem has made solution techniques an ongoing research topic since the problem was first introduced by Carpentier in 1962 [50]. Many OPF solution techniques have been proposed, including successive quadratic programs, Lagrangian relaxation, genetic algorithms, particle swarm optimization, and interior point methods. See [51–55] for relevant survey papers.

This section next provides a mathematical description of the OPF problem as it is classically formulated. Consider an n-bus power system, where $\mathcal{N} = \{1, 2, \ldots, n\}$ represents the set of all buses, $\mathcal{G}$ represents the set of generator buses, and $\mathcal{L}$ represents the set of all lines. Let $P_{Dk} + jQ_{Dk}$ represent the active and reactive load demand at each bus $k \in \mathcal{N}$. Let $V_k = V_{dk} + jV_{qk}$ represent the voltage phasors in rectangular coordinates at each bus $k \in \mathcal{N}$. Let $P_{Gk} + jQ_{Gk}$ represent the generation at generator buses $k \in \mathcal{G}$. Let S_{lm} represent the apparent power flow on the line $(l, m) \in \mathcal{L}$. Superscripts "max" and "min" denote specified upper and lower limits. Let $\mathbf{Y} = \mathbf{G} + j\mathbf{B}$ denote the network admittance matrix.

Define an objective function associated with the active power output of each generator $k \in \mathcal{G}$, typically representing a dollar/hour variable operating cost.

$$f_k\left(P_{Gk}\right) = c_{k2}P_{Gk}^2 + c_{k1}P_{Gk} + c_{k0} \tag{1.3}$$

The classical OPF problem is then

$$\min_{P_G, Q_G, V_d, V_q, S} \quad \sum_{k \in \mathcal{G}} f_k\left(P_{Gk}\right) \qquad \text{subject to} \tag{1.4a}$$

$$P_{Gk}^{\min} \leq P_{Gk} \leq P_{Gk}^{\max} \qquad \forall k \in \mathcal{G} \tag{1.4b}$$

$$Q_{Gk}^{\min} \leq Q_{Gk} \leq Q_{Gk}^{\max} \qquad \forall k \in \mathcal{G} \tag{1.4c}$$

$$\left(V_k^{\min}\right)^2 \leq V_{dk}^2 + V_{qk}^2 \leq \left(V_k^{\max}\right)^2 \qquad \forall k \in \mathcal{N} \tag{1.4d}$$

$$|S_{lm}| \leq S_{lm}^{\max} \qquad \forall\, (l,m) \in \mathcal{L} \tag{1.4e}$$

$$P_{Gk} - P_{Dk} = V_{dk} \sum_{i=1}^{n} \left(\mathbf{G}_{ik} V_{di} - \mathbf{B}_{ik} V_{qi}\right) + V_{qk} \sum_{i=1}^{n} \left(\mathbf{B}_{ik} V_{di} + \mathbf{G}_{ik} V_{qi}\right) \qquad \forall k \in \mathcal{N} \tag{1.4f}$$

$$Q_{Gk} - Q_{Dk} = V_{dk} \sum_{i=1}^{n} \left(-\mathbf{B}_{ik} V_{di} - \mathbf{G}_{ik} V_{qi}\right) + V_{qk} \sum_{i=1}^{n} \left(\mathbf{G}_{ik} V_{di} - \mathbf{B}_{ik} V_{qi}\right) \qquad \forall k \in \mathcal{N} \tag{1.4g}$$

Note that this formulation limits the apparent power flow measured at each end of a given line, recognizing that active and reactive line losses can cause these quantities to differ.

This classical formulation is sufficient for modeling most small test systems; Chapter 3 contains a more detailed formulation of the OPF problem suitable for realistic system models that include parallel lines; the possibility of multiple generators at the same bus; piecewise-linear objective functions, which are commonly used in electricity market contexts; and ZIP load models, which have constant impedance, constant current, and constant power components.

1.4 Semidefinite Programming

Semidefinite programming is a type of convex optimization that minimizes a linear objective function over the intersection of a cone of positive semidefinite matrices (i.e., symmetric matrices constrained to have all non-negative eigenvalues) and an affine plane. Semidefinite programming has been successful in solving or approximating the solutions of many practical problems that are otherwise computationally challenging, including NP-hard optimization problems. Semidefinite programming finds applications in such areas as Lyapunov stability analysis, relaxations of discrete design variables in combinatorial optimization problems, and maximum cut problems in

graph theory [56]. Overviews of semidefinite programming theory and practice are available in references [56–58].

The primal form of a semidefinite program is

$$\min_{\mathbf{W}} \ \operatorname{trace}(\mathbf{BW}) \qquad \text{subject to} \tag{1.5a}$$

$$\operatorname{trace}(\mathbf{A}_i\mathbf{W}) = c_i$$

$$\mathbf{W} \succeq 0 \tag{1.5b}$$

for specified vector c, specified symmetric matrices $\mathbf{A}_i$ and $\mathbf{B}$, and symmetric matrix decision variable $\mathbf{W}$, where trace indicates the trace operator (i.e., the sum of the corresponding matrix's diagonal entries) and the symbol $\succeq$ indicates that the corresponding matrix is positive semidefinite [57]. Note that the trace of a matrix product is analogous to a "matrix dot product" which sums the product of the corresponding matrix entries. For $n \times n$ matrices $\mathbf{A}$ and $\mathbf{B}$, $\operatorname{trace}(\mathbf{AB}) = \sum_{i=1}^{n}\sum_{k=1}^{n}\mathbf{A}_{ik}\mathbf{B}_{ik}$.

The corresponding dual form is

$$\max_{\lambda} \ c^T\lambda \qquad \text{subject to} \tag{1.6a}$$

$$\left[\mathbf{B} - \sum_{i=1}^{n}\mathbf{A}_i\lambda_i\right] \succeq 0 \tag{1.6b}$$

for decision variable vector of Lagrangian dual variables λ with length n. Superscript T indicates the transpose operator.

Semidefinite programs can be solved efficiently (i.e., in polynomial time) for a globally optimal solution with robust primal–dual interior point methods. Example solution codes for semidefinite programs are SeDuMi [59], CSDP [60], SDPA [61], and SDPT3 [62].

Chapter 5 uses extensions to semidefinite programming to develop sufficient conditions for power flow insolvability and voltage stability margins that consider reactive power limited generators. Chapter 5 first uses mixed-integer semidefinite programming, which has both positive

semidefinite matrix constraints and integer variable constraints. Current mixed-integer semidefinite programming solvers are relatively immature, and unlike algorithms for semidefinite programs, solvers are not assured to run in polynomial time. However, this is an active area of research, and more capable algorithms will likely become available. Existing tools [63, 64] can solve the proposed formulation for small power system models, and Chapter 5 discusses potential modifications that improve the computational tractability of the proposed formulation with respect to solution algorithms in the literature [65, 66].

Chapter 5 also uses the concept of infeasibility certificates from the field of real algebraic geometry [67]. Infeasibility certificates for polynomial equations are calculated using sum-of-squares decompositions that are themselves computed with semidefinite optimization programs. Specifically, infeasibility certificates use the Positivstellensatz theorem, which states that there exists an algebraic identity to certify the non-existence of real solutions to every infeasible system of polynomial equalities and inequalities [67]. Overviews of both mixed-integer semidefinite programming and sum-of-squares programming are provided in Chapter 5.

1.5 Semidefinite Relaxation of the Power Flow Equations

Recently, significant research attention has focused on a semidefinite programming relaxation of the power flow equations and the optimal power flow problem [6, 7]. By appropriate selection of $\mathbf{A}_i$ matrices, the power flow equations in rectangular voltage coordinates can be written in the form $x^T \mathbf{A}_i x = c_i$, where x is a vector of orthogonal voltage components.

$$x = \begin{bmatrix} V_{d1} & V_{d2} & \dots & V_{dn} & V_{q1} & V_{q2} & \dots & V_{qn} \end{bmatrix}^T \tag{1.7}$$

By defining the matrix $\mathbf{W} = xx^T$, the power flow equations (1.2) can then be rewritten as the combination of the linear equations $\mathrm{trace}\,(\mathbf{A}_i \mathbf{W}) = c_i$ and the condition $\mathrm{rank}\,(\mathbf{W}) = 1$. Consider, for example, an expression for V_1^2, the square of the voltage magnitude at bus 1, which is equal to $V_{d1}^2 + V_{q1}^2$. The desired formulation for this expression is given in (1.8).

$$V_1^2 = \text{trace}\left(\begin{bmatrix} 1 & 0 & \cdots & 0 & \cdots & 0 \\ 0 & 0 & \cdots & 0 & \cdots & 0 \\ \vdots & \vdots & \ddots & \vdots & \cdots & \vdots \\ 0 & 0 & \cdots & 1 & \cdots & 0 \\ \vdots & \vdots & \cdots & \vdots & \ddots & \vdots \\ 0 & 0 & \cdots & 0 & \cdots & 0 \end{bmatrix} \underbrace{\begin{bmatrix} V_{d1}^2 & V_{d1}V_{d2} & \cdots & V_{d1}V_{q1} & \cdots & V_{d1}V_{qn} \\ V_{d1}V_{d2} & V_{d2}^2 & \cdots & V_{d2}V_{q1} & \cdots & V_{d2}V_{qn} \\ \vdots & \vdots & \ddots & \vdots & \ddots & \vdots \\ V_{d1}V_{q1} & V_{d2}V_{q1} & \cdots & V_{q1}^2 & \cdots & V_{q1}V_{qn} \\ \vdots & \vdots & \ddots & \vdots & \ddots & \vdots \\ V_{d1}V_{qn} & V_{d2}V_{qn} & \cdots & V_{q1}V_{qn} & \cdots & V_{qn}^2 \end{bmatrix}}_{\mathbf{W}=xx^T} \right) \tag{1.8}$$

Since the trace operator is a linear function, the non-convexity in this formulation of the power flow equations is entirely due to the rank condition. The semidefinite relaxation of the power flow equations does not enforce the rank condition; rather, the constraint $\mathbf{W} \succeq 0$ is used to define a convex feasible space. When an objective function is specified, the resulting semidefinite program provides a lower bound on the optimal objective value of the OPF problem. If the solution to the semidefinite program satisfies the rank condition, the semidefinite relaxation is "tight" (i.e., the lower bound provided by the semidefinite relaxation equals the globally optimal objective value of the OPF problem). See [7] and [58] for further details.

One of the first works applying semidefinite programming methods to OPF problems [7] uses the phrase "duality gap" to describe the gap between the original, rank-constrained problem and a convex relaxation. This is *not* the gap between primal and dual formulations of a single optimization problem (i.e., it is not the gap between the primal and dual forms of the semidefinite relaxation). Rather, the gap of interest is between two different but closely related optimization problems: the original, rank-constrained problem and an optimization problem formed by a convex relaxation of the original problem's constraint set. Therefore, this dissertation deviates from prior practice by using the phrase "relaxation gap" to refer to the gap between the original, rank-constrained problem and its semidefinite relaxation (i.e., the "duality gap" as used in other power systems literature, such as [7], on convex relaxations).

For a zero relaxation gap solution to the semidefinite program, a voltage profile satisfying the power flow equations can be obtained from an eigenvector associated with a non-zero eigenvalue of the solution's $\mathbf{W}$ matrix [7]. The voltage profile obtained from a semidefinite programming relaxation of the OPF problem is guaranteed to be a globally optimal solution if the rank condition is satisfied. The ability to find a global solution is a significant advantage of semidefinite programming over traditional solution techniques.

Existing literature [7] claims that the rank condition is satisfied for most practical power system models, including the IEEE test systems [68]. However, the rank condition is not always satisfied, which means that semidefinite relaxations do not give physically meaningful solutions for all realistic power system models. An example case that does not satisfy the rank condition is presented in Chapter 2 of this dissertation. Recent research has investigated the conditions under which the rank condition is satisfied; to date, sufficient conditions for rank condition satisfaction include requirements on power injection and voltage magnitude limits and either radial networks (typical of distribution system models) or appropriate placement of controllable phase shifting transformers [69–75]. There is limited existing research on the reasons for non-zero relaxation gap solutions; expanding on the limited existing literature [76, 77], Chapter 7 of this dissertation explores non-zero relaxation gap solutions.

In addition to theoretical concerns regarding satisfaction of the rank condition, practical computational issues are also of interest. Semidefinite programming relaxations of the OPF problem constrain a $2n \times 2n$ symmetric matrix to be positive semidefinite, where n is the number buses in the system. The semidefinite program size thus grows as the square of the number of buses, which makes solution of OPF problems by semidefinite programming computationally challenging for large systems. Recent work using matrix completion [78–80] reduces the computational burden inherent in solving large systems by taking advantage of the sparse matrix structure created by realistic power system models. Sojoudi and Lavaei [71], Bai and Wei [81], and Jabr [82] present formulations that decompose the single large $2n \times 2n$ positive semidefinite matrix constraint into

positive semidefinite constraints on many smaller matrices. If the matrices from these decompositions satisfy a rank condition, the $2n \times 2n$ matrix also satisfies the rank condition and an optimal solution can be obtained.

1.6 Organization

This dissertation is organized around two major themes: 1.) economic operation of power systems using a semidefinite programming relaxation of the optimal power flow problem and 2.) tools for improving power system reliability using semidefinite programming. Chapter 2 introduces the semidefinite programming relaxation of the optimal power flow problem and discusses instances where the relaxation fails to yield physically meaningful solutions (i.e., the solution exhibits nonzero relaxation gap). Chapter 3 provides modeling and computational advances necessary for solving semidefinite relaxations of the optimal power flow problem for realistic, large-scale power system models. Specific modeling advances regard parallel lines; multiple generators at the same bus; and constant impedance, constant current, constant power (ZIP) load models. Computational advances include a preprocessing method that significantly reduces solver time using matrix completion decompositions, a technique for recovering an optimal voltage profile from the solution to a decomposed semidefinite program, and an improvement to an existing decomposition that enables application to more general power systems. This chapter also proposes a sufficient condition test for global optimality of a candidate OPF solution using the Karush-Kuhn-Tucker (KKT) conditions for optimality of the semidefinite relaxation of the OPF problem.

The dissertation next details investigation into techniques for improving power system reliability. Chapter 4 presents a sufficient condition, calculated using a semidefinite program, for the insolvability of the power flow equations. As a byproduct of this sufficient condition, voltage stability margins are developed that give bounds on the distance to the power flow solvability boundary. The sufficient condition for power flow insolvability proposed in Chapter 4 models generators as ideal voltage sources that maintain fixed voltage magnitude regardless of reactive power output. Chapter 5 formulates sufficient conditions for power flow insolvability considering reactive power

limited generators. The first of these conditions uses mixed-integer semidefinite programming and the second uses infeasibility certificates and sum-of-squares programming.

Next, Chapter 6 provides a counterexample to a claim in the existing literature about the ability of a continuation-based algorithm to reliably find all power flow solutions. With this counterexample, current literature appears to offer no computationally tractable technique for reliably finding all power flow solutions. Chapter 6 continues with a discussion of the use of the semidefinite relaxation of the power flow equations to find multiple power flow solutions.

By illustrating the feasible spaces for power system optimization problems and their semidefinite relaxations, Chapter 7 studies semidefinite program solutions with non-zero relaxation gaps. Three applications of the semidefinite relaxation of the power flow equations are considered: the optimal power flow problem (i.e., work from Chapters 2 and 3), a formulation used to determine voltage stability margins (i.e., work from Chapters 4 and 5), and a formulation for calculating multiple power flow solutions (i.e., work from Chapter 6).

The remainder of the dissertation summarizes these developments and discusses future work. Proposed areas of future work include the extension of the semidefinite relaxation to more flexible distribution system models (i.e., modeling unbalanced loading among phases) and integrating the voltage stability margins developed in Chapters 4 and 5 into an OPF problem to explore a potential trade-off between stability and cost in determining a power system operating point. Other future work includes application of mixed-integer semidefinite programming to other power systems problems (e.g., the unit commitment problem). Results from the semidefinite relaxation of large OPF problems in Chapters 3 and 7 suggest future directions for investigating non-zero relaxation gap solutions. Specifically of interest are development of methods for identifying non-convexities in OPF problems and creation of methods for perturbing an OPF problem to obtain a zero relaxation gap solution (i.e., finding the closest OPF problem for which the semidefinite relaxation is tight).

1.7 Contributions

The contributions of this dissertation can be organized in two major areas: 1.) theoretical, computational, and modeling advances in the semidefinite programming relaxation of the power flow equations, and 2.) techniques for improving power system reliability involving conditions for power flow insolvability and the calculation of multiple solutions to the power flow equations.

A theoretical contribution is the publishing of counterexamples to a claim in the literature that the semidefinite programming relaxation gives physically meaningful solutions (i.e., satisfies the rank condition) for most practical optimal power flow problems. (See Chapter 2.)

Other theoretical contributions include detailed analyses of non-zero relaxation gap solutions. The three specific applications of the semidefinite relaxation of the power flow equations considered are the optimal power flow problem, a formulation used to determine voltage stability margins, and a formulation for determining multiple solutions to the power flow equations. (See Chapter 7.)

A modeling contribution is the incorporation of flow limits on parallel lines and transformers, potentially including off-nominal voltage ratios and non-zero phase shifts, in the semidefinite programming relaxation of the power flow equations. An additional modeling contribution is the incorporation of multiple generators at the same bus. Generator cost functions may be either quadratic or piecewise-linear. Another modeling contribution is an approximate representation of ZIP loads in the semidefinite relaxation of the power flow equations. (See Chapter 3.)

This dissertation contributes several computational advances in the semidefinite relaxation of the power flow equations. The first computational advance presented in this dissertation is a modification to existing matrix completion decomposition techniques. These techniques exploit power system sparsity to reduce computation time. The modification to the existing techniques described in this dissertation further reduces computation time by a factor between two and three for typical test cases. (See Chapter 3.)

The second computational advance is the extension of the applicability of an existing matrix completion decomposition. The matrix completion decomposition described by Jabr [82] performs a Cholesky factorization of the absolute value of the imaginary part of the bus admittance matrix.

However, lack of positive definiteness for some systems precludes the ability to perform a Cholesky factorization. This dissertation presents a different matrix that is guaranteed to be positive definite and whose Cholesky factorization can be substituted in the matrix completion decomposition procedure. (See Chapter 3.)

The third computational advance is a method for recovering an optimal voltage profile from the decomposed problem. Existing literature discusses decomposition algorithms, but does not present specific steps for recovering an optimal voltage profile from a decomposed problem. (See Chapter 3.)

The fourth computational advance is a sufficient condition test for global optimality of a candidate optimal power flow solution. This condition combines the global optimality advantage of the semidefinite relaxation with the maturity and speed of existing optimal power flow algorithms. (See Chapter 3.)

The dissertation next contributes to tools for improving power system reliability. First, this dissertation introduces a power flow insolvability condition based on the semidefinite programming relaxation of the power flow equations. The semidefinite program used to evaluate this condition is shown to be feasible for practical power system models using a proof of solution existence for a modified form of the power flow equations. The insolvability condition is valid regardless of the rank characteristics of the semidefinite program solution. Note that this condition does not consider reactive power limited generators. (See Chapter 4.)

The optimization problem used to evaluate the insolvability condition also yields margins to the power flow solvability boundary (i.e., the set of operating points where a solution exists, but small perturbations may result in the insolvability of the power flow equations). Specifically, a controlled voltage margin measures the distance to the solvability boundary in terms of proportional changes in all controlled voltages. A power injection margin measures the distance to the solvability boundary in terms of uniform, constant-power-factor changes in power injections at all buses. These margins are obtained from a single semidefinite program evaluation. (See Chapter 4.)

Sufficient conditions for power flow insolvability with consideration of reactive power limited generators are another contribution of this dissertation. Two such conditions are presented, the first

of which uses mixed-integer semidefinite programming and the second of which uses infeasibility certificates and sum-of-squares programming. Voltage stability margins to the power flow solvability boundary, with consideration of reactive power limited generators, are developed from both insolvability conditions. (See Chapter 5.)

Further contributions regard finding multiple solutions to the power flow equations. A counterexample is provided to a claim in the literature that a continuation-based algorithm is capable of finding all power flow solutions. With this counterexample, there is currently no computationally tractable method for reliably calculating all power flow solutions. (See Chapter 6.)

This dissertation also provides a method for calculating multiple power flow solutions using the semidefinite programming relaxation of the power flow equations with an objective function specified in terms of squared voltage magnitudes. Voltage magnitude properties of desired solutions are thus directly specified in this method. (See Chapter 6.)

Finally, open source MATLAB code implementing these contributions is under review for public release as part of the MATPOWER [55] package. Publicly available code will speed research progress by eliminating the need for researchers to independently implement these semidefinite formulations and will quickly distribute the contributions of this dissertation.

Chapter 2

Application of Semidefinite Programming to the OPF Problem

2.1 Introduction

The optimal power flow (OPF) problem seeks decision variable values to yield an optimal operating point for an electric power system in terms of a specified objective and subject to a wide range of engineering limits on active and reactive power generation, bus voltage magnitudes, transmission line and transformer flows, and possibly network stability constraints. Total generation cost is the typical objective; other objectives, such as loss minimization, may be considered.

The non-convexity of the OPF problem has made solution techniques an ongoing research topic since the problem was first introduced in 1962 by Carpentier [50]. Non-convexity in typical OPF formulations enters largely through the non-linear power flow equations representing physical constraints on the electric grid [49]. The long literature reflects a wide range of proposed solution techniques including successive quadratic programs, Lagrangian relaxation, genetic algorithms, particle swarm optimization, and interior point methods [51–55].

Recent research has pursued the application of semidefinite programming to the OPF problem [6,7]. Semidefinite programming formulations create a convex relaxation of the OPF problem; a global solution of the relaxed problem can be found in polynomial time. If the relaxed problem has a zero relaxation gap solution (i.e., the semidefinite relaxation is "tight"), a global optimum of the original OPF problem can be obtained. Traditional methods do not offer such a means to guarantee a global optimum, and hence the semidefinite relaxation has attracted significant interest.

While this approach is promising, the relaxation inherent in the semidefinite formulation may yield solutions that are not physically meaningful (i.e., the solutions exhibit non-zero relaxation

gap, meaning that the semidefinite relaxation is not "tight"). However, with their success on a significant number of standard IEEE test cases, Lavaei and Low claim that the semidefinite relaxation will satisfy a condition ensuring zero relaxation gap solutions for most practical OPF problems [7].

This chapter explores a counterexample to this assertion: a three-bus system with a constraint on the magnitude of complex power flow ("apparent power") on a transmission line. This example represents a power system with parameters in realistic ranges, operated with a commonly imposed constraint. (In AC power flow models, line flows are typically limited in terms of apparent power flow (MVA) because both active and reactive components of line flows contribute to line losses and associated line heating.) The semidefinite relaxation yields a physically meaningful solution when the line-flow limit is reasonably large, but fails (i.e., has a non-zero relaxation gap solution) when a stricter line-flow limit is enforced.

Additionally, as part of a discussion on properties of zero relaxation gap solutions, Lavaei and Low indicate that solutions with negative Lagrange multipliers associated with active power balance constraints (i.e., negative locational marginal prices (LMP) in an electricity market context) are not expected to have zero relaxation gap solutions [7]; these solutions are considered "abnormal." This chapter uses publicly available prices from a large wholesale electricity market (MidwestISO) to demonstrate that such solutions are not abnormal and occur with regularity in practical OPF problems.

This chapter is organized as follows. Section 2.2 presents a semidefinite programming relaxation of the classical formulation of the OPF problem given in (1.4). Section 2.3 discusses cases where the semidefinite relaxation of the OPF problem fails to provide physically meaningful results. This includes both a discussion of solutions with negative Lagrange multipliers associated with active power balance constraints and a three-bus example system for which the semidefinite relaxation fails with a strict line-flow constraint. This work is published as [83].

2.2 Semidefinite Relaxation of the Optimal Power Flow Problem

This section presents a semidefinite programming relaxation of the OPF problem (1.4). This relaxation is adopted from [7]. The formulation of the relaxation given in this section is suitable for many small test systems; a more flexible formulation tailored to large-scale systems is presented in Chapter 3.

Consider an n-bus power system, where $\mathcal{N} = \{1, 2, \ldots, n\}$ represents the set of all buses, $\mathcal{G}$ represents the subset of generator buses in $\mathcal{N}$, and $\mathcal{L}$ represents the set of all lines modeled as Π-equivalent circuits. Let $P_{Dk} + jQ_{Dk}$ represent the active and reactive load demand at each bus $k \in \mathcal{N}$. Let $V_k = V_{dk} + jV_{qk}$ represent the voltage phasors in rectangular coordinates at each bus $k \in \mathcal{N}$. Let $P_{Gk} + jQ_{Gk}$ represent the generation at generator buses $k \in \mathcal{G}$. Let S_{lm} represent the apparent power flow on the line $(l, m) \in \mathcal{L}$. Superscripts "max" and "min" denote specified upper and lower limits. Let $\mathbf{Y} = \mathbf{G} + j\mathbf{B}$ denote the network admittance matrix.

Define a quadratic objective function associated with each generator $k \in \mathcal{G}$, typically representing a dollar/hour variable operating cost:

$$f_k\left(P_{Gk}\right) = c_{k2}P_{Gk}^2 + c_{k1}P_{Gk} + c_{k0} \tag{2.1}$$

Let e_k denote the k^{th} standard basis vector in $\mathbb{R}^n$. Define the matrix $Y_k = e_k e_k^T \mathbf{Y}$, where the superscript T indicates the transpose operation. Define the matrix $Y_{lm} = \left(\frac{jb_{lm}}{2} + y_{lm}\right) e_l e_l^T - \left(y_{lm}\right) e_l e_m^T$, where b_{lm} is the total shunt susceptance and y_{lm} is the series admittance of the line (see Figure 2.1, $y_{lm} = \left(R_{lm} + jX_{lm}\right)^{-1}$). Each line is required to have a small minimum resistance $R_{lm} > 0$.

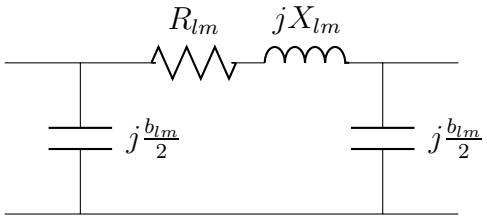

Figure 2.1 Transmission Line Π-Circuit Model

Matrices employed in the semidefinite relaxation are given as

$$\mathbf{Y}_k = \frac{1}{2}\begin{bmatrix} \mathrm{Re}\left(Y_k + Y_k^T\right) & \mathrm{Im}\left(Y_k^T - Y_k\right) \\ \mathrm{Im}\left(Y_k - Y_k^T\right) & \mathrm{Re}\left(Y_k\ + Y_k^T\right) \end{bmatrix} \tag{2.2a}$$

$$\bar{\mathbf{Y}}_k = -\frac{1}{2}\begin{bmatrix} \mathrm{Im}\left(Y_k + Y_k^T\right) & \mathrm{Re}\left(Y_k - Y_k^T\right) \\ \mathrm{Re}\left(Y_k^T - Y_k\right) & \mathrm{Im}\left(Y_k + Y_k^T\right) \end{bmatrix} \tag{2.2b}$$

$$\mathbf{M}_k = \begin{bmatrix} e_k e_k^T & \mathbf{0} \\ \mathbf{0} & e_k e_k^T \end{bmatrix} \tag{2.2c}$$

$$\mathbf{Y}_{lm} = \frac{1}{2}\begin{bmatrix} \mathrm{Re}\left(Y_{lm} + Y_{lm}^T\right) & \mathrm{Im}\left(Y_{lm}^T - Y_{lm}\right) \\ \mathrm{Im}\left(Y_{lm} - Y_{lm}^T\right) & \mathrm{Re}\left(Y_{lm}\ + Y_{lm}^T\right) \end{bmatrix} \tag{2.2d}$$

$$\bar{\mathbf{Y}}_{lm} = -\frac{1}{2}\begin{bmatrix} \mathrm{Im}\left(Y_{lm} + Y_{lm}^T\right) & \mathrm{Re}\left(Y_{lm} - Y_{lm}^T\right) \\ \mathrm{Re}\left(Y_{lm}^T - Y_{lm}\right) & \mathrm{Im}\left(Y_{lm} + Y_{lm}^T\right) \end{bmatrix} \tag{2.2e}$$

This section next details a semidefinite relaxation of the power flow equations using the same notation as [7]. To write the semidefinite relaxation, first define the vector of voltage coordinates

$$x = \begin{bmatrix} V_{d1} & V_{d2} & \dots & V_{dn} & V_{q1} & V_{q2} & \dots & V_{qn} \end{bmatrix} \tag{2.3}$$

Then define the rank one matrix

$$\mathbf{W} = xx^T \tag{2.4}$$

Replacement of the rank one constraint (2.4) by the less stringent constraint $\mathbf{W} \succeq 0$, where $\succeq$ indicates the corresponding matrix is positive semidefinite, yields the semidefinite relaxation. The semidefinite relaxation is "tight" (i.e., has zero relaxation gap) if the $\mathbf{W}$ matrix of a globally optimal solution has rank one.

The semidefinite relaxation of the OPF problem is

$$\min_{\mathbf{W}} \sum_{k\in\mathcal{G}} \alpha_k \qquad \text{subject to} \tag{2.5a}$$

$$P_{Gk}^{\min} - P_{Dk} \le \text{trace}\left(\mathbf{Y}_k\mathbf{W}\right) \le P_{Gk}^{\max} - P_{Dk} \qquad \forall k \in \mathcal{N} \tag{2.5b}$$

$$Q_{Gk}^{\min} - Q_{Dk} \le \text{trace}\left(\bar{\mathbf{Y}}_k\mathbf{W}\right) \le Q_{Gk}^{\max} - Q_{Dk} \qquad \forall k \in \mathcal{N} \tag{2.5c}$$

$$\left(V_k^{\min}\right)^2 \le \text{trace}\left(\mathbf{M}_k\mathbf{W}\right) \le \left(V_k^{\max}\right)^2 \qquad \forall k \in \mathcal{N} \tag{2.5d}$$

$$\begin{bmatrix} (S_{lm}^{max})^2 & -\text{trace}\left(\mathbf{Y}_{lm}\mathbf{W}\right) & -\text{trace}\left(\bar{\mathbf{Y}}_{lm}\mathbf{W}\right) \\ -\text{trace}\left(\mathbf{Y}_{lm}\mathbf{W}\right) & 1 & 0 \\ -\text{trace}\left(\bar{\mathbf{Y}}_{lm}\mathbf{W}\right) & 0 & 1 \end{bmatrix} \succeq 0 \qquad \forall\,(l,m) \in \mathcal{L} \tag{2.5e}$$

$$\begin{bmatrix} \alpha_k - c_{k1}\left(\text{trace}\left(\mathbf{Y}_k\mathbf{W}\right) + P_{Dk}\right) - c_{k0} & -\sqrt{c_{k2}}\left(\text{trace}\left(\mathbf{Y}_k\mathbf{W}\right) + P_{Dk}\right) \\ -\sqrt{c_{k2}}\left(\text{trace}\left(\mathbf{Y}_k\mathbf{W}\right) + P_{Dk}\right) & 1 \end{bmatrix} \succeq 0 \qquad \forall k \in \mathcal{G} \tag{2.5f}$$

$$\mathbf{W} \succeq 0 \tag{2.5g}$$

Active and reactive power and voltage magnitude limits are enforced in (2.5b), (2.5c), and (2.5d), respectively. Line-flow limits in (2.5e) and quadratic generator costs in (2.5f) are implemented using a Schur complement [58]. A solution to the semidefinite relaxation (2.5) has zero relaxation gap if it satisfies

$$\text{rank}\left(\mathbf{W}\right) \le 2 \tag{2.6}$$

A rank one matrix can be obtained from a matrix satisfying (2.6) by specifying the reference angle, which then allows for obtaining a globally optimal voltage profile [7].

This section next presents the dual form of the semidefinite relaxation. Define vectors of Lagrange multipliers associated with lower inequality bounds (2.5b), (2.5c), and (2.5d) as $\underline{\lambda}_k$, $\underline{\gamma}_k$, and $\underline{\mu}_k$, and those associated with upper bounds as $\bar{\lambda}_k$, $\bar{\gamma}_k$, and $\bar{\mu}_k$, respectively. Define 3×3 symmetric matrices to represent generalized Lagrange multipliers for the line-flow limits (2.5e): $\mathbf{H}_{lm}$, with $\mathbf{H}_{lm}^{ik}$ the (i,k) element of $\mathbf{H}_{lm}$. Define 2×2 symmetric matrices to represent generalized Lagrange multipliers for the quadratic cost functions (2.5f): $\mathbf{R}_k$, with $\mathbf{R}_k^{ik}$ the (i,k) element of $\mathbf{R}_k$.

Define aggregate multipliers λ_k, γ_k, and μ_k for all $k \in \mathcal{N}$.

$$\lambda_k = \begin{cases} \bar{\lambda}_k - \underline{\lambda}_k + c_{k1} + 2\sqrt{c_{k2}}\,\mathbf{R}_k^{12} & \text{if } k \in \mathcal{G} \\ \bar{\lambda}_k - \underline{\lambda}_k & \text{otherwise} \end{cases} \tag{2.7a}$$

$$\gamma_k = \bar{\gamma}_k - \underline{\gamma}_k \tag{2.7b}$$

$$\mu_k = \bar{\mu}_k - \underline{\mu}_k \tag{2.7c}$$

Finally, define a scalar real-valued function h and matrix-valued function $\mathbf{A}$.

$$\begin{aligned} h = &\sum_{k\in\mathcal{N}} \Big\{ \underline{\lambda}_k P_k^{\min} - \bar{\lambda}_k P_k^{\max} + \lambda_k P_{Dk} + \underline{\gamma}_k Q_k^{\min} - \bar{\gamma}_k Q_k^{\max} + \gamma_k Q_{Dk} + \underline{\mu}_k \big(V_k^{\min}\big)^2 - \bar{\mu}_k (V_k^{\max})^2 \Big\} \\ &+ \sum_{k\in\mathcal{G}} \big(c_{k0} - \mathbf{R}_k^{22}\big) - \sum_{(l,m)\in\mathcal{L}} \big\{ (S_{lm}^{\max})^2\, \mathbf{H}_{lm}^{11} + \mathbf{H}_{lm}^{22} + \mathbf{H}_{lm}^{33} \big\} \end{aligned} \tag{2.8}$$

$$\mathbf{A} = \sum_{k\in\mathcal{N}} \big\{ \lambda_k \mathbf{Y}_k + \gamma_k \bar{\mathbf{Y}}_k + \mu_k \mathbf{M}_k \big\} + 2 \sum_{(l,m)\in\mathcal{L}} \big\{ \mathbf{H}_{lm}^{12} \mathbf{Y}_{lm} + \mathbf{H}_{lm}^{13} \bar{\mathbf{Y}}_{lm} \big\} \tag{2.9}$$

The dual semidefinite problem is then

$$\max_{\underline{\lambda}, \bar{\lambda}, \underline{\gamma}, \bar{\gamma}, \underline{\mu}, \bar{\mu}, \mathbf{R}, \mathbf{H}} \quad h \qquad \text{subject to} \tag{2.10a}$$

$$\mathbf{A} \succeq 0 \tag{2.10b}$$

$$\mathbf{H}_{lm} \succeq 0 \qquad \forall\, (l,m) \in \mathcal{L} \tag{2.10c}$$

$$\mathbf{R}_k \succeq 0, \quad \mathbf{R}_k^{11} = 1 \qquad \forall k \in \mathcal{G} \tag{2.10d}$$

$$\underline{\lambda}_k \geq 0,\ \bar{\lambda}_k \geq 0,\ \underline{\gamma}_k \geq 0,\ \bar{\gamma}_k \geq 0,\ \underline{\mu}_k \geq 0,\ \bar{\mu}_k \geq 0 \qquad \forall k \in \mathcal{N} \tag{2.10e}$$

If the $\mathbf{A}$ matrix corresponding to the dual formulation's optimal solution has two-dimensional nullspace, Lavaei and Low demonstrate that a rank one $\mathbf{W}$ can be obtained (i.e., the solution has zero relaxation gap). (The additional degree of freedom in the nullspace of $\mathbf{A}$ corresponds to the lack of an angle reference specification in (2.10).) A globally optimal voltage profile is then extracted from the zero relaxation gap solution [7].

2.3 Discussion on the Semidefinite Relaxation's Ability to Provide Physically Meaningful Results

It is important to note that the semidefinite relaxation does not enforce a two-dimensional nullspace for $\mathbf{A}$ or the corresponding rank condition on $\mathbf{W}$. If the solution to the semidefinite relaxation has a nullspace of $\mathbf{A}$ with dimension greater than two, the relaxation gap is non-zero and $\mathbf{W}$ does not yield a solution to the OPF problem. Lavaei and Low argue that "practical systems operating at normal conditions" will have zero relaxation gap solutions based on their experience with a number of IEEE test systems [7]. However, in general, the semidefinite relaxation of the OPF problem offers three possible outcomes: a zero relaxation gap solution, and hence a globally optimal solution to the OPF problem; a solution to the semidefinite relaxation with a higher rank $\mathbf{W}$, and hence physically meaningless as a solution to the original OPF problem; and the semidefinite relaxation may not be feasible.

This section first discusses a class of solution that Lavaei and Low discount as being abnormal and for which they argue one may not expect a zero relaxation gap solution: that of negative Lagrange multipliers associated with active power balance constraints [7].

2.3.1 Non-Zero Relaxation Gap in the Case of Negative LMPs

The Lagrange multipliers λ_k for the active power constraints given in (1.4f) and (2.7a) are, in the terminology of electric power markets, locational marginal prices (LMP). These are commonly computed and updated many times daily in wholesale electricity markets in the United States. Simple intuition regarding unconstrained markets might lead one to believe an OPF solution with negative λ_k, (i.e., consumers at some locations are paid to consume) could be considered "abnormal" and excluded from consideration. Lavaei and Low do so, stating that the semidefinite relaxation is not guaranteed to yield a solution with zero relaxation gap under these conditions [7]. However, electricity markets often operate at conditions with negative LMPs.

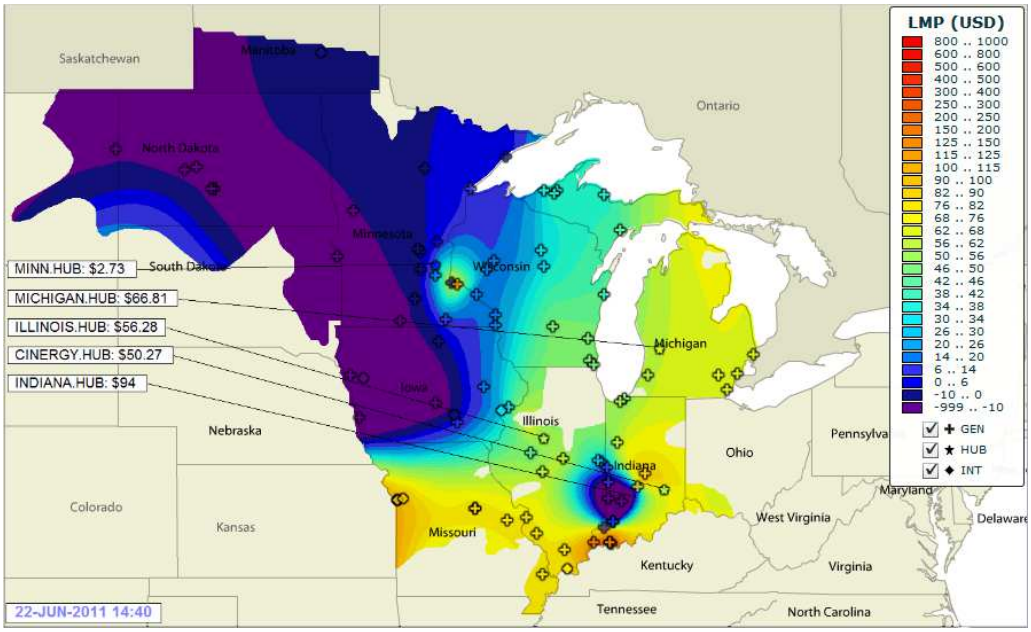

Figure 2.2 Negative LMPs (Lagrange Multipliers) in the MidwestISO Market

Along with generation market participants willing to submit negative price offers to sell,[1] binding line-flow constraints can cause negative LMPs. In systems with binding line-flow constraints, it is possible that increasing the power delivered to certain buses may relieve congestion elsewhere in the system. Reducing transmission congestion allows for greater output from cheaper generators, thus decreasing overall system costs. Negative LMPs will occur at buses where increasing power consumption leads to decreased overall system costs.

MidwestISO, which operates one the largest wholesale power markets in the United States, displays a color-coded contour map of LMPs throughout its system on its publicly accessible website [84], updating the LMP values at five-minute intervals. This market regularly sees periods of negative LMPs. A sample LMP contour from June 2011 is shown in Figure 2.2. In this example, 32 of the 190 commercial pricing nodes in the MidwestISO market displayed negative LMPs, with the most negative being a price of $-112 per MWh at a node in the Hoosier Energy control area. Inability to reliably compute OPF solutions for situations that yield negative LMPs appears to be a practical limitation of the semidefinite relaxation.

[1] Such negative price offers are common when a generator has an out-of-market revenue stream, such as wind energy production credits.

2.3.2 Non-Zero Relaxation Gap in the Case of Strict Line-Flow Constraints

This section next provides an example system to demonstrate that the semidefinite relaxation of the OPF problem may also fail to produce physically meaningful solutions in the presence of line-flow constraints. The semidefinite relaxation of the OPF problem was solved using YALMIP version 3 [64] and SeDuMi version 1.3 [59] for a simple three-bus example system. For comparison purposes, the classical formulation of the OPF problem was solved using an interior point method implemented in MATPOWER version 4.0 [55].

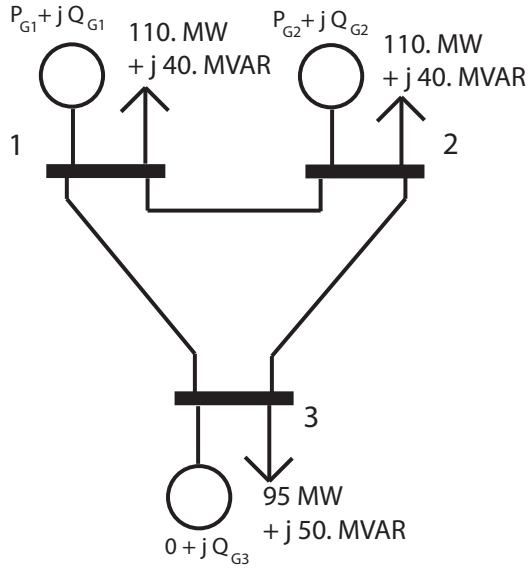

Figure 2.3 Three-Bus Example System

The three-bus example power system is depicted in Figure 2.3, where the numeric values indicate the $P_{Dk} + jQ_{Dk}$ load demands in MW and MVAR. This example uses a 100 MVA base. The active and reactive power outputs of the generators at buses 1 and 2 have large, non-binding limits. The "generator" at bus 3 is a synchronous condenser (i.e., it produces only reactive power). The reactive power limits for the generator at bus 3 are large enough to be non-binding. The quadratic generator cost curves for the generators at buses 1 and 2 are given in Table 2.1 for power generation in MWh, where c_2 is the coefficient of the squared term, c_1 is the coefficient of the linear term, and c_0 is a constant. There is no cost associated with generator 3 since it produces no active power. The network data using per unit representation are given in Table 2.2. Line shunt susceptances are

specified for the entire line (see Figure 2.1 for the Π-model circuit representation). The voltage magnitudes at all buses are constrained to the range 1.1 to 0.9 per unit.

Generator	c_2	c_1	c_0
1	\$0.11 per $(\text{MWh})^2$	\$5 per MWh	\$0
2	\$0.085 per $(\text{MWh})^2$	\$1.2 per MWh	\$0

Table 2.1 Three-Bus System Generator Cost Data

From Bus	To Bus	R	X	b
1	3	0.065	0.620	0.450
3	2	0.025	0.750	0.700
1	2	0.042	0.900	0.300

Table 2.2 Three-Bus System Network Data

First consider a line-flow limit of 60 MVA enforced on both ends of the line between bus 2 and bus 3 (all other lines have no flow limits). The semidefinite relaxation yields a physically meaningful result, as evidenced by the two-dimensional nullspace of $\mathbf{A}$, that matches the solution of the classical formulation. The solution is shown in Tables 2.3 and 2.4, and aggregate Lagrange multipliers (LMPs) for active and reactive power obtained from (2.7a) and (2.7b) are given in Table 2.5. The optimal objective values for both the semidefinite relaxation and classical formulations are \$5707.07 per hour.

	Bus 1	Bus 2	Bus 3
$\lvert V\rvert$ (per unit)	1.069	1.028	1.001
δ (degrees)	0	9.916	-13.561
P_g (MW)	131.09	185.93	0
Q_g (MVAR)	17.02	-3.50	0.06

Table 2.3 Solution to Three-Bus System with Line-Flow Limit of 60 MVA (Classical and Semidefinite Relaxation)

From Bus	To Bus	From MVA	To MVA
1	3	43.90	47.47
3	2	60.00	60.00
1	2	22.72	28.69

Table 2.4 Line-Flow Data for Three-Bus System with Line-Flow Limit of 60 MVA (Classical and Semidefinite Relaxation)

	Bus 1	Bus 2	Bus 3
$\lambda\,(\$/\mathrm{MWh})$	33.84	32.81	35.96
$\gamma\,(\$/\mathrm{MVAR\text{-}hour})$	0	0	0

Table 2.5 Aggregate Lagrange Multipliers for Three-Bus System with Line-Flow Limit of 60 MVA

Now reduce the line-flow limit to 50 MVA while leaving the other parameters unchanged. The solution to the semidefinite relaxation has an $\mathbf{A}$ matrix with four-dimensional nullspace. The solution therefore has non-zero relaxation gap and is not physically meaningful. However, the classical formulation solved via an interior point method in MATPOWER does yield a (at least locally optimal) solution as shown in Tables 2.6 and 2.7. Aggregate Lagrange multipliers (prices) for active and reactive power obtained using MATPOWER are given in Table 2.8. The aggregate Lagrange multipliers at the non-zero relaxation gap solution to the semidefinite relaxation are given in Table 2.9. Note that all aggregate Lagrange multipliers in both the classical and semidefinite relaxation formulations are non-negative, and the active power balance Lagrange multipliers λ are strictly positive. The relaxation gap/loss-of-physically-meaningful semidefinite relaxation solution cannot, therefore, be attributed to negative Lagrange multipliers. Also note that the $\mathbf{H}$ and $\mathbf{R}$ matrices at this solution are rank one; the relaxation gap is evident solely from the dimension of the nullspace of the $\mathbf{A}$ matrix.

	Bus 1	Bus 2	Bus 3
$\|V\|$ (per unit)	1.100	0.926	0.900
δ (degrees)	0	7.259	-17.267
P_g (MW)	148.07	170.01	0
Q_g (MVAR)	54.70	-8.79	-4.84

Table 2.6 Solution to Three-Bus System with Line-Flow Limit of 50 MVA (Classical Formulation)

From Bus	To Bus	From MVA	To MVA
1	3	52.29	60.28
3	2	50.00	50.00
1	2	14.02	33.33

Table 2.7 Line-Flow Data for Three-Bus System with Line-Flow Limit of 50 MVA (Classical Formulation)

	Bus 1	Bus 2	Bus 3
λ (\$/MWh)	37.57	30.10	45.54
γ (\$/MVAR-hour)	0	0	0

Table 2.8 Aggregate Lagrange Multipliers for Three-Bus System with Line-Flow Limit of 50 MVA (Classical Formulation)

	Bus 1	Bus 2	Bus 3
λ (\$/MWh)	35.78	31.62	40.83
γ (\$/MVAR-hour)	0	0	0

Table 2.9 Aggregate Lagrange Multipliers for Three-Bus System with Line-Flow Limit of 50 MVA (Semidefinite Relaxation)

The optimal objective value for the semidefinite relaxation is \$5789.87 per hour, whereas the optimal objective value to the classical formulation is \$5812.60 per hour (a difference of 0.4%). Thus, as expected, the objective function value of the solution to the semidefinite relaxation lower bounds that of the classical formulation. Larger example systems also showed these same properties in which the semidefinite relaxation yielded an $\mathbf{A}$ matrix with nullspace dimension greater than two, and hence failed to provide a physically meaningful OPF solution. Again, the problematic cases appeared as sufficiently strict line-flow limits were imposed.

In [71], Sojoudi and Lavaei consider a modified form of the three-bus system in Figure 2.3 with line-flow limits based on active power flows rather than apparent power flows. They correctly note that when the modified OPF problem is feasible, the semidefinite programming relaxation yields a physically meaningful solution for all positive active power flow limits on the line between buses 2 and 3. However, this property does not hold for the original three-bus system presented in Figure 2.3; when an active power line-flow limit of 30 MW is imposed in this system, the semidefinite program solution has non-zero relaxation gap. Using active power line-flow limits instead of apparent power line-flow limits is not a panacea for obtaining physically meaningful solutions.

There might remain useful information to be garnered from non-zero relaxation gap solutions, particularly in cases for which $\mathbf{W}$ is close to a rank one matrix. As a pragmatic heuristic, the binding constraints for the non-zero relaxation gap solution to the semidefinite relaxation might be assumed to be the same as those for the actual optimal solution. For an n-bus system with $2n$ binding constraints, the values of all unknown variables are fully determined, and, with a sufficiently close initial guess, could be computed via standard Newton-Raphson algorithms. In cases for which the binding constraints do not yield a fully determined system, the dimension of the feasible space is still significantly reduced, and, by using an eigen decomposition, the closest rank one approximation to $\mathbf{W}$ could be employed to yield an initial guess to an alternative OPF algorithm.

It is important to note, however, that a solution to the semidefinite relaxation with non-zero relaxation gap is not necessarily a good approximation of the actual OPF solution. For instance, when applied to the three-bus example system in Figure 2.3 with line-flow limits of 50 MVA, the

DC OPF, a common linear approximation to the OPF problem [85], yields more accurate active power generation and active power Lagrange multipliers (LMPs), as compared to the solution of the classical formulation in Table 2.6, than the non-zero relaxation gap solution to the semidefinite relaxation. Even when line-flow limits are based on active power flows, rather than apparent power flows, non-zero relaxation gap solutions to the semidefinite relaxation can be less accurate approximations than solutions from a DC OPF (e.g., the three-bus system in Figure 2.3 with an active power line-flow limit of 30 MW on line between buses 2 and 3).

2.4 Conclusion

This chapter has investigated application of a semidefinite programming relaxation to the optimal power flow problem and presented practical system conditions where the semidefinite relaxation may fail to give physically meaningful results. The first was already identified in the discussion of [7], but was not recognized as a commonly occurring practical system condition: that of negative bus LMPs. In a new result, this chapter has also provided a numerical OPF example to demonstrate that a non-zero relaxation gap solution may arise from the semidefinite relaxation as a line-flow inequality constraint is progressively "tightened." Under these conditions, the semidefinite relaxation fails to provide a physically meaningful solution to the original OPF problem of interest. The examples examined in this chapter demonstrate that the semidefinite relaxation in its present development is not capable of reliably solving the OPF problem in several practical operating conditions of interest.

Chapter 3

Applications of the Semidefinite Relaxation to Large-Scale OPF Problems

3.1 Introduction

Although the semidefinite relaxation does not find zero relaxation gap solutions to all OPF problems, the ability to find global optima for many OPF problems in polynomial time is a significant advantage of this solution technique. Solving large-scale OPF problems that reflect features common in practical power system applications requires overcoming several modeling and computational limitations inherent to the formulation presented in Chapter 2. The work detailed in this chapter addresses these limitations.

In Section 3.2, this chapter first focuses on modeling aspects that must be addressed in order to apply the semidefinite relaxation to OPF problems with general power system models. The first issue addressed is that of allowing multiple generators at the same bus. Whereas existing formulations only allow a single generator to exist at a bus, this chapter uses analogy to the concept of equal marginal generation cost to produce a formulation that allows for multiple generators at the same bus, each with separate cost functions and generation limits. This chapter considers both quadratic and piecewise-linear generator cost functions.

A method for incorporating flow limits on parallel lines is then presented. Existing formulations limit the total flow between two buses, which cannot account for parallel lines with different electrical properties and limits. In contrast, the formulation in this chapter limits the flow on each individual line. This formulation allows lines with off-nominal voltage ratios and/or non-zero phase shifts.

The next contribution regards load models. Power system analyses benefit from flexible and detailed representation of load behavior; specifying load models to best capture physical behvaior is an active research topic [86, 87]. Static analyses often use ZIP load models that consist of constant impedance, constant current, and constant power components [87, 88]. The ZIP load model is used in such commercial power system software packages as Power System Simulation for Engineering (PSS/E) [89], Positive Sequence Load Flow (PSLF) [90], and PowerWorld [91].

Existing semidefinite relaxations of the OPF problem explicitly consider constant power load models, in which complex power demand is independent of voltage magnitude. Constant impedance loads, for which demands are functions of the square of voltage magnitudes, are easily incorporated in existing semidefinite formulations using shunt admittances. However, constant current loads are linear functions of voltage magnitude, and hence are not easily incorporated into semidefinite formulations.

Section 3.2.4 presents an approximate method for incorporating constant current loads, and therefore ZIP models, into the semidefinite relaxation of the OPF problem. This formulation uses a rank relaxation to approximate a linear function of voltage magnitude.

Section 3.3 next advances research in the computational tractability of applying semidefinite programming to large power system models. It should be noted that the feature of providing a provably polynomial time solution does not necessarily imply practical computation time for large-scale problems. Semidefinite programming relaxations of the OPF problem constrain a $2n \times 2n$ symmetric matrix to be positive semidefinite, where n is the number buses in the system. The semidefinite program size thus grows as the square of the number of buses, which makes solution of the OPF problem by semidefinite programming computationally challenging for large systems. Recent work using matrix completion [78–80] reduces the computational burden inherent in solving large systems by taking advantage of the sparse matrix structure created by realistic power system models. Sojoudi and Lavaei [71], Jabr [82], and Bai and Wei [81] present formulations that decompose the single large $2n \times 2n$ positive semidefinite matrix constraint into positive semidefinite constraints on many smaller matrices. If the matrices from these decompositions satisfy a rank condition, the $2n \times 2n$ matrix also satisfies the rank condition and an optimal solution can be

obtained. Sojoudi and Lavaei's decomposition [71] uses a cycle basis of the network. The matrix decomposition approach used by both Jabr [82] and Bai and Wei [81] is based on the maximal cliques of a chordal extension of the network.

Computational contributions of this chapter involve several enhancements to the existing decompositions. Specifically, this chapter presents a heuristic algorithm for combining some of the small matrices resulting from the decomposition. Since linking constraints are required in order to equate elements of the decomposed matrices that refer to the same element in the $2n \times 2n$ matrix, it is not always advantageous to create the smallest possible matrices. Combining matrices eliminates some of these linking constraints, which can result in significant computational speed increases. The claim that the proposed algorithm can substantially increase computational speed is justified using both theoretical arguments and several test cases.

Exploitation of power system sparsity enables analysis of the relaxation gap properties for large OPF problems. This analysis suggests that non-convexities in small subsections of the network may result in non-zero relaxation gap solutions.

Note that this chapter considers a centralized application of these decompositions in the sense of creating one semidefinite program that is solved on a single computer as opposed to creating many subproblems that are solved using decentralized techniques as in [92]. Centralized application allows for solution with existing generic semidefinite programming solvers.

A further enhancement presented in this chapter is a technique for recovering an optimal voltage profile from the decomposed matrices. While the steps are relatively straightforward, existing literature does not detail a method for actually obtaining an optimal voltage profile from a solution to a decomposed formulation.

Although this chapter focuses on the maximal clique decomposition proposed by both Jabr [82] and Bai and Wei [81] due to the voluminous literature on matrix completion with chordal extensions (e.g., [78–80]), both of these enhancements could be applied to Sojoudi and Lavaei's decomposition [71] as well.

This chapter also describes a modification to the maximal clique decomposition as formulated by Jabr [82] that allows for application to general power systems. This formulation creates

a chordal extension of the network using a Cholesky factorization of the absolute value of the imaginary part of the bus admittance matrix. However, this matrix may fail to be positive definite (for instance, in networks with significant shunt capacitive compensation), thus preventing calculation of a Cholesky factorization. This chapter proposes an alternative matrix that is always positive definite and gives an equivalent chordal extension, thus broadening the applicability of this decomposition to general networks.

Despite these computational advances, solution of the semidefinite relaxation is still significantly slower than mature OPF algorithms, such as interior point methods [55]. It would be beneficial to pair the solution speed of mature OPF solution algorithms with the global optimality guarantee of the semidefinite relaxation. Section 3.4 next proposes a sufficient condition derived from the Karush-Kuhn-Tucker (KKT) conditions for optimality of the semidefinite relaxation of the OPF problem [93]. A candidate solution obtained from a mature OPF solution algorithm that satisfies the KKT conditions of complementarity and feasibility is guaranteed to be globally optimal. However, satisfaction of these conditions is not necessary for global optimality.

This chapter is organized as follows. Section 3.2 provides both the classical formulation of the OPF problem and a proposed semidefinite programming relaxation that incorporates multiple generators at the same bus and parallel lines, including lines with off-nominal voltage ratios and/or non-zero phase-shifts. An approximate representation of ZIP loads is also described in this section. Section 3.3 gives an overview of the maximal clique decomposition and presents three advances in decompositions for large-scale system models: an algorithm that improves computation speed by combining matrices, a modification to Jabr's maximal clique decomposition that extends its applicability to general power system networks, and a technique for recovering an optimal voltage profile from a solution to a decomposed formulation. Section 3.3 next discusses rank condition satisfaction for large system models. Finally, Section 3.4 proposes a sufficient condition test for global optimality of a candidate OPF solution.

The work in Sections 3.2 and 3.3 is accepted for publication as [94]. The work in Section 3.2.4 is submitted for publication as [95]. The work in Section 3.4 is accepted for publication as [96].

3.2 The OPF Problem and Modeling Issues

This section first presents the OPF problem as it is classically formulated. Specifically, this formulation is in terms of rectangular voltage coordinates, active and reactive power generation, and apparent-power line-flow limits. Each bus may have multiple generators with either convex quadratic or convex piecewise-linear cost functions and parallel lines are allowed. This classical OPF formulation is generally non-convex. This section then describes a semidefinite programming relaxation of the OPF problem adopted from [7] that handles the modeling issues of multiple generators at the same bus and parallel lines. This section finally describes an approximate method for integrating ZIP models into the semidefinite relaxation of the OPF problem.

3.2.1 Classical OPF Formulation

Consider an n-bus power system, where $\mathcal{N} = \{1, 2, \ldots, n\}$ represents the set of all buses. Define $\mathcal{G}$ as the set of all generators, with $\mathcal{G}_i$ the set of generators at bus i. Let $\mathcal{G}^q$ represent the set of all generators with quadratic cost functions, with $\mathcal{G}_i^q$ those such generators at bus i. Let $\mathcal{G}^{pw}$ represent the set of generators with piecewise-linear cost functions, with $\mathcal{G}_i^{pw}$ those such generators at bus i. (Some of these sets may be empty.) $P_{Gg} + jQ_{Gg}$ represents the active and reactive power output of generator $g \in \mathcal{G}$. $P_{Di} + jQ_{Di}$ represents the active and reactive load demand at each bus $i \in \mathcal{N}$. $V_i = V_{di} + jV_{qi}$ represents the voltage phasor in rectangular coordinates at each bus $i \in \mathcal{N}$. Superscripts "max" and "min" denote specified upper and lower limits. Let $\mathbf{Y} = \mathbf{G} + j\mathbf{B}$ denote the network admittance matrix.

$\mathcal{L}$ represents the set of all lines, where line $k \in \mathcal{L}$ has terminals at buses l_k and m_k, with parallel lines allowed (i.e., more than one line between the same terminal buses). Let S_k represent the apparent power flow on the line $k \in \mathcal{L}$.

Define a cost function associated with each generator, typically representing a dollar/hour variable operating cost. This chapter considers quadratic and piecewise-linear cost functions in (3.1a) and (3.1b), respectively. In (3.1a), the terms c_{g2}, c_{g1}, and c_{g0} represent the convex quadratic cost coefficients for generator $g \in \mathcal{G}^q$. In (3.1b), generator $g \in \mathcal{G}^{pw}$ has a convex piecewise-linear

cost function composed of r_g line segments specified by slopes $m_{g1}, \ldots, m_{gr_g}$ and breakpoints $(a_{gt}, b_{gt}),\ t = 1, \ldots, r_g$, where a_{gt} is the power generation coordinate and b_{gt} is the cost coordinate for the breakpoint.

$$\mathcal{C}_g^q\left(P_{Gg}\right) = c_{g2}P_{Gg}^2 + c_{g1}P_{Gg} + c_{g0} \tag{3.1a}$$

$$\mathcal{C}_g^{pw}\left(P_{Gg}\right) = \begin{cases} m_{g1}\left(P_{Gg} - a_{g1}\right) + b_{g1}, & P_{Gg} \le a_{g1} \\ m_{g2}\left(P_{Gg} - a_{g2}\right) + b_{g2}, & a_{g1} < P_{Gg} \le a_{g2} \\ \vdots & \vdots \\ m_{gr}\left(P_{Gg} - a_{gr}\right) + b_{gr}, & a_{gr} < P_{Gg} \end{cases} \tag{3.1b}$$

The classical OPF problem is then

$$\min_{P_G, Q_G, S, V_d, V_q} \sum_{g\in\mathcal{G}^q} \mathcal{C}_g^q\left(P_{Gg}\right) + \sum_{g\in\mathcal{G}^{pw}} \mathcal{C}_g^{pw}\left(P_{Gg}\right) \qquad \text{subject to} \tag{3.2a}$$

$$P_{Gg}^{\min} \le P_{Gg} \le P_{Gg}^{\max} \qquad \forall g \in \mathcal{G} \tag{3.2b}$$

$$Q_{Gg}^{\min} \le Q_{Gg} \le Q_{Gg}^{\max} \qquad \forall g \in \mathcal{G} \tag{3.2c}$$

$$\left(V_i^{\min}\right)^2 \le V_{di}^2 + V_{qi}^2 \le \left(V_i^{\max}\right)^2 \qquad \forall i \in \mathcal{N} \tag{3.2d}$$

$$|S_k| \le S_k^{\max} \qquad \forall k \in \mathcal{L} \tag{3.2e}$$

$$\sum_{g\in\mathcal{G}_i}\left(P_{Gg}\right) - P_{Di} = V_{di}\sum_{h=1}^{n}\left(\mathbf{G}_{ih}V_{dh} - \mathbf{B}_{ih}V_{qh}\right) + V_{qi}\sum_{h=1}^{n}\left(\mathbf{B}_{ih}V_{dh} + \mathbf{G}_{ih}V_{qh}\right) \qquad \forall i \in \mathcal{N} \tag{3.2f}$$

$$\sum_{g\in\mathcal{G}_i}\left(Q_{Gg}\right) - Q_{Di} = V_{di}\sum_{h=1}^{n}\left(-\mathbf{B}_{ih}V_{dh} - \mathbf{G}_{ih}V_{qh}\right) + V_{qi}\sum_{h=1}^{n}\left(\mathbf{G}_{ih}V_{dh} - \mathbf{B}_{ih}V_{qh}\right) \qquad \forall i \in \mathcal{N} \tag{3.2g}$$

Note that this formulation limits the apparent power flow measured at each end of a given line, recognizing that active and reactive line losses can cause these quantities to differ.

3.2.2 Semidefinite Programming Relaxation of the OPF Problem

This section describes the semidefinite relaxation of the OPF problem, including the capability to incorporate parallel lines and multiple generators at the same bus. Let e_i denote the i^{th} standard basis vector in $\mathbb{R}^n$. Define the matrix $Y_i = e_i e_i^T \mathbf{Y}$, where transpose is indicated by superscript T.

Matrices employed in the bus power injection and voltage magnitude constraints are

$$\mathbf{Y}_i = \frac{1}{2}\begin{bmatrix} \mathrm{Re}\left(Y_i + Y_i^T\right) & \mathrm{Im}\left(Y_i^T - Y_i\right) \\ \mathrm{Im}\left(Y_i - Y_i^T\right) & \mathrm{Re}\left(Y_i\ + Y_i^T\right) \end{bmatrix} \tag{3.3}$$

$$\bar{\mathbf{Y}}_i = -\frac{1}{2}\begin{bmatrix} \mathrm{Im}\left(Y_i + Y_i^T\right) & \mathrm{Re}\left(Y_i - Y_i^T\right) \\ \mathrm{Re}\left(Y_i^T - Y_i\right) & \mathrm{Im}\left(Y_i + Y_i^T\right) \end{bmatrix} \tag{3.4}$$

$$\mathbf{M}_i = \begin{bmatrix} e_i e_i^T & \mathbf{0} \\ \mathbf{0} & e_i e_i^T \end{bmatrix} \tag{3.5}$$

A "line" in this formulation includes both transmission lines and transformers, where transformers may have both a phase shift and/or an off-nominal voltage ratio. That is, line k is modeled as a Π circuit (with series admittance $g_k + jb_k$ and shunt capacitances $\frac{b_{sh,\,k}}{2}$) in series with an ideal transformer (with turns ratio $1 : \tau_k e^{j\theta_k}$) as in [55]. Note that a small minimum resistance is enforced on all lines in accordance with [7]. Define f_i as the i^{th} standard basis vector in $\mathbb{R}^{2n}$. Matrices employed in the line-flow constraints are

$$\begin{aligned} \mathbf{Z}_{k_l} = {} & \frac{g_k}{\tau_k^2}\left(f_{l_k} f_{l_k}^T + f_{l_k+n} f_{l_k+n}^T\right) - c_l\left(f_{l_k} f_{m_k}^T + f_{m_k} f_{l_k}^T + f_{l_k+n} f_{m_k+n}^T + f_{m_k+n} f_{l_k+n}^T\right) \\ & + s_l\left(f_{l_k} f_{m_k+n}^T + f_{m_k+n} f_{l_k}^T - f_{l_k+n} f_{m_k}^T - f_{m_k} f_{l_k+n}^T\right) \end{aligned} \tag{3.6}$$

$$\begin{aligned} \mathbf{Z}_{k_m} = {} & g_k\left(f_{m_k} f_{m_k}^T + f_{m_k+n} f_{m_k+n}^T\right) - c_m\left(f_{l_k} f_{m_k}^T + f_{m_k} f_{l_k}^T + f_{l_k+n} f_{m_k+n}^T + f_{m_k+n} f_{l_k+n}^T\right) \\ & + s_m\left(f_{l_k+n} f_{m_k}^T + f_{m_k} f_{l_k+n}^T - f_{l_k} f_{m_k+n}^T - f_{m_k+n} f_{l_k}^T\right) \end{aligned} \tag{3.7}$$

$$\begin{aligned} \bar{\mathbf{Z}}_{k_l} = {} & -\left(\frac{2b_k + b_{sh,k}}{2\tau_k^2}\right)\left(f_{l_k} f_{l_k}^T + f_{l_k+n} f_{l_k+n}^T\right) \\ & + c_l\left(f_{l_k} f_{m_k+n}^T + f_{m_k+n} f_{l_k}^T - f_{l_k+n} f_{m_k}^T - f_{m_k} f_{l_k+n}^T\right) \\ & + s_l\left(f_{l_k} f_{m_k}^T + f_{m_k} f_{l_k}^T + f_{l_k+n} f_{m_k+n}^T + f_{m_k+n} f_{l_k+n}^T\right) \end{aligned} \tag{3.8}$$

$$\begin{aligned} \bar{\mathbf{Z}}_{k_m} = {} & -\left(b_k + \frac{b_{sh,k}}{2}\right)\left(f_{m_k} f_{m_k}^T + f_{m_k+n} f_{m_k+n}^T\right) \\ & + c_m\left(f_{l_k+n} f_{m_k}^T + f_{m_k} f_{l_k+n}^T - f_{l_k} f_{m_k+n}^T - f_{m_k+n} f_{l_k}^T\right) \\ & + s_m\left(f_{l_k} f_{m_k}^T + f_{m_k} f_{l_k}^T + f_{l_k+n} f_{m_k+n}^T + f_{m_k+n} f_{l_k+n}^T\right) \end{aligned} \tag{3.9}$$

where, for notational convenience,

$$c_l = \left(g_k \cos\left(\theta_k\right) + b_k \cos\left(\theta_k + \frac{\pi}{2}\right)\right) / \left(2\tau_k\right) \tag{3.10}$$

$$c_m = \left(g_k \cos\left(-\theta_k\right) + b_k \cos\left(-\theta_k + \frac{\pi}{2}\right)\right) / \left(2\tau_k\right) \tag{3.11}$$

$$s_l = \left(g_k \sin\left(\theta_k\right) + b_k \sin\left(\theta_k + \frac{\pi}{2}\right)\right) / \left(2\tau_k\right) \tag{3.12}$$

$$s_m = \left(g_k \sin\left(-\theta_k\right) + b_k \sin\left(-\theta_k + \frac{\pi}{2}\right)\right) / \left(2\tau_k\right) \tag{3.13}$$

To write the semidefinite relaxation, first define the vector of voltage coordinates

$$x = \begin{bmatrix} V_{d1} & V_{d2} & \dots & V_{dn} & V_{q1} & V_{q2} & \dots & V_{qn} \end{bmatrix} \tag{3.14}$$

Then define the rank one matrix

$$\mathbf{W} = xx^T \tag{3.15}$$

The active and reactive power injections at bus i are then given by $\mathrm{trace}\left(\mathbf{Y}_i\mathbf{W}\right)$ and $\mathrm{trace}\left(\bar{\mathbf{Y}}_i\mathbf{W}\right)$, respectively, where trace indicates the matrix trace operator (i.e., sum of the diagonal elements). The square of the voltage magnitude at bus i is given by $\mathrm{trace}\left(\mathbf{M}_i\mathbf{W}\right)$.

Similarly, the active and reactive line flows for line $k \in \mathcal{L}$ at terminal bus l are given by $\mathrm{trace}\left(\mathbf{Z}_{k_l}\mathbf{W}\right)$ and $\mathrm{trace}\left(\bar{\mathbf{Z}}_{k_l}\mathbf{W}\right)$. Due to the asymmetry introduced by allowing transformers with off-nominal voltage ratios and non-zero phase shifts, separate matrices are required to represent active and reactive power flows from the other terminal of line k at bus m: $\mathrm{trace}\left(\mathbf{Z}_{k_m}\mathbf{W}\right)$ and $\mathrm{trace}\left(\bar{\mathbf{Z}}_{k_m}\mathbf{W}\right)$.

Replacing the rank one constraint (3.15) by the less stringent constraint $\mathbf{W} \succeq 0$, where $\succeq$ indicates positive semidefiniteness, yields the semidefinite relaxation. The semidefinite relaxation is "tight" when the solution has zero relaxation gap. The relaxation gap for a solution to the semidefinite relaxation refers to the difference between an optimal objective value for the semidefinite relaxation and the objective value for a global solution to the classical formulation of the OPF problem (3.2). A solution to the semidefinite relaxation has zero relaxation gap if and only if the rank condition $\mathrm{rank}\left(\mathbf{W}\right) \leq 2$ is satisfied. For a solution with zero relaxation gap, a unique rank one matrix $\mathbf{W}$ is recovered by enforcing the known voltage angle at the reference bus [7].

The semidefinite relaxation of the OPF problem is

$$\min_{\mathbf{W},\, P_G,\, \alpha,\, \beta} \sum_{g \in \mathcal{G}^q} \alpha_g + \sum_{g \in \mathcal{G}^{pw}} \beta_g \qquad \text{subject to} \tag{3.16a}$$

$$P_{Gg}^{\min} \leq P_{Gg} \leq P_{Gg}^{\max} \qquad \forall g \in \mathcal{G} \quad (3.16b)$$

$$-P_{Di} + \sum_{g \in \mathcal{G}_i} P_{Gg} = \operatorname{trace}\left(\mathbf{Y}_i \mathbf{W}\right) \qquad \forall i \in \mathcal{N} \quad (3.16c)$$

$$Q_i^{\min} \leq \operatorname{trace}\left(\bar{\mathbf{Y}}_i \mathbf{W}\right) \leq Q_i^{\max} \qquad \forall i \in \mathcal{N} \quad (3.16d)$$

$$\left(V_i^{\min}\right)^2 \leq \operatorname{trace}\left(\mathbf{M}_i \mathbf{W}\right) \leq \left(V_i^{\max}\right)^2 \qquad \forall i \in \mathcal{N} \quad (3.16e)$$

$$\begin{bmatrix} \left(S_k^{\max}\right)^2 & -\operatorname{trace}\left(\mathbf{Z}_{k_l} \mathbf{W}\right) & -\operatorname{trace}\left(\bar{\mathbf{Z}}_{k_l} \mathbf{W}\right) \\ -\operatorname{trace}\left(\mathbf{Z}_{k_l} \mathbf{W}\right) & 1 & 0 \\ -\operatorname{trace}\left(\bar{\mathbf{Z}}_{k_l} \mathbf{W}\right) & 0 & 1 \end{bmatrix} \succeq 0 \qquad \forall k \in \mathcal{L} \quad (3.16f)$$

$$\begin{bmatrix} \left(S_k^{\max}\right)^2 & -\operatorname{trace}\left(\mathbf{Z}_{k_m} \mathbf{W}\right) & -\operatorname{trace}\left(\bar{\mathbf{Z}}_{k_m} \mathbf{W}\right) \\ -\operatorname{trace}\left(\mathbf{Z}_{k_m} \mathbf{W}\right) & 1 & 0 \\ -\operatorname{trace}\left(\bar{\mathbf{Z}}_{k_m} \mathbf{W}\right) & 0 & 1 \end{bmatrix} \succeq 0 \qquad \forall k \in \mathcal{L} \quad (3.16g)$$

$$\begin{bmatrix} \alpha_g - c_{g1} P_{Gg} + c_{g0} & -\sqrt{c_{g2}} P_{Gg} \\ -\sqrt{c_{g2}} P_{Gg} & 1 \end{bmatrix} \succeq 0 \qquad \forall g \in \mathcal{G}^q \quad (3.16h)$$

$$\left\{\beta_g \geq m_{gt}\left(P_{Gg} - a_{gt}\right) + b_{gt} \qquad \forall t = 1, \ldots, r_g\right\} \qquad \forall g \in \mathcal{G}^{pw} \quad (3.16i)$$

$$\mathbf{W} \succeq 0 \tag{3.16j}$$

where apparent-power line-flow limits and quadratic generator cost functions are implemented using Schur's complement formula in (3.16f)–(3.16g) and (3.16h), respectively; in (3.16i), piecewise-linear generator cost functions are implemented using the "constrained cost variable" method as in [55]; and, for notational convenience, the maximum and minimum reactive power injections at each bus are defined as

$$Q_i^{\max} = -Q_{Di} + \sum_{g \in \mathcal{G}_i} Q_{Gg}^{\max} \tag{3.17}$$

$$Q_i^{\min} = -Q_{Di} + \sum_{g \in \mathcal{G}_i} Q_{Gg}^{\min} \tag{3.18}$$

The dual form of the semidefinite relaxation (i.e., the dual of (3.16)) requires definition of Lagrange multipliers corresponding to each constraint in (3.16). Define vectors of Lagrange multipliers associated with lower inequality bounds on active power, reactive power, and squared voltage magnitude as $\underline{\psi}_k$, $\underline{\gamma}_i$, and $\underline{\mu}_i$, and those associated with upper bounds as $\bar{\psi}_k$, $\bar{\gamma}_i$, and $\bar{\mu}_i$, respectively. Define a scalar variable λ_i as the aggregate Lagrange multiplier (i.e., the locational marginal price (LMP)) of active power at each bus i. Note that λ_i is not constrained to be non-negative. Define two 3×3 symmetric matrices per line for the line-flow limits measured from each line terminal: $\mathbf{H}_{k_l}$ and $\mathbf{H}_{k_m}$, with $\mathbf{H}_{k_l}^{cd}$ and $\mathbf{H}_{k_m}^{cd}$ indicating the (c, d) element of the corresponding matrix. Define 2×2 symmetric matrices for each generator with a quadratic cost function: $\mathbf{R}_g$, with $\mathbf{R}_g^{cd}$ the (c, d) element of $\mathbf{R}_g$. Define a Lagrange multiplier ζ_{gt} for each line segment t of each generator g with a piecewise-linear cost function.

Define a matrix-valued function $\mathbf{A}$.

$$\begin{aligned}\mathbf{A} = &\sum_{i \in \mathcal{N}} \left\{ \lambda_i \mathbf{Y}_i + \left(\bar{\gamma}_i - \underline{\gamma}_i \right) \bar{\mathbf{Y}}_i + \left(\bar{\mu}_i - \underline{\mu}_i \right) \mathbf{M}_i \right\} \\ &+ 2 \sum_{k \in \mathcal{L}} \left\{ \mathbf{H}_{k_l}^{12} \mathbf{Z}_{k_l} + \mathbf{H}_{k_m}^{12} \mathbf{Z}_{k_m} + \mathbf{H}_{k_l}^{13} \bar{\mathbf{Z}}_{k_l} + \mathbf{H}_{k_m}^{13} \bar{\mathbf{Z}}_{k_m} \right\} \end{aligned} \tag{3.19}$$

Define a scalar real-valued function ρ.

$$\begin{aligned}\rho = &\sum_{i \in \mathcal{N}} \left\{ \lambda_i P_{Di} + \underline{\gamma}_i Q_i^{\min} - \bar{\gamma}_i Q_i^{\max} + \underline{\mu}_i \left(V_i^{\min} \right)^2 - \bar{\mu}_i \left(V_i^{\max} \right)^2 \right. \\ &\left. + \sum_{g \in \mathcal{G}_i^q} \left(\underline{\psi}_g P_{Gg}^{\min} - \bar{\psi}_g P_{Gg}^{\max} + c_{g0} - \mathbf{R}_g^{22} \right) - \sum_{g \in \mathcal{G}_i^{pw}} \sum_{t=1}^{r_g} \left(\zeta_{gt} \left(m_{gt} a_{gt} - b_{gt} \right) \right) \right\} \\ &- \sum_{k \in \mathcal{L}} \left\{ \left(S_k^{\max} \right)^2 \left(\mathbf{H}_{k_l}^{11} + \mathbf{H}_{k_m}^{11} \right) + \mathbf{H}_{k_l}^{22} + \mathbf{H}_{k_m}^{22} + \mathbf{H}_{k_l}^{33} + \mathbf{H}_{k_m}^{33} \right\} \end{aligned} \tag{3.20}$$

The dual form of the semidefinite programming relaxation of the OPF problem is then

$$\max_{\lambda,\underline{\psi},\bar{\psi},\underline{\gamma},\bar{\gamma},\underline{\mu},\bar{\mu},\zeta,\mathbf{H},\mathbf{R}} \quad \rho \qquad \text{subject to} \tag{3.21a}$$

$$\mathbf{A} \succeq 0 \tag{3.21b}$$

$$\mathbf{H}_{k_l} \succeq 0, \quad \mathbf{H}_{k_m} \succeq 0 \qquad \forall k \in \mathcal{L} \tag{3.21c}$$

$$\mathbf{R}_g \succeq 0, \quad \mathbf{R}_g^{11} = 1 \qquad \forall g \in \mathcal{G}^q \tag{3.21d}$$

$$\sum_{t=1}^{r_g} \zeta_{gt} = 1 \qquad \forall g \in \mathcal{G}^{pw} \tag{3.21e}$$

$$\left\{ \lambda_i = c_{g1} + 2\sqrt{c_{g2}}\mathbf{R}_g^{12} + \bar{\psi}_g - \underline{\psi}_g \qquad \forall g \in \mathcal{G}_i^q \right\} \qquad \forall i \in \mathcal{N} \tag{3.21f}$$

$$\left\{ \lambda_i = \sum_{t=1}^{r_g} \zeta_{gt} m_{gt} \qquad \forall g \in \mathcal{G}_i^{pw} \right\} \qquad \forall i \in \mathcal{N} \tag{3.21g}$$

$$\underline{\psi}_g \geq 0,\ \bar{\psi}_g \geq 0,\ \underline{\gamma}_i \geq 0,\ \bar{\gamma}_i \geq 0,\ \underline{\mu}_i \geq 0,\ \bar{\mu}_i \geq 0,\ \zeta_{gt} \geq 0 \tag{3.21h}$$

The semidefinite relaxation has zero relaxation gap and yields a physically meaningful solution if and only if the solution to (3.21) satisfies the rank condition $\dim(\mathrm{null}(\mathbf{A})) \leq 2$. (The additional degree of freedom in the nullspace of $\mathbf{A}$ corresponds to the lack of an angle reference specification in (3.21).)

3.2.3 Semidefinite Programming Formulation Discussion

Several aspects of the semidefinite programming formulation deserve special attention. This discussion focuses on those aspects that differ from previous formulations (e.g., [7]) due to the proposed formulation's allowing of multiple generators at the same bus and parallel lines.

The semidefinite relaxation includes the possibility of multiple generators at the same bus. As shown in (3.21f) and (3.21g), all generators at the same bus i must have the same aggregate active power Lagrange multiplier λ_i. This is related to the principle of equal marginal costs in the economic dispatch problem [9]. Since generator reactive power injections do not appear in the cost function of (3.2), reactive power Lagrange multipliers are only needed for each generator bus rather than for each generator. This is seen in (3.17) and (3.18), which determine the allowed range of bus i reactive power injection.

The semidefinite relaxation also includes the possibility of parallel lines (i.e., multiple lines with the same terminal buses) and the ability to represent transformers with off-nominal voltage ratios and/or non-zero phase-shifts. Previous formulations limited line flows by constraining the total power flow between two buses, thus precluding the ability to separately limit line flows on parallel lines. This modeling flexibility comes at the price of additional complexity. Incorporating parallel lines removes the ability to form the line-flow matrices directly from the bus admittance matrix, instead requiring the more complicated expressions in (3.6)–(3.9). Incorporating off-nominal voltage ratios and non-zero phase shifts breaks the symmetry of the Π model such that different line-flow matrices are required for each line terminal (i.e., $\mathbf{Z}_{k_l}$ in (3.6) and $\bar{\mathbf{Z}}_{k_l}$ in (3.8) for active and reactive power flows measured from the sending terminal and $\mathbf{Z}_{k_m}$ in (3.7) and $\bar{\mathbf{Z}}_{k_m}$ in (3.9) for the receiving terminal).

For large system models, numerical difficulties in the semidefinite programming solver may prevent convergence to acceptable precision. There are several pragmatic techniques that reduce numerical difficulties with large systems. First, ignore engineering limits that will clearly not be binding at the solution. Many power system data sets specify large values for limits that are intended to be unconstrained, particularly for reactive power generation and line-flow limits. Terms corresponding to very large limits are not incorporated. Similarly, some generators specified with quadratic cost functions actually have linear cost functions (i.e., $c_{g2} = 0$). The corresponding $\mathbf{R}_g$ matrix is eliminated. These techniques do not affect the optimality of the resulting solution.

Numerical difficulties often occur when the system model has very "tight" limits. For instance, the active power generation of a synchronous condenser is constrained to be zero. A second technique for reducing numerical difficulties is to use equality constraints rather than inequality constraints to model these limits. When the power output of a generator is constrained to a very small range, fix the generator at the midpoint of this range and directly add the associated generation cost to the objective function. The degree of suboptimality of the resulting solution can be estimated by multiplying the Lagrange multiplier corresponding to the equality constraint by the half of the difference between the maximum and minimum limits.

3.2.4 Approximate Representation of ZIP Loads in a Semidefinite Relaxation of the OPF Problem

Power system analyses benefit from flexible and detailed representation of load behavior. Static analyses often use ZIP load models which consist of constant impedance, constant current, and constant power components. The ZIP load model is used in such commercial power system software packages as Power System Simulation for Engineering (PSS/E) [89], Positive Sequence Load Flow (PSLF) [90], and PowerWorld [91].

Existing semidefinite relaxations of the OPF problem explicitly consider constant power load models which demand constant complex power for any voltage magnitude. Constant impedance loads, for which demands are functions of the square of voltage magnitudes, are easily incorporated in existing semidefinite relaxations using shunt admittances. As linear functions of voltage magnitude, constant current loads are not easily incorporated into semidefinite formulations.

This section next presents an approximate method for integrating constant current loads, and therefore ZIP models, into a semidefinite relaxation of the OPF problem. This method uses a rank relaxation to obtain a linear function of voltage magnitude.

3.2.4.1 Overview of the ZIP Load Model

The constant impedance, constant current, and constant power components of a ZIP load are represented by a second-order polynomial in bus voltage magnitude V_i [87, 88].

$$P_{Di}\left(V_i\right) = a_{1i}V_i^2 + a_{2i}V_i + a_{3i} \tag{3.22a}$$

$$Q_{Di}\left(V_i\right) = b_{1i}V_i^2 + b_{2i}V_i + b_{3i} \tag{3.22b}$$

where a_{1i}, a_{2i}, a_{3i} and b_{1i}, b_{2i}, b_{3i} are scalar parameters for bus i active and reactive power demand, respectively. The constant impedance ("Z"), constant current ("I"), and constant power ("P") components are specified using a_{1i} and b_{1i}, a_{2i} and b_{2i}, and a_{3i} and b_{3i}, respectively. This load model comprises the load demand terms P_{Di} and Q_{Di} in the active and reactive power balance equations of an OPF problem (i.e., (3.2f) and (3.2g)).

3.2.4.2 A Semidefinite Programming Formulation of the ZIP Load Model

The ZIP load model is composed of constant, linear, and squared functions of voltage magnitude. Consider a rank one matrix $\mathbf{\Gamma}_i$ to represent these terms at bus i.

$$\mathbf{\Gamma}_i = \begin{bmatrix} 1 \\ V_i \end{bmatrix} \begin{bmatrix} 1 & V_i \end{bmatrix} = \begin{bmatrix} 1 & V_i \\ V_i & V_i^2 \end{bmatrix} \tag{3.23}$$

Let matrix superscripts denote the corresponding (row, column) element. With constraints $\mathbf{\Gamma}_i^{11} = 1$ and $\mathbf{\Gamma}_i^{22} = V_i^2$, linear functions of voltage magnitude are obtained using $\mathbf{\Gamma}_i^{12}$. (Squared voltage magnitudes V_i^2 are easily formulated in the semidefinite relaxation of the OPF problem.)

To form a semidefinite-programming-suitable convex relaxation, the rank one condition on $\mathbf{\Gamma}_i$ is replaced by a positive semidefinite constraint $\mathbf{\Gamma}_i \succeq 0$. This rank relaxation forms an upper bound on a convex feasible space in the $\mathbf{\Gamma}_i^{22}$ vs. $\mathbf{\Gamma}_i^{12}$ plane on the curve $\mathbf{\Gamma}_i^{12} = \sqrt{\mathbf{\Gamma}_i^{22}}$. Rather than necessarily lying on this curve, the variables $\mathbf{\Gamma}_i^{12}$ and $\mathbf{\Gamma}_i^{22}$ must be within this feasible space, which is shown in Figure 3.1. An exact solution (i.e., a solution on the curve $\mathbf{\Gamma}_i^{12} = \sqrt{\Gamma_i^{22}}$, which is indicated by the red line in Figure 3.1) is obtained when $\text{rank}\,(\mathbf{\Gamma}_i) = 1$.

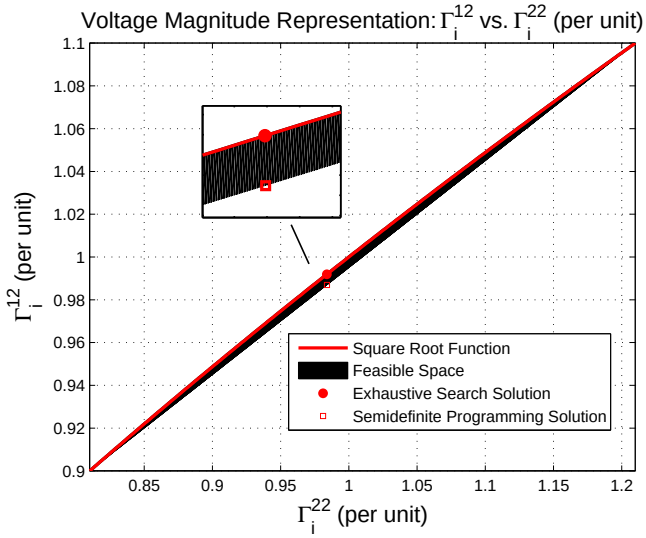

Figure 3.1 Feasible Space for Voltage Magnitude Representation

To enforce voltage magnitudes between V_i^{min} and V_i^{max}, constrain $\left(V_i^{min}\right)^2 \leq \mathbf{\Gamma}_i^{22} \leq \left(V_i^{max}\right)^2$. The line connecting the points $\left(\left(V_i^{min}\right)^2,\, V_i^{min}\right)$ and $\left(\left(V_i^{max}\right)^2,\, V_i^{max}\right)$ lower bounds the feasible space, which is the convex hull of the square root function between the voltage magnitude limits.

To represent the ZIP load model in terms of $\mathbf{\Gamma}_i$, define the constant matrices

$$\mathbf{T}_i = \begin{bmatrix} a_{3i} & \frac{a_{2i}}{2} \\ \frac{a_{2i}}{2} & a_{1i} \end{bmatrix} \tag{3.24a}$$

$$\bar{\mathbf{T}}_i = \begin{bmatrix} b_{3i} & \frac{b_{2i}}{2} \\ \frac{b_{2i}}{2} & b_{1i} \end{bmatrix} \tag{3.24b}$$

The proposed representation for ZIP loads is then

$$P_{Di} = \text{trace}\left(\mathbf{T}_i \mathbf{\Gamma}_i\right) \tag{3.25a}$$

$$Q_{Di} = \text{trace}\left(\bar{\mathbf{T}}_i \mathbf{\Gamma}_i\right) \tag{3.25b}$$

3.2.4.3 ZIP Model Example

Consider a two-bus system with a generator at bus 1 that has no limits on active or reactive power outputs and a ZIP load at bus 2. The line has impedance of $0.05 + j0.15$ per unit and has no flow limit. The ZIP load has per unit parameters $a_{12} = b_{12} = 0.01$, $a_{22} = b_{22} = 0.02$, and $a_{32} = b_{32} = 0.50$. Bus voltage magnitudes are in the range $[0.90,\, 1.10]$ per unit. Denote the bus i voltage phasor as $V_{di} + jV_{qi}$. Specific a 100 MVA base power.

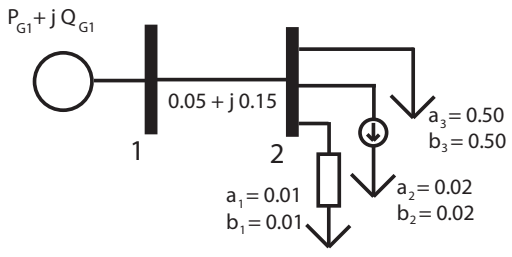

Figure 3.2 Two-Bus Test System with ZIP Load

Define an OPF problem that minimizes the active power generation by specifying that the generator costs \$1/MWh. Use bus 1 to provide the reference angle (i.e., $V_{q1} = 0$ and $V_{d1} = V_1$). For specified V_1, the feasible space has two degrees of freedom (i.e., V_{d2} and V_{q2}) constrained by the active and reactive power balance equations at bus 2. Exhaustive search of the feasible space is conducted by varying V_1 between 0.90 and 1.10 per unit while solving for V_{d2} and V_{q2} with the quadratic equation. This yields a globally optimal solution to the OPF problem with objective value of \$55.82 per hour, $V_1 = 1.100$, and $V_2 = 0.992$ per unit ($V_{d2} = 0.991$ and $V_{q2} = -0.048$ per unit), which is marked by the circle in Figure 3.1. Minimum total cost is achieved by balancing the trade-off between raising voltages to reduce line losses and higher demand from the ZIP load.

The solution to the semidefinite relaxation closely approximates this global solution obtained through exhaustive search. The solution to the semidefinite relaxation has optimal objective value \$55.81 per hour and $V_1 = 1.100$ per unit. $\mathbf{\Gamma}_2^{22} = 0.984$, which implies that $V_2 = 0.992$, while $\mathbf{\Gamma}_2^{12}$ implies that $V_2 = 0.987$ per unit (i.e., a voltage magnitude difference of 0.005 per unit or 0.5%). This solution, which is marked by the square in Figure 3.1, indicates that the semidefinite relaxation selects a slightly larger value for $\mathbf{\Gamma}_2^{22}$ in order to minimize losses as compared to a smaller value for $\mathbf{\Gamma}_2^{12}$ to reduce the demand of the ZIP load. The matrix $\mathbf{\Gamma}_2$ has eigenvalues of 0.005 and 1.979, so this matrix is close to being rank one. The proposed model thus closely approximates but does not exactly match ZIP load behavior for this system.

3.2.4.4 ZIP Model Discussion

Reducing active power demand at ZIP loads often results in lower cost solutions to OPF problems. Active power demands of the constant current components of ZIP loads with positive a_{2i} are reduced by minimizing voltage magnitudes. Thus, solutions to the semidefinite relaxation will tend to have smaller values of $\mathbf{\Gamma}_i^{12}$ relative to the value of V_i implied by $\sqrt{\mathbf{\Gamma}_i^{22}}$, which results in rank two $\mathbf{\Gamma}_i$ matrices. Although such solutions are not exact, they closely approximate ZIP load behavior. The maximum error in the voltage magnitude approximation is given in (3.26).

$$\max_{\left(V_i^{min}\right)^2 \leq \mathbf{\Gamma}_i^{22} \leq \left(V_i^{max}\right)^2} \left\{ \sqrt{\mathbf{\Gamma}_i^{22}} - \mathbf{\Gamma}_i^{12} \right\} = \frac{\left(V_i^{max} - V_i^{min}\right)^2}{4\left(V_i^{max} + V_i^{min}\right)} \quad \text{per unit} \tag{3.26}$$

This maximum occurs at $\mathbf{\Gamma}_i^{22} = \left(V_i^{max} + V_i^{min}\right)^2 / 4$. The error is small for typical values of V_i^{max} and V_i^{min} (e.g., a maximum error of 0.005 per unit occurs at $\mathbf{\Gamma}_i^{22} = 1.00$ and $\mathbf{\Gamma}_i^{12} = 0.995$ per unit for $V_i^{max} = 1.10$ and $V_i^{min} = 0.90$).

Note that negative a_{2i} values in ZIP load models correspond to constant current components that inject active power into the network. For these cases, the semidefinite relaxation will typically yield an exact solution because it tends to maximize the magnitudes of these negative injections. For instance, specifying $a_{22} = -0.02$ per unit gives the exact solution to the two-bus example system (i.e., $\text{rank}\left(\mathbf{\Gamma}_2\right) = 1$).

3.3 Advances in Matrix Completion Decompositions

This section describes several advances in the decomposition techniques used to reduce the computational burden of semidefinite relaxations of large OPF problems. First, this section reviews the maximal clique decomposition as introduced by Jabr [82]. Next, this section proposes a matrix combination algorithm that significantly reduces the required computation time of this decomposition. This section then presents a modification to Jabr's formulation of the maximal clique decomposition that extends this decomposition to general networks rather than only networks with admittance matrices that satisfy a positive definiteness requirement. This section then describes a technique for obtaining an optimal voltage profile from the decomposed matrices.

3.3.1 Overview of Jabr's Maximal Clique Decomposition

Jabr's formulation of the maximal clique decomposition uses a matrix completion theorem [78]. Several graph theoretic definitions aid understanding of this theorem. A "clique" is a subset of the graph vertices for which each vertex in the clique is connected to all other vertices in the clique. A "maximal clique" is a clique that is not a proper subset of another clique. A graph is "chordal" if each cycle of length four or more nodes has a chord, which is an edge connecting two nodes that

are not adjacent in the cycle. The maximal cliques of a chordal graph can be determined in linear time [97]. See [82] and [98] for more details on these definitions.

The matrix completion theorem can now be stated. Let $\bar{\mathbf{A}}$ be a symmetric matrix with partial information (i.e., not all entries of $\bar{\mathbf{A}}$ have known values) with an associated undirected graph. Note that the graph of interest has the power system buses as vertices and the branch susceptances as edge weights. The matrix $\bar{\mathbf{A}}$ can be completed to a positive semidefinite matrix (i.e., the unknown entries of $\bar{\mathbf{A}}$ can be chosen such that $\bar{\mathbf{A}} \succeq 0$) if and only if the submatrices associated with each of the maximal cliques of the graph associated with $\bar{\mathbf{A}}$ are all positive semidefinite.

The matrix completion theorem allows replacing the single large $2n \times 2n$ positive semidefinite constraint (3.21b) with many smaller matrices that are each constrained to be positive semidefinite. This significantly reduces the problem size for large, sparse power networks.

There are two important aspects of this decomposition that are relevant to the advances in this section. First, since the maximal cliques can have non-empty intersection (i.e., contain some of the same buses), different matrices may contain elements that refer to the same element in the $2n \times 2n$ matrix. Therefore, linking constraints are required to force equality between elements that are shared between maximal cliques. To specify these linking constraints, Jabr recommends forming a "clique tree": a maximum weight spanning tree of a graph with nodes corresponding to the maximal cliques and the edge weights between each node pair given by the number of shared buses in each clique pair. A maximal weight spanning tree of this graph, which can be calculated using Prim's algorithm [99], is used to reduce the number of linking constraints: equality constraints are only enforced between the appropriate elements in maximal cliques that are adjacent in the maximal weight spanning tree.

Second, graphs corresponding to realistic power networks are not chordal. A chordal extension of the graph is thus required in order to use the matrix completion theorem. A chordal extension adds edges between non-physically connected nodes (i.e., edges in the chordal extension of the graph may exist between buses that are not connected by a line in the power system) to obtain a chordal graph. Jabr recommends obtaining a chordal extension using a Cholesky factorization of the absolute value of the imaginary part of the network's admittance matrix. To reduce the

total number of edges, a Cholesky factorization with minimum fill-in is obtained from a minimum degree ordering of the row/column indices [100].

3.3.2 Matrix Combination Algorithm

This section next describes a modification to the maximal clique decomposition that yields a significant computational speed improvement. This modification accounts for the trade-off between the size of maximal cliques and the number of linking constraints. Smaller maximal cliques generally reduce the total size of the positive semidefinite constrained matrices. The overlap between maximal cliques, as determined by the clique tree approach, establishes the number of linking constraints.

The maximal clique decomposition uses a Cholesky factorization with minimum fill-in to obtain small maximal cliques as a heuristic for minimizing the number of variables in the positive semidefinite matrix constraints. This approach does not account for the computational burden of the linking constraints. The optimization literature provides theoretical support for the concept of reducing computational burden by combining matrices (see [78] and Section 4 of [79]). Specifically, this literature discusses the potential trade-off in solver time between the sizes of the semidefinite-constrained matrices and the number of linking constraints, which require solution of a system of linear equations in the semidefinite program algorithm. Combining matrices eliminates the need for linking constraints between the matrices at the computational price of a larger matrix. A heuristic for combining matrices to gain the benefits of small matrices while reducing linking constraints thus has the potential for computational speed improvements.

Many common semidefinite program solvers, such as SeDuMi [59] and SDPT3 [62], use primal–dual methods that solve both the primal and dual problems simultaneously. Moreover, since a primal constraint corresponds to a dual variable, the "size" of the semidefinite program can be estimated by adding the total number of scalar variables required to form the matrices with the number of linking constraints. This approximation for the "size" of a semidefinite program forms the basis of the proposed matrix combination heuristic. In a greedy manner, this approach

repeatedly combines the pair of matrices that most reduces the "size" of the semidefinite program as measured by the total number of variables plus the number of linking constraints.

This section next details the matrix combination heuristic. Let L be a parameter specifying the maximum number of matrices. Consider a semidefinite program formed from the chordal extension of a power system network, with maximal clique i containing d_i buses. Since the matrices corresponding to the maximal cliques are symmetric and contain both real and imaginary voltage components, matrix i (corresponding to maximal clique i) has $d_i\,(2d_i + 1)$ variables. If maximal cliques i and k, adjacent in the clique tree, share s_{ik} buses, then $s_{ik}\,(2s_{ik} + 1)$ linking constraints are required between the corresponding matrices. For each pair of adjacent maximal cliques in the clique tree, the change in the optimization problem "size" Δ_{ik} if the cliques i and k were combined is given by

$$\Delta_{ik} = d_{ik}\,(2d_{ik} + 1) - d_i\,(2d_i + 1) - d_k\,(2d_k + 1) - s_{ik}\,(2s_{ik} + 1) \tag{3.27}$$

where $d_{ik} = d_i + d_k - s_{ik}$ is the number of buses in the combined clique.

While the number of matrices is greater than L, combine a pair of adjacent maximal cliques with smallest Δ_{ik}. Then recalculate the value of Δ_{ik} for all maximal cliques adjacent to the newly combined clique. Repeat until the number of matrices is equal to L. Constrain the resulting set of matrices to be positive semidefinite in the OPF formulation.

This heuristic is next tested using two large system models: the IEEE 300-bus system [68] and a 3012-bus model of the Polish system for evening peak demand in winter 2007-2008 [55]. These systems were chosen to examine how the heuristic scales with system size. Matrix decomposition techniques do not result in a notable speed improvement for small systems; no matrix decomposition significantly reduced the computational time for the IEEE 14, 30, and 57-bus systems [68].

The OPF formulation in (3.21) was implemented using YALMIP version 3 [64], SeDuMi version 1.3 [59], and MATLAB R2011a. One computer with an 64-bit Intel i7-2600 Quad Core CPU at 3.40 GHz with 16 GB of RAM was used to run the formulation. By using the matrix completion decompositions to exploit the inherent sparsity, these computational resources were sufficient for

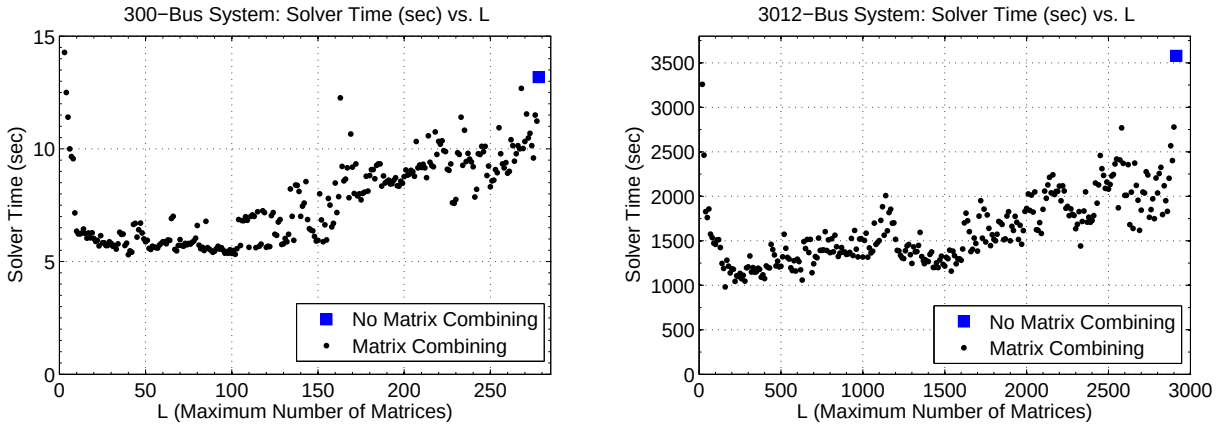

(a) Solver time versus L for the IEEE 300-Bus System

(b) Solver time versus L for the 3012-Bus System

Figure 3.3 Solver Time versus L. For the IEEE 300-bus system, the time with $L = 1$ of 69.5 seconds is not shown on the plot. For the 3012-bus system, the time with $L = 2$ of approximately 1×10^5 seconds is not shown on the plot and the system could not be solved with $L = 1$.

the 300 and 3012-bus system models. A tolerance of 1×10^{-9} for SeDuMi's `eps` was used in the calculation of the results.

Figures 3.3a and 3.3b show variation in total solver time (i.e., the time used by the semidefinite programming solver SeDuMi), with the parameter L. These figures do not include the setup time required to initialize the formulation. The setup time is typically 15% to 20% of the solver time.

The solver times for Jabr's formulation of the maximal clique decomposition are the rightmost points (no matrix combinations) in Figures 3.3a and 3.3b. As L decreases from the rightmost point, the solver times decrease by, at most, approximately a factor of 2.5 for the 300-bus system and a factor of 3.6 for the 3012-bus system as compared to the solver time without combining matrices.

The solution time graphs in Figures 3.3a and 3.3b appear to be "noisy," which is attributable to differences in the number of iterations needed to reach the specified tolerance. That is, solver times can vary among choices of L if the solver requires one additional iteration to reach the desired solution tolerance. Despite this noise, there is a clear trend. The plots show that reducing L results in significant improvements in solver time as compared to the case without matrix combining. However, as L continues to decrease, the speed improvements from removing linking constraints are overcome by the additional variables required for the larger matrices (in the extreme, returning

to a single $2n \times 2n$ matrix for $L = 1$). Thus, the solver times exhibit a steep increase for small L. (Solution times for very small L are not shown on Figures 3.3a and 3.3b. For the 300-bus system, the full $2n \times 2n$ matrix constraint corresponding to $L = 1$ solved in 69.5 seconds. The 3012-bus system could not be solved with $L = 1$; the system required approximately 1.0×10^5 seconds for $L = 2$.)

Rather than combining matrices until below a specified parameter value, an alternative approach combines matrices until no pair of adjacent maximal cliques had a negative value of Δ_{ik} (i.e., stop combining matrices once the heuristic indicated no further advantage to doing so). Numerical experience indicates that this approach typically does not identify a set of matrices that minimizes solver times. The number of matrices for which no remaining adjacent pairs of maximal cliques has negative Δ_{ik} is $L = 150$ for the 300-bus system and $L = 1376$ for the 3012-bus system. In both systems, faster solver times are obtained for smaller values of L. This reinforces the fact that the measure of semidefinite program size (3.27) is a heuristic approximation of the computational burden.

Based on these empirical results, choosing L equal to 10% of the initial number of matrices appears to give near minimum solver times. (Expressing L as a percentage of the original number of matrices allows for easy comparison between systems.) Experience to date indicates that minimum computational time consistently appears at approximately this value of L for the available power system models. However, limited diversity of available large system models precludes more general comments on this value. System models that are strongly interconnected (i.e., have a relatively low amount of sparsity) will inherently have large maximal cliques and will probably not benefit from as many matrix combinations as compared to more sparsely connected system models. A larger value of L is expected to be appropriate for strongly interconnected models.

Note that solution times are not greatly affected by the addition of parallel lines or multiple generators at the same bus; models with these features have comparable computational burden relative to other models with the same total numbers of lines and generators.

Table 3.1 summarizes these results by providing the solver times for each system / decomposition pair along with a "speed up factor" for the improvement of the matrix combination approach

System	$2n \times 2n$	No Combining	Combining ($L = 10\%$)	Speed Up Factor
IEEE 118-bus	6.63	4.84	2.06	2.349
IEEE 300-bus	69.45	13.18	5.71	2.309
Polish 3012-bus	–	3578.5	1197.4	2.989

Table 3.1 Solver Times (seconds) for Various Algorithms

with $L = 10\%$ of the original number of matrices as compared to not combining matrices. Results using the full $2n \times 2n$ matrix for the 3012-bus system could not be computed. Note that solver times with $L = 10\%$ for other models of the Polish system that is represented in the 3012-bus system model are available in Table 3.2. Also note that the proposed heuristic yields improvements for the intermediate-sized IEEE 118-bus system.

Several alternatives to the proposed heuristic were attempted. These included a variant of the proposed algorithm that, at each step, randomly (weighted by Δ_{ik}) selects a pair of maximal cliques to combine; the heuristic proposed in [79]; and a "top-down" approach that groups maximal cliques using a normalized cut algorithm on the clique tree. These alternatives sometimes had comparable but not substantially faster solution times than the proposed heuristic.

3.3.3 Analysis of Relaxation Gap Properties of Solution to OPF Problems for Large System Models

While solutions to many OPF problems satisfy the rank condition and thus have zero relaxation gaps [7], it is known that some small system models yield non-zero relaxation gap solutions [76, 83]. Until the recent exploitation of power system sparsity, computational challenges have precluded investigation of the rank properties of the semidefinite relaxation for large system models. Harnessing the computational methods described in this chapter allows for investigating rank condition satisfaction for large system models. Note that, as in the previous section, the results in this section are calculated with a minimum line resistance of 1×10^{-4} per unit in accordance with [7] and with SeDuMi's tolerance parameter `eps` set to 1×10^{-9}.

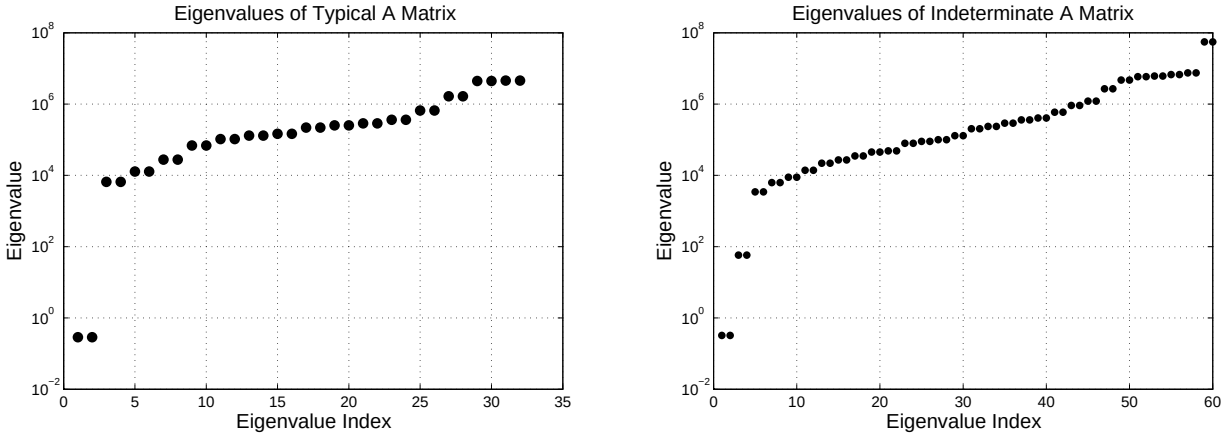

(a) Eigenvalues for a Typical $\mathbf{A}$ Matrix

(b) Eigenvalues for an Indeterminate $\mathbf{A}$ Matrix

Figure 3.4 Eigenvalues for Selected $\mathbf{A}$ Matrices of the Solution to the 3012-Bus System

When using a matrix completion decomposition, solutions to the dual formulation of the semidefinite relaxation consist of a set of $\mathbf{A}$ matrices. For a solution that satisfies the rank condition, the nullspaces of all $\mathbf{A}$ matrices have dimension less than or equal to two. However, for numerical reasons, solvers do not yield a "hard zero" value for the eigenvalues corresponding to the nullspaces of these matrices. Therefore, it can be difficult to determine when an $\mathbf{A}$ matrix has nullspace with dimension two. For illustration of this challenge, Figure 3.4 shows the eigenvalues, sorted in order of ascending magnitude, for selected $\mathbf{A}$ matrices from the $L = 10\%$ decomposition of the Polish 3012-bus system model. With two smallest eigenvalues that are four orders of magnitude below the next smallest eigenvalues, Figure 3.4a shows a typical matrix that has nullspace with dimension two. Conversely, the smallest eigenvalues in Figure 3.4b are only two orders of magnitude below the next smallest eigenvalues; the nullspace dimension for this matrix is more difficult to determine. Characterizing the overall satisfaction of the rank condition for the Polish 3012-bus system is correspondingly difficult.

To evaluate the satisfaction of the rank condition, this section proposes the following metric to measure closeness to a nullspace with dimension two. The metric is based on the ratio between the third and second smallest magnitude eigenvalues. The minimum such ratio among all the $\mathbf{A}$ matrices is termed the "minimum eigenvalue ratio." If the solution did yield "hard zeros" for zero

System Model	Min Eigenvalue Ratio	Max Mismatch	Solver Time ($L = 10\%$)
IEEE 118-bus	2.86×10^{9}	3.9×10^{-5} MVAr	2.1 sec
IEEE 300-bus	2.25×10^{2}	4.7×10^{0} MVAr	5.7 sec
2383-bus (wp)	7.90×10^{2}	2.9×10^{2} MVAr	730 sec
2736-bus (sp)	3.07×10^{4}	2.7×10^{-2} MVAr	622 sec
2737-bus (sop)	4.11×10^{4}	3.7×10^{-1} MVAr	607 sec
2746-bus (wp)	8.65×10^{4}	5.5×10^{-2} MW	752 sec
2746-bus (wop)	1.95×10^{4}	1.4×10^{-1} MW	738 sec
3012-bus (wp)	1.72×10^{2}	4.1×10^{2} MVAr	1197 sec
3120-bus (sp)	5.84×10^{2}	4.6×10^{1} MVAr	1619 sec
3375-bus (wp)	1.64×10^{2}	5.2×10^{2} MVAr	1457 sec

Table 3.2 Measures of Rank Condition Satisfaction and Solver Times for Various System Models

eigenvalues, the second smallest eigenvalue would be zero and the third smallest eigenvalue would be non-zero, resulting in a minimum eigenvalue ratio of infinity. In practice, numerical issues result in minimum eigenvalue ratios that are large (typical values are greater than 1×10^{7} for small systems that are known to satisfy the rank condition). Further, if the solution does not satisfy the rank condition, both the second and third smallest eigenvalues will have similar magnitudes near zero, therefore yielding a small value for the minimum eigenvalue ratio. Thus, a large value for the minimum eigenvalue ratio indicates a solution with zero relaxation gap while a small value indicates a non-zero relaxation gap solution. Note that more sophisticated metrics than the proposed minimum eigenvalue ratio are possible; the proposed metric is intended to be a simple but meaningful measure.

Table 3.2 shows the minimum eigenvalue ratios for several test systems. The solution times with $L = 10\%$ are also given. The systems with more than 300 buses are representations of the Polish grid with various levels of modeling detail and different loading scenarios (winter peak (wp), winter off peak (wop), summer peak (sp), and summer off peak (sop)). These results indicate

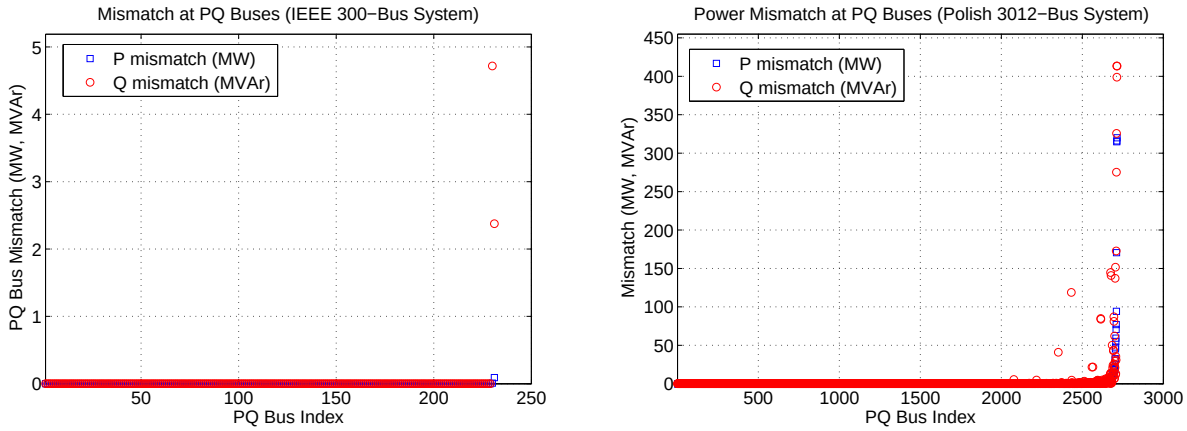

(a) Power Mismatch for IEEE 300-Bus System

(b) Power Mismatch for Polish 3012-Bus System

Figure 3.5 Active and Reactive Power Mismatch at PQ Buses

that, according to the proposed metric, the large system models do not satisfy the rank condition as well as many smaller system models, which generally have minimum eigenvalue ratios greater than 1×10^7 when they satisfy the rank condition. Since, other than the IEEE 118 and 300-bus systems, the large system models all represent the same Polish system, the lack of more diverse system models limits the ability to make more general statements concerning satisfaction of the rank condition for large system models.

An alternative test for satisfaction of the rank condition is based on the mismatch between the calculated and specified active and reactive power injections at PQ buses. Recovering a candidate voltage profile is accomplished by forming the closest rank one matrix to the solution's $\mathbf{W}$ matrix using the eigenvector associated with the largest eigenvalue of $\mathbf{W}$. If the solution has zero relaxation gap, the $\mathbf{W}$ matrix is rank one and the resulting voltage profile will satisfy the power injection equality constraints at the PQ buses. Conversely, the closest rank one matrix to a solution with non-zero relaxation gap will typically not yield a voltage profile that satisfies the power injection equality constraints at PQ buses. Thus, the mismatch between the calculated and specified power injections at PQ buses provides an alternative measure for satisfaction of the rank condition.

Figures 3.5a and 3.5b show the mismatch between the specified and calculated active and reactive power injections at PQ buses for the 300 and 3012-bus systems, respectively, sorted in

order of increasing active power mismatch. The voltage profile yields small mismatches for the majority of buses, but a few buses display large mismatches in both active and reactive power. The large power mismatches indicate non-zero relaxation gap solutions. With small mismatch at the majority of PQ buses, such non-zero relaxation gap solutions may provide good starting points for a local search algorithm. Table 3.2 shows the maximum mismatch, considering both active and reactive powers, for a variety of test systems. Solutions to several of these system models have relatively large power mismatches; for instance, mismatches for all test systems in Table 3.2 except for the IEEE 118-bus and Polish 2736 and 2746 (wp) bus systems are greater than the default Newton solution tolerance of 0.1 MW/MVAr used by the power flow solution package PSS/E [89]. Large power mismatches indicate that the corresponding solutions do not satisfy the rank condition. Note the correlation between the minimum eigenvalue ratio and the maximum power mismatch, which supports the validity of these measures of rank condition satisfaction.

3.3.4 Extending Jabr's Formulation of the Maximal Clique Decomposition

The first step in Jabr's formulation creates a chordal extension of the network using a Cholesky factorization of the absolute value of the imaginary part of the bus admittance matrix (i.e., $\mathrm{chol}\left(\left|\mathrm{Im}\left(\mathbf{Y}\right)\right|\right)$). Only positive definite matrices have Cholesky factorizations. Since not all power system networks have positive definite $\left|\mathrm{Im}\left(\mathbf{Y}\right)\right|$ matrices (e.g., networks with sufficiently large shunt capacitances), Jabr's formulation cannot be universally applied to such networks.

Jabr's formulation only uses the *sparsity pattern* (i.e., location of the non-zero elements) of the Cholesky factorization. Thus, an alternative, positive definite matrix whose Cholesky factorization exhibits the same sparsity pattern would extend Jabr's formulation to general power systems. This section next presents such an alternative matrix.

Let $\mathbf{D}$ represent the incidence matrix associated with the network (i.e., each row of $\mathbf{D}$ corresponds to a line and has two non-zero elements: $+1$ in the column corresponding to the line's "from" bus and -1 in the column corresponding to the line's "to" bus). The matrix $\mathbf{E}$ in (3.28) has a Cholesky factorization with the same sparsity pattern as $\mathrm{chol}\left(\left|\mathrm{Im}\left(\mathbf{Y}\right)\right|\right)$.

$$\mathbf{E} = \mathbf{D}^T\mathbf{D} + \mathbf{I}_{n\times n} \tag{3.28}$$

where $\mathbf{I}_{n\times n}$ is the $n \times n$ identity matrix.

Since $\mathbf{D}^T\mathbf{D}$ has a Laplacian structure, it is positive semidefinite. Adding an identity matrix increases all eigenvalues by one, and thus $\mathbf{E}$ is positive definite. Note that the common modification for making a Laplacian matrix positive definite via adding the matrix $\mathbb{1} \cdot \mathbb{1}^T$, where $\mathbb{1}$ is the vector of all ones, is not appropriate due to the fact that this modification makes the Cholesky factorization of $\mathbf{E}$ dense.

The bus admittance matrix $\mathbf{Y}$ has generalized Laplacian structure with weightings from the line admittances plus diagonal terms corresponding to shunt admittances. The $\mathbf{E}$ matrix's similar construction implies that its Cholesky factorization has the same sparsity pattern as the Cholesky factorization of $|\mathrm{Im}\,(\mathbf{Y})|$. Using the Cholesky factorization of $\mathbf{E}$ therefore extends Jabr's method to general power networks.

3.3.5 Obtaining an Optimal Voltage Profile

The solution to the dual formulation (3.21) of a decomposed problem is a set of positive semidefinite matrices. (A similar procedure is applicable for a solution to the primal formulation (3.16).) If all the matrices have nullspaces with appropriate dimension, the key solution information of practical use, an optimal voltage profile can be recovered [7, 82]. (For formulations that separate real and imaginary voltage components, like (3.21), the nullspace of all matrices must have dimension less than or equal to two.) However, existing literature does not give specific steps for recovering the optimal voltage profile. This section next describes a technique for obtaining the optimal voltage profile.

An overview of this technique follows. First obtain vectors in the nullspaces (hereafter referred to as nullvectors) of each positive semidefinite constrained matrix. Note that calculation of these nullvectors can be carried out in parallel since the nullspace computation for each matrix can be performed independently. These nullvectors, when rearranged such that they correspond to complex "phasor" voltages, can each be multiplied by a different complex scalar and remain in their

respective nullspaces. Since a bus can be in multiple maximal cliques, elements in different vectors may correspond to the same bus voltage phasor. The complex scalars are chosen such that elements of different vectors that correspond to the same bus voltage are equal. A centrally computed linear nullspace calculation of a specified matrix gives an appropriate choice of the scalar values. This allows for specification of a vector that is a scalar multiple of the optimal voltage profile. Using a single binding constraint, the resulting vector is scaled to obtain the optimal voltage profile.

This section next presents the details of this technique. Consider an optimal solution to (3.21) consisting of d positive semidefinite matrices $\bar{\mathbf{A}}_i$ with $\dim\left(\text{null}\left(\bar{\mathbf{A}}_i\right)\right) \leq 2,\ \forall i \in \{1,\ldots,d\}$. Let $u^{(i)}$ be a nullvector of $\bar{\mathbf{A}}_i$. Let r_i be the number of buses in the maximal clique corresponding to matrix i. Convert each vector $u^{(i)}$ to complex "phasor" form: $\underline{u}^{(i)} = u^{(i)}_{1:r_i} + j u^{(i)}_{r_i+1:2r_i}$, where subscript $1:r_i$ indicates the first through r_i^{th} elements of the corresponding vector.

Vectors $\underline{u}^{(i)}$ remain in their corresponding nullspace after multiplication by complex scalars α_i. This property is used to enforce consistency between elements of different vectors that correspond to the same bus voltage phasor. Obtaining the optimal voltage profile requires determining values of α_i that create agreement between all elements representing the same voltage from the nullvectors of different matrices. This can be visualized by forming a table with rows corresponding to bus indices and columns corresponding to maximal clique indices. If maximal clique j contains bus i, the (i,j) entry of the table is α_j multiplied by the element of $\underline{u}^{(j)}$ corresponding to bus i. If maximal clique j does not contain bus i, the (i,j) entry of the table is empty.

Since each row of the table represents a voltage phasor at the corresponding bus, values of $\alpha_i\ \forall i = 1,\ldots,d$ are chosen such that all entries in each row are equal. Appropriate values of α_i are obtained using a nullvector of an appropriately specified matrix. Specifically, use the following procedure to create a matrix $\mathbf{C}$ with d columns that enforces equality of all entries of each row of the table. For each row i of the table, find the first non-empty entry and store the corresponding column index j. (All rows of the table will have at least one non-empty entry because each bus is contained in at least one maximal clique.) While there exists a non-empty entry in row i with column index greater than j (let the non-empty entry exist in column k), add a row to the matrix $\mathbf{C}$

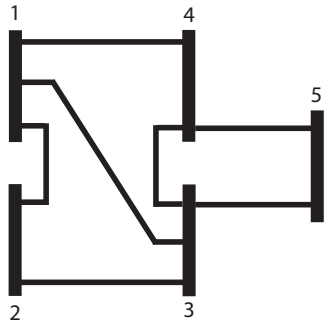

Figure 3.6 Voltage Profile Recovery Example Network

Bus \ Clique Index	1	2	3
1	$\alpha_1 \underline{u}_1^{(1)}$	$\alpha_2 \underline{u}_1^{(2)}$	
2	$\alpha_1 \underline{u}_2^{(1)}$		
3	$\alpha_1 \underline{u}_3^{(1)}$	$\alpha_2 \underline{u}_2^{(2)}$	$\alpha_3 \underline{u}_1^{(3)}$
4		$\alpha_2 \underline{u}_3^{(2)}$	$\alpha_3 \underline{u}_2^{(3)}$
5			$\alpha_5 \underline{u}_3^{(3)}$

Table 3.3 Voltage Profile Recovery Example Table

that enforces equality of the (i, j) and (i, k) entries. Set $j = k$ and repeat until no other non-empty entries exist in row i with column indices greater than j. Then proceed to row $i + 1$.

Consider the illustrative example system network in Figure 3.6 and corresponding Table 3.3. This system has three maximal cliques composed of buses $\{1,\ 2,\ 3\}$, $\{1,\ 3,\ 4\}$, and $\{3,\ 4,\ 5\}$. The corresponding equation for the example is

$$\mathbf{C}\alpha = \begin{bmatrix} \underline{u}_1^{(1)} & -\underline{u}_1^{(2)} & 0 \\ \underline{u}_3^{(1)} & -\underline{u}_2^{(2)} & 0 \\ 0 & \underline{u}_2^{(2)} & -\underline{u}_1^{(3)} \\ 0 & \underline{u}_3^{(2)} & -\underline{u}_2^{(3)} \end{bmatrix} \begin{bmatrix} \alpha_1 \\ \alpha_2 \\ \alpha_3 \end{bmatrix} = \begin{bmatrix} 0 \\ 0 \\ 0 \\ 0 \end{bmatrix} \tag{3.29}$$

The nullspace calculation has a non-trivial solution if all $\bar{\mathbf{A}}_i$ matrices of the solution have nullspaces with dimension less than or equal to two. (For a solution to the semidefinite relaxation where some of the $\bar{\mathbf{A}}$ matrices have nullspace dimension greater than two, the nullspace calculation may only have the trivial solution $\alpha = 0$, indicating that a consistent voltage profile cannot be obtained.) A nullvector α yields a table where all entries of each row have the same value. Create a vector η of length n where η_i is equal to the value of an entry in the i^{th} row of the table. The vector η is a scalar multiple of the optimal voltage vector.

Since α has one degree of freedom in its length, the optimal voltage profile is a scalar multiple χ of η. To determine the value of χ, one additional piece of information is required from a binding constraint. Reference [7] suggests the use of a binding voltage magnitude constraint. However, not all solutions have a binding voltage magnitude constraint (e.g., the three-bus system in [83]). Optimal solutions to OPF problems have at least one binding constraint, but not necessarily a binding voltage magnitude constraint.

A binding constraint is identified by a non-zero value of the corresponding Lagrange multiplier. Consider a solution with a binding voltage magnitude constraint. Let $\bar{V}_k$ be the value of a binding voltage magnitude constraint at bus k. The value of χ is chosen using this voltage magnitude:

$$\chi = \frac{\bar{V}_k}{|\eta_k|} \tag{3.30}$$

For solutions without a binding voltage magnitude constraint, use an alternative binding constraint to determine χ.

The optimal voltage profile is then constructed by scaling η by χ and rotating the resulting vector to obtain zero reference angle.

$$V^{opt} = \chi\eta e^{-j\theta_{ref}} \tag{3.31}$$

where θ_{ref} is the angle of the element of η corresponding to the reference bus.

3.4 A Sufficient Condition for Global Optimality of Solutions to the Optimal Power Flow Problem

The semidefinite relaxation of the OPF problem is computationally limited by a positive semidefinite constraint on a $2n \times 2n$ matrix, where n is the number of buses in the system. Thus, despite being provably polynomial time, the semidefinite relaxation is computationally challenging for large systems. As shown in Section 3.3, matrix completion decompositions speed computation by exploiting power system sparsity. These decompositions make solution of the semidefinite relaxation feasible for large systems.

However, solution of the semidefinite relaxation is still significantly slower than mature OPF algorithms, such as interior point methods [55]. It would be beneficial to pair the computational speed of mature OPF solution algorithms with the global optimality guarantee of the semidefinite relaxation. This section proposes a sufficient condition derived from the Karush-Kuhn-Tucker (KKT) conditions for optimality of the semidefinite relaxation of the OPF problem [93]. A candidate solution obtained from a mature OPF solution algorithm that satisfies the KKT conditions of complementarity and feasibility is guaranteed to be globally optimal. However, satisfaction of these conditions is not necessary for global optimality.

3.4.1 Development of a Sufficient Condition for Global Optimality

A solution to classical formulation of the OPF problem (3.2) consists of vectors of voltage phasors $V = V_d + jV_q$, power injections $P + jQ$, and Lagrange multipliers. Denote the Lagrange multipliers associated with the voltage magnitude equation (3.2d) as ξ, those associated with the apparent-power line-flow equation (3.2e) as ζ, those associated with the active power balance equation (3.2f) as λ, and those associated with the reactive power balance equation (3.2g) as γ.

The sufficient condition for global optimality requires the $\mathbf{W}$ and $\mathbf{A}$ matrices of the primal (3.16) and dual (3.21) forms of the semidefinite relaxation of the OPF problem. As in Section 3.2.2, define the rank one matrix $\mathbf{W} = xx^T$ where $x = \begin{bmatrix} V_{d1} & \cdots & V_{dn} & V_{q1} & \cdots & V_{qn} \end{bmatrix}^T$.

The $\mathbf{A}$ matrix of the dual semidefinite problem requires Lagrange multipliers in terms of the square of voltage magnitudes (denoted as μ) rather than the voltage magnitudes themselves. Use the chain rule of differentiation for the conversion

$$\mu_k = \xi_k \left(\frac{1}{2V_{k_0}} \right) \tag{3.32}$$

where V_{k_0} is the solution's voltage magnitude at bus k. Additionally, the solution to the classical formulation of the OPF problem (3.2) gives line-flow limit Lagrange multipliers ζ in terms of apparent power (MVA), but the dual semidefinite problem requires separate multipliers in terms of active and reactive power flows (denoted as α_k and β_k, respectively, for all lines $k \in \mathcal{L}$ with terminals at buses l and m). Using the relationship

$$S_{k_l} = \sqrt{P_{k_l}^2 + Q_{k_l}^2} \tag{3.33}$$

where P_{k_l} and Q_{k_l} are the active and reactive flows, respectively, on the line k from bus l to bus m, the appropriate conversions are

$$\alpha_{k_l} = \zeta_{k_l} \left(\frac{\partial S_{k_l}}{\partial P_{k_l}} \right) = \zeta_{k_l} \left(\frac{P_{k_l}^{\circ}}{S_{k_l}^{\circ}} \right) \tag{3.34a}$$

$$\beta_{k_l} = \zeta_{k_l} \left(\frac{\partial S_{k_l}}{\partial Q_{k_l}} \right) = \zeta_{k_l} \left(\frac{Q_{k_l}^{\circ}}{S_{k_l}^{\circ}} \right) \tag{3.34b}$$

where $P_{k_l}^{\circ}$ and $Q_{k_l}^{\circ}$ are the solution's flows on line k from bus l to bus m.

The $\mathbf{A}$ matrix is then

$$\mathbf{A} = \sum_{i \in \mathcal{N}} \left\{ \lambda_i \mathbf{Y}_i + \gamma_i \bar{\mathbf{Y}}_i + \mu_i \mathbf{M}_i \right\} + \sum_{k \in \mathcal{L}} \left\{ \alpha_{k_l} \mathbf{Z}_{k_l} + \alpha_{k_m} \mathbf{Z}_{k_m} + \beta_{k_l} \bar{\mathbf{Z}}_{k_l} + \beta_{k_m} \bar{\mathbf{Z}}_{k_m} \right\} \tag{3.35}$$

When feasible, the semidefinite relaxation has a global solution that satisfies the KKT conditions for optimality [93]. A candidate OPF solution may satisfy these KKT conditions, in which case the solution is globally optimal. Using $\mathbf{W} = xx^T$ and $\mathbf{A}$ from (3.35), the first KKT condition of complementarity is

$$\text{trace}\,(\mathbf{AW}) = 0 \tag{3.36}$$

The second regards feasibility of the $\mathbf{W}$ and $\mathbf{A}$ matrices. These matrices are feasible in the semidefinite relaxation if they are positive semidefinite. The matrix $\mathbf{W} = xx^T$ is positive semidefinite by construction. Thus, the relevant feasibility condition is

$$\mathbf{A} \succeq 0 \tag{3.37}$$

3.4.2 Global Optimality Condition Discussion

Satisfaction of both (3.36) and (3.37) implies global optimality regardless of the rank characteristics of the $\mathbf{A}$ matrix (i.e., $\dim(\mathrm{null}(\mathbf{A})) \leq 2$ is not required). Non-zero branch resistances, as necessary in [7], are not required. However, enforcing small minimum branch resistances may result in satisfaction of (3.36) and (3.37) for problems that would not otherwise satisfy these conditions.

If either (3.36) or (3.37) is not satisfied, global optimality is indeterminate. Failure to satisfy these conditions may result when the semidefinite relaxation does not satisfy the rank condition [76, 83], in which case the solution may still be globally optimal but is not guaranteed to be so. Alternatively, failure to satisfy (3.36) and (3.37) may indicate that a better solution exists.

When applied to the IEEE test systems [68] without minimum resistances, global optimality of solutions from MATPOWER's interior point algorithm [55] was verified for the 14, 30, and 57-bus systems, but not for the 118 and 300-bus systems due to non-satisfaction of the feasibility condition (3.37). With a minimum branch resistance of 1×10^{-4} per unit, the solution to the 118-bus system (but not the 300-bus system) was verified to be globally optimal. Note that tight solution tolerances are often needed to obtain satisfactory numerical results.

The most challenging aspect of implementing the proposed condition for global optimality regards evaluation of the feasibility condition (3.37). This condition holds if and only if the algebraically smallest eigenvalue of $\mathbf{A}$ is non-negative. Calculating eigenvalues of large matrices can be computationally difficult, particularly for poorly conditioned matrices. Since the $\mathbf{A}$ matrices for solutions to some large OPF problems are poorly conditioned (e.g., the $\mathbf{A}$ matrix for a global solution to the Polish 2736-bus system has a smallest eigenvalue equal to zero and a largest eigenvalue equal to 1.57×10^8), an alternative to calculating the smallest eigenvalue is beneficial.

Rather than calculate the smallest eigenvalue of $\mathbf{A}$, attempt to form a Cholesky decomposition of the matrix $\mathbf{A} + \epsilon\mathbf{I}$ for some small positive scalar ϵ. A matrix has a Cholesky decomposition if and only if the matrix is positive definite. Adding $\epsilon\mathbf{I}$ increases all eigenvalues by ϵ, thus ensuring that a Cholesky decomposition exists if $\mathbf{A}$ is positive semidefinite. If a Cholesky decomposition exists for $\mathbf{A} + \epsilon\mathbf{I}$, the $\mathbf{A}$ matrix is positive semidefinite to within a tolerance of ϵ. Performing a Cholesky decomposition is computationally efficient for matrices permuted with a minimum degree ordering [100].

As an example of the computational benefits of the global optimality condition, solving the Polish 2736-bus system with minimum branch resistances of 1×10^{-4} using MATPOWER [55] to a tolerance of 1×10^{-10} took 3.4 seconds and verifying global optimality using a Cholesky decomposition took 6.8 seconds. Thus, the total time to find and verify a globally optimal solution to this OPF problem is only 1.6% of the 622 seconds required solve the semidefinite relaxation.

3.5 Conclusion

This chapter has addressed two categories of practical issues associated with implementing a large-scale optimal power flow solver based on semidefinite programming: modeling issues associated with realistic power systems and methods for improving computational efficiency. Specific modeling issues addressed include multiple generators at the same bus, limiting flows on parallel lines, and incorporating ZIP loads in the semidefinite relaxation of the OPF problem. Multiple generators at the same bus are incorporated in the proposed formulation by analogy with the "equal marginal cost" criterion of the economic dispatch problem. Both convex quadratic and convex piecewise-linear generator cost functions are considered. Parallel lines, including lines with off-nominal voltage ratios and non-zero phase shifts, are incorporated in the model using a "line-by-line" approach rather than existing "point-to-point" approaches such that the flows on each line can be individually limited. An approximate representation of ZIP loads in the semidefinite relaxation is introduced and analyzed for worst case error.

This chapter next provided three computational advances for exploiting power system sparsity using matrix completion decompositions. First, a proposed matrix combination algorithm considers the impact of "linking constraints" between elements in certain decomposed matrices that refer to the same element in the original $2n \times 2n$ matrix. Since combining matrices eliminates linking constraints, matrix combination can reduce computation time. Calculations using test systems demonstrate the efficacy of the matrix combination approach: the IEEE 300-bus system shows a factor of approximately 2.3 decrease in solver time and a 3012-bus model of the Polish system shows a factor of 3.0 decrease in solver time compared to not combining matrices. The rank characteristics of solutions to OPF problems for large system models were also examined.

Next, Jabr's formulation of the maximal clique decomposition [82] was extended to general power system networks. This formulation uses a Cholesky factorization of the absolute value of the imaginary part of the bus admittance matrix. Since a Cholesky factorization requires a positive definite matrix, this approach cannot be used for some networks (e.g., networks with large shunt capacitive compensation). Jabr's formulation only uses the sparsity pattern of the Cholesky factorization. This chapter proposes an alternative positive definite matrix with the same sparsity pattern to extend Jabr's formulation to general power system networks.

Another computational advance is a method for constructing an optimal voltage profile from a solution consisting of decomposed matrices. Although existing literature discusses the use of matrix decompositions [71, 81, 82], it does not give a detailed method for obtaining an optimal voltage profile.

Finally, using the KKT conditions of a semidefinite relaxation of the OPF problem, this chapter has proposed a sufficient condition test for global optimality of a candidate OPF solution. This pairs an advantage of the semidefinite relaxation with the speed of mature OPF solvers.

Chapter 4

A Sufficient Condition for Power Flow Insolvability with Applications to Voltage Stability Margins

4.1 Introduction

The previous chapter focused on solving the optimal power flow problem to find the least-cost operating point for a power system. This chapter considers the problem of assessing power system operation in terms of security margins. To this end, this chapter again examines the power flow equations but now solutions are measured using the distance to truly insolvable conditions.

The non-linear power flow equations may not have any solutions (the power flow equations are said to be insolvable). That is, it is possible to choose a set of power injections for which no valid corresponding voltage profile exists. Practical cases that may fail to have a solution include long-range planning studies in which the studied system may not be able to support projected loads and contingency studies for which the loss of one or more components may yield a network configuration that is similarly inoperable for the specified injections. This chapter presents a practically computable sufficient condition, that, when satisfied, rigorously classifies a specified case as insolvable. This method also provides controlled voltage and power injection margins that characterize a distance to the power flow solvability boundary.

In engineering practice, large-scale non-linear power flow equations are typically solved using iterative numerical techniques, most commonly Newton-Raphson or its variants [9]. These rely on an initial guess of the solution voltage magnitudes and angles and are only locally convergent. They generally do not converge to a particular solution from an arbitrary initial guess [11], and may show very high sensitivity and highly complex behavior with respect to initial conditions

for certain study cases. It is well recognized that the power flow equations may generally have a very large number of solutions; for example, the work of [35] establishes cases for which the number of solutions grows faster than polynomial with respect to network size. For cases having multiple solutions, each solution has a set of initial conditions that converges to that solution in Newton-Raphson iteration. Characterization of Newton-Raphson regions of attraction was the subject of [41], which demonstrated cases for which the boundaries of these attractive sets were factual in nature. So despite the fact that very large-scale problems (10's or 100's of thousands of unknowns) are solved in power engineering practice, the behavior of these equations can be highly complex as parameters move outside of routine operating ranges. Convergence failure for a Newton-Raphson-based commercial software package is far from a reliable indication that no solution exists.

The properties of the Newton-Raphson iteration guarantee (under suitable differentiability assumptions) that the iteration must converge to the solution for an initial condition selected in a sufficiently small neighborhood about that solution [12]. However, when a selected initial condition (or some set of multiple initial conditions) fails to yield convergence, the user of a Newton-Raphson-based software package is left with an indeterminate outcome: does the specified problem have no solution, or has the initial condition(s) simply failed to fall within the attractive set of a solution that does exist?

Development of conditions that guarantee existence of solutions to the power flow equations has been an active topic of study. See Section 1.2 for a review of relevant literature on conditions for power flow solution existence. Note that existing conditions often rely on methods that are only locally convergent, are overly conservative (i.e., a solution may exist for a much larger range of operating points than satisfy the sufficient conditions), or use approximations of the power flow equations (e.g., the decoupled active power-voltage angle, reactive power-voltage magnitude power flow model).

Another active research topic is developing measures of the distance to the solvability boundary (the set of operating points where a solution exists, but small perturbations may result in power flow insolvability [18]). Such measures are desirable in order to ensure that power systems are operated

with security margins. If a solution does not exist for a specified set of power injections, a measure of the distance to the solvability boundary indicates how close the power flow equations are to having a solution. If a power flow solution exists, desired margins indicate distances to solution non-existence at the solvability boundary. See Section 1.2 for a review of existing work in this area. Note that existing work has the limitation of exclusively relying on methods that are only guaranteed to find locally optimal measures of the distance to the power flow solvability boundary.

This chapter presents a sufficient condition under which the power flow equations are guaranteed to be insolvable. By-products of the computation are controlled voltage and power injection margins to the power flow solvability boundary. In contrast to existing techniques that are almost universally Newton-based, local solution methods, the semidefinite program in the method proposed here yields a global solution to the optimization problem that is formulated from the originally specified power flow. This global optimum enables the guarantee of solution non-existence upon satisfaction of a sufficient condition. No such guarantee can be made with existing Newton-based methods whose conditions for convergence are inherently local in nature. Furthermore, rather than requiring repeated power flow calculations, the proposed method uses a single evaluation of a semidefinite optimization problem.

The sufficient condition for power flow insolvability is based on an optimization problem that includes a relaxation of certain equality constraints in the power flow equations. Specifically, in this optimization problem, the voltages at slack and PV buses are not fixed, but instead have a one-dimensional degree of freedom (i.e., they are allowed to change in constant proportion). Section 4.2 provides a proof showing that the extra degree of freedom guarantees that the modified power flow equations have at least one solution. In an idealized lossless case, one may interpret this as follows: a sufficiently high voltage profile allows the system to meet any specified power injections. By continuity from the lossless case, this property may be expected to continue to hold for modest losses, as is typical of models for bulk transmission. With the relaxed problem feasible for some (sufficiently high) voltage profile, the feasible set of the optimization problem is non-empty.

With a non-empty feasible set established, the optimization problem then seeks to minimize the slack bus voltage magnitude (using the one-degree-of-freedom in the voltage profile), subject to the active and reactive power injection constraints of the power flow equations. Importantly, a relaxed version of this optimization problem is a convex semidefinite programming problem, and hence has a practically computable global minimum. If the global minimum slack bus voltage obtained from this optimization problem is greater than the originally specified slack bus voltage, there can be no solution to the originally specified power flow equations. However, due to the nature of the relaxation, one may not draw a firm conclusion from the converse: if the minimum slack bus voltage is less than or equal to the specified slack bus voltage, the power flow equations may or may not be solvable.

The ratio of the specified slack bus voltage to the minimum slack bus voltage gives a "controlled voltage margin" to the power flow solvability boundary. For a provably insolvable case, this margin is the multiplicative factor by which the controlled voltages must be increased to allow for the possibility of power flow solution existence.

The power flow equations are quadratic in the complex voltage vector when these voltages are expressed in rectangular form. Exploiting this fact, an analogous power injection margin can also be calculated; here the new, one degree of freedom introduced represents a constant power factor scaling in injections at each bus in proportion to the specified injections. When the power flow equations do not have a solution, the power injection margin provides the scaling factor by which the power injections must be decreased to admit the possibility of power flow solution existence.

These margins are non-conservative bounds. Thus, for an insolvable set of specified values, a change in voltage by *at least* the amount indicated by the voltage margin (or a change in power injections by at least the amount indicated by the power injection margin) is required for the power flow equations to be *potentially* solvable. More precisely, the margin identifies the shortest distance (as measured in voltage setpoint changes for the controlled voltage margin and power injection changes for the power injection margin) to a point at which the sufficient condition for power flow insolvability fails to be satisfied; equivalently, this is the smallest distance to a point at which the associated necessary condition for power flow solvability is first satisfied.

A relaxation of the optimization problem used in the sufficient condition is written as a semidefinite program. In contrast to the original non-convex optimization problem [49], the feasible space of the semidefinite program is convex. The optimal objective value obtained from the semidefinite program is a lower bound on the objective function value. Thus, if the sufficient condition holds based on the lower bound from the semidefinite program, one can be assured that the originally formulated power flow equations admit no solution.

Note that generator reactive power limits are not considered in this chapter; generators are modeled as ideal voltage sources with no limits on reactive power output. Generator limits are relevant to power flow solvability since non-existence of power flow solutions may result from limit-induced bifurcations [30, 31]. Development of methods that consider reactive power limits is discussed in Chapter 5.

The organization of this chapter is as follows. Section 4.2 provides the existence proof that shows the feasibility of the optimization problem used by the proposed condition. Section 4.3 describes the sufficient condition for power flow insolvability and defines voltage and power injection margins. Numeric examples are then provided in Section 4.4. Research detailed in this chapter is published as [101] with extended version available in [102].

4.2 Solution Existence Proof

The sufficient condition for power flow insolvability requires the evaluation of an optimization problem in which the feasible set is defined by a modified form of the power flow equations. The modification introduces one new degree of freedom, allowing voltage magnitudes at the slack and PV buses to vary; this variation is restricted to a one-degree-of-freedom "ray," with all voltage magnitudes changing in constant proportion to their base-case values. This section proves that the feasible space is non-empty for any lossless power system (i.e., all line conductances are zero) without generator reactive power limits. Using standard results of basic circuit theory and continuity, the problem must retain a non-empty feasible set when perturbed with sufficiently small line conductances. Note that modest line conductance values are typical in bulk transmission (i.e., low active power losses in high-voltage transmission lines).

The proof of solution existence may be outlined as follows. The proof first establish that a solution must exist for any lossless system with zero power injections without generator reactive power limits. The implicit function theorem is then used to establish that solutions continue to exist for injections within small ball around zero. Hence, within this ball must exist a ray that aligns with the originally specified vector of non-zero power injections. Exploiting the quadratic nature of the power flow equations allows for "scaling up" voltage magnitudes along the one degree of freedom, observing that the power injections must likewise move along the previously identified ray. It follows that there exists a scaling of voltages such that the specified power injections are realized, yielding a solution to the modified power flow equations.

4.2.1 Existence of a Zero Power Injection Solution

Consider a generic lossless power system with all active and reactive power injections at PQ buses set to zero and all active power injections at PV buses set to zero. As the goal is accomplished upon establishing existence of one solution, restrict attention to candidate solutions in which all buses have the same voltage angle of zero.

First, since zero power injection at a PQ bus implies zero nodal current injection, such buses have only branch admittances incident (i.e., from a circuit perspective, these are nodes with no independent source connected). They can be eliminated from the network, and the network admittance matrix algebraically reduced via standard results of linear circuit theory. The proof generically assumes that the reduced network does not result in any zero impedance lines. (Such a zero impedance line outcome can be eliminated by an arbitrarily small perturbation to the underlying line parameter data.)

Next, the substitution theorem [8] guarantees that at any PV bus that has an associated non-zero reactive power injection, there must exist a shunt admittance of appropriate value such that, when substituted in place of the reactive injection, an identical solution for bus voltages is preserved. The injections replaced are purely reactive, ensuring that the associated admittances will be purely imaginary; i.e., susceptances only.

With PQ buses eliminated and reactive injections at PV buses replaced by equivalent susceptances, the resulting network has the property that active and reactive power injections at all non-slack buses are identically zero. The remaining network constraints of interest can be written as linear voltage/current relationships:

$$\left[\begin{array}{c} I_{\text{slack}} \\ \hline \mathbf{0} \end{array}\right] = \left[\begin{array}{c|c} jb_1 & jb_2 \\ \hline jb_2^T & j\mathbf{B}_3 + j\text{diag}\left(\Delta d\right) \end{array}\right] \left[\begin{array}{c} V_{\text{slack}} \\ \hline V_{\text{PV}} \end{array}\right] \tag{4.1}$$

where Δd is a vector of shunt element susceptances, $\text{diag}\left(\Delta d\right)$ denotes the diagonal matrix with elements of Δd on the diagonal, $\mathbf{B} = \left[\begin{array}{c|c} b_1 & b_2 \\ \hline b_2^T & \mathbf{B}_3 \end{array}\right]$ is the bus susceptance matrix, and superscript T indicates the transpose operator. V_{slack} and I_{slack} are the voltage and current injection at the slack bus, respectively, and V_{PV} is the vector of PV bus voltages. Note that the lossless assumption implies that the network admittance matrix is purely imaginary.

Solving (4.1) for Δd yields

$$\Delta d = \left(\text{diag}\left(V_{\text{PV}}\right)\right)^{-1}\left(-b_2 V_{\text{slack}} - \mathbf{B}_3 V_{\text{PV}}\right) \tag{4.2}$$

Because the desired voltage profile solution has the same voltage angle at all buses and a non-zero voltage magnitude at the slack bus, it follows that the voltage at every bus must be non-zero and $\text{diag}\left(V_{\text{PV}}\right)$ is invertible. Hence, for a lossless system under the assumptions specified, (4.2) yields a unique solution for the shunt susceptance values whose existence follows from the substitution theorem.

Thus, the vector $\left[\begin{array}{c} V_{\text{slack}} \\ \hline V_{\text{PV}} \end{array}\right]$ provides a zero power injection solution to the reduced network that resulted from elimination of PQ buses; voltages at PQ buses can be trivially reconstructed. Thus, any lossless system is guaranteed to have a zero power injection solution.

To illustrate that this need not be the case for systems with large conductive elements in their bus admittance matrix (i.e., high transmission losses), consider the two-bus system with a slack bus and a PV bus shown in Figure 4.1. The transmission line admittance is $g + jb$; note that in this

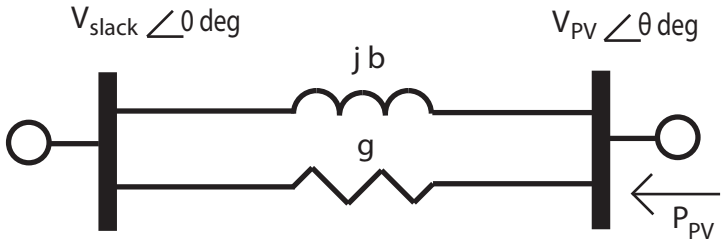

Figure 4.1 Two-Bus System

admittance representation, the conductive term g and the susceptance term jb appear as parallel branch elements between the two buses. The voltage at the slack bus is denoted by V_{slack}, and the voltage at the PV bus is represented by V_{PV} with angle θ.

The power injection at the PV bus is

$$P_{PV} = gV_{PV}^2 - V_{PV}V_{slack}\left(g\cos\left(\theta\right) + b\sin\left(\theta\right)\right) \tag{4.3}$$

The two-bus system has a zero power injection solution for a given set of parameters g, b, V_{PV}, and V_{slack} if a value of θ_0 exists such that $P_{PV}\left(\theta_0\right) = 0$. The existence of such a value of θ_0 depends on the ratio of V_{PV} to V_{slack} and the ratio of b to g. A zero power injection solution to this system exists when line resistances are small relative to line reactances and voltage magnitude differences are small; specifically, for the system in Figure 4.1

$$\left(\frac{V_{PV}}{V_{slack}}\right)^2 \leq 1 + \left(\frac{b}{g}\right)^2 \tag{4.4}$$

Since voltage magnitudes differences and line resistance to reactance ratios are small in realistic power systems, typical systems are expected to have zero power injection solutions. Consistent with this observation, all the IEEE power flow test cases [68] have zero power injection solutions. However, (4.4) confirms that the two-bus example will fail to have a zero injection solution when the conductance values relative to the susceptances are sufficiently large.

4.2.2 Implicit Function Theorem

The implicit function theorem [103] is next applied at a zero power injection solution, which requires a non-singular power flow Jacobian. This proof therefore investigates the Jacobian evaluated at a zero power injection solution.

The power flow Jacobian obtained using polar voltage coordinates at a zero power injection solution of a lossless system is

$$\mathbf{J} = \begin{bmatrix} \mathbf{J}_{11} & \mathbf{0} \\ \mathbf{0} & \mathbf{J}_{22} \end{bmatrix} \tag{4.5a}$$

where

$$\mathbf{J}_{11} = \frac{\partial P}{\partial \delta} = -\mathrm{diag}\left(V\right)\left(\mathbf{B}\,\mathrm{diag}\left(V\right) - \mathrm{diag}\left(\mathbf{B}V\right)\right) \tag{4.5b}$$

$$\mathbf{J}_{22} = \frac{\partial Q}{\partial V} = -\mathrm{diag}\left(V\right)\mathbf{B} - \mathrm{diag}\left(\mathbf{B}V\right) \tag{4.5c}$$

Since active and reactive power injections at the slack bus are unconstrained, the rows and columns corresponding to the slack bus are removed from both $\mathbf{J}_{11}$ and $\mathbf{J}_{22}$. Similarly, since the reactive power injections at PV buses are unconstrained, the rows and columns corresponding to PV buses are removed from $\mathbf{J}_{22}$. Note that both $\frac{\partial P}{\partial V}$ and $\frac{\partial Q}{\partial \delta}$ equal zero for the voltage profile with the same voltage angle at all buses corresponding to a zero power injection solution of a lossless system.

The implicit function theorem can be applied at a zero power injection solution so long as the power flow Jacobian at this solution is non-singular. In the lossless case, this requires that $\mathbf{J}$ in (4.5) is non-singular. This proof next shows that the Jacobian for a lossless power system is non-singular at a zero power injection solution, provided that all lines are inductive and that the network is connected (i.e., no islands).

The matrix $\mathbf{J}$ in (4.5) is non-singular if both $\mathbf{J}_{11}$ and $\mathbf{J}_{22}$ are non-singular. The matrix $\mathrm{diag}\left(\mathbf{B}V\right)$ in $\mathbf{J}_{22}$ is equivalent to $\mathrm{diag}\left(I\right)$, where I is the vector of current injections. Since all rows and columns in $\mathbf{J}_{22}$ correspond to PQ buses with zero current injections, this term is zero. The matrix $\mathrm{diag}\left(V\right)$ is non-singular since all voltages are non-zero for the voltage profile with the same

voltage angle at all buses. With the slack bus row and column removed, $\mathbf{B}$ is non-singular for a connected power system with inductive lines. Thus, $\mathbf{J}_{22}$ is non-singular.

Since $\operatorname{diag}(V)$ is non-singular, $\mathbf{J}_{11}$ is non-singular if

$$(\mathbf{B}\operatorname{diag}(V) - \operatorname{diag}(\mathbf{B}V)) = \begin{bmatrix} \mathbf{B}_{12}V_2 + \ldots + \mathbf{B}_{1n}V_n & \cdots & -\mathbf{B}_{1n}V_n \\ \vdots & \ddots & \vdots \\ -\mathbf{B}_{n1}V_1 & \cdots & \mathbf{B}_{n1}V_1 + \ldots + \mathbf{B}_{n(n-1)}V_{(n-1)} \end{bmatrix} \tag{4.6}$$

is non-singular. Note that the diagonal elements in (4.6) are the negative of the sum of the off-diagonal elements in the corresponding row. Under the assumption of inductive lines, all off-diagonal elements are negative, and this matrix has weak diagonal dominance. With the slack bus row and column removed, the remaining matrix has at least one row where the diagonal element is strictly greater than the sum of the off-diagonal elements (i.e., strict diagonal dominance exists for this row). Since the power system network is connected (i.e., no islands), the digraph associated with the matrix in (4.6) is strongly connected. This implies that the matrix is irreducible [104]. Since the matrix is irreducible, weakly diagonally dominant, and has at least one row with strict diagonal dominance, the matrix is irreducibly diagonally dominant. The Levy–Desplanques theorem then establishes that $\mathbf{J}_{11}$ is non-singular [104]. Thus, the Jacobian for a connected, lossless system at a zero power injection solution is invertible, under the assumption of inductive lines.

Although the assumptions of lossless systems and inductive lines are required for the above proof, non-singularity of the Jacobian at a zero power injection solution generically holds for more general systems (e.g., lossless systems with some capacitive lines and lossy systems). A singular Jacobian would imply marginal stability at the zero power injection solution with multiple solutions coalescing at a bifurcation point. There is no reason to expect this to occur at a zero power injection solution. Computational experience shows that all IEEE power flow test cases [68] have non-singular Jacobians at their zero power injection solution points.

If the Jacobian of the power flow equations is non-singular at the zero power injection solution, the implicit function theorem indicates that a solution must persist for all power injections in a

small ball around the zero power injection. Thus, there exists some voltage magnitude and angle perturbation $\Delta V \angle \Delta\delta$ such that

$$f\left(V + \Delta V \angle \Delta\delta\right) = \Delta P + j\Delta Q \tag{4.7}$$

for any small ΔP and ΔQ, where V is the voltage profile for the zero power injection solution, ΔP and ΔQ are small perturbations to the active and reactive power injections, and f represents the power flow equations relating the voltages and power injections.

4.2.3 Scaling Up Voltages

The solution existence proof is completed by expanding the small ball around the zero power injection solution to obtain a voltage profile that yields the originally specified power injections. Since the power flow equations are quadratic in voltage magnitudes V, scaling all voltage magnitudes also scales the power injections. That is, scaling the voltage magnitudes in (4.7) by the scalar β gives

$$f\left(\beta\left(V + \Delta V \angle \Delta\delta\right)\right) = \beta^2\left(\Delta P + j\Delta Q\right) \tag{4.8}$$

Choose a $\Delta P + j\Delta Q$ that is in the direction of the specified power injections and obtain a corresponding voltage profile $V + \Delta V \angle \Delta\delta$. Then increase β until the power injections given by $f\left(\beta\left(V + \Delta V \angle \Delta\delta\right)\right)$ match the specified power injections. The voltage profile $\beta\left(V + \Delta V \angle \Delta\delta\right)$ then yields the specified power injections.

4.3 Sufficient Condition for Power Flow Insolvability

The proof in Section 4.2 shows that there exists a voltage profile satisfying the power injection equations. Next, this section develops a sufficient condition for power flow insolvability by determining whether any such voltage profile could match the specified slack bus and PV bus voltages. No solution exists if it is impossible to obtain a voltage profile that yields the specified power injections while also matching the specified voltage magnitudes at slack and PV buses. After developing this insolvability condition, this section further describes two margins to the power flow solvability boundary in terms of controlled voltages and power injections.

4.3.1 Condition Description

This section first describes a sufficient condition for power flow insolvability. This condition determines whether any voltage profile that satisfies the power injection equations could also match the specified controlled voltage magnitudes. One way to determine if such a valid voltage profile exists is to find the voltage profile with the lowest possible slack bus voltage. If the minimum possible slack bus voltage is greater than the specified slack bus voltage, no voltage profile will satisfy the power flow equations and thus the power flow equations are insolvable. This condition indicates that no power flow solution exists when the minimum slack bus voltage obtainable while satisfying the power injection equations (with PV bus voltage magnitudes scaled proportionally) is greater than the specified slack bus voltage magnitude. An optimization problem with objective function minimizing the slack bus voltage and constraints on power injections and PV bus voltage magnitudes, as shown in (4.9), is used to evaluate this condition.

$$\min_{V,\,\delta} \quad V_{slack} \qquad \text{subject to} \tag{4.9a}$$

$$V_k \sum_{i=1}^{n} V_i \left(\mathbf{G}_{ik} \cos\left(\delta_k - \delta_i\right) + \mathbf{B}_{ik} \sin\left(\delta_k - \delta_i\right)\right) = P_k \qquad \forall\, k \in \{\mathcal{PQ},\, \mathcal{PV}\} \tag{4.9b}$$

$$V_k \sum_{i=1}^{n} V_i \left(\mathbf{G}_{ik} \sin\left(\delta_k - \delta_i\right) - \mathbf{B}_{ik} \cos\left(\delta_k - \delta_i\right)\right) = Q_k \qquad \forall\, k \in \mathcal{PQ} \tag{4.9c}$$

$$V_k = \alpha_k V_{\text{slack}} \qquad \forall\, k \in \mathcal{PV} \tag{4.9d}$$

where $\mathcal{PQ}$ is the set of PQ buses, $\mathcal{PV}$ is the set of PV buses, and V_{slack} is the slack bus voltage magnitude. α_k represents the specified ratio of the PV bus k and slack bus voltage magnitudes. The minimum achievable slack bus voltage (i.e., the optimal objective value of (4.9)) is denoted as V_{slack}^{min}.

The optimization problem (4.9) is in general non-convex [49], and hence solution for a global optimum is not assured. A global minimum is required in order to ensure the validity of the sufficient condition for power flow solution non-existence. A semidefinite relaxation is used to provide a lower bound on the global minimum of (4.9). Solution algorithms assure finding a

global solution to the semidefinite formulation. The primal form of the semidefinite relaxation of (4.9) is

$$\min_{\mathbf{W}} \quad \operatorname{trace}\left(\mathbf{M}_{\text{slack}}\mathbf{W}\right) \qquad \text{subject to} \tag{4.10a}$$

$$\operatorname{trace}\left(\mathbf{Y}_k\mathbf{W}\right) = P_k \qquad \forall\, k \in \{\mathcal{PQ},\, \mathcal{PV}\} \tag{4.10b}$$

$$\operatorname{trace}\left(\bar{\mathbf{Y}}_k\mathbf{W}\right) = Q_k \qquad \forall\, k \in \mathcal{PQ} \tag{4.10c}$$

$$\operatorname{trace}\left(\mathbf{M}_k\mathbf{W}\right) = \alpha_k^2 \operatorname{trace}\left(\mathbf{M}_{\text{slack}}\mathbf{W}\right) \qquad \forall\, k \in \mathcal{PV} \tag{4.10d}$$

$$\mathbf{W} \succeq 0 \tag{4.10e}$$

The symbol $\succeq$ indicates that the corresponding matrix is constrained to be positive semidefinite. Matrices employed in (4.10) are defined in Chapter 2. As a relaxation of a feasible optimization problem, the primal formulation of (4.10) is also feasible.

The dual form of the semidefinite relaxation is

$$\max_{\lambda,\,\gamma,\,\mu} \quad \sum_{k\in\{\mathcal{PQ},\,\mathcal{PV}\}} \left(\lambda_k P_k\right) + \sum_{k\in\mathcal{PQ}} \left(\gamma_k Q_k\right) \qquad \text{subject to} \tag{4.11a}$$

$$\mathbf{A}\left(\lambda,\gamma,\mu\right) = \left[\mathbf{M}_{\text{slack}} - \sum_{k\in\mathcal{PQ}} \left(\lambda_k\mathbf{Y}_k + \gamma_k\bar{\mathbf{Y}}_k\right) - \sum_{k\in\mathcal{PV}} \left(\lambda_k\mathbf{Y}_k + \mu_k\left(\mathbf{M}_k - \alpha_k^2\mathbf{M}_{\text{slack}}\right)\right)\right] \succeq 0 \tag{4.11b}$$

where free variables λ_k, γ_k, and μ_k are the Lagrange multipliers for active power (4.9b), reactive power (4.9c), and PV bus voltage magnitude ratio (4.9d) equality constraints, respectively, associated with bus k. The dual formulation (4.11) is always feasible since the point $\lambda_i = 0$, $\gamma_i = 0$, $\mu_i = 0$ for all i implies $\mathbf{A} = \mathbf{M}_{slack} \succeq 0$.

The semidefinite relaxation provides a lower bound on the minimum slack bus voltage in (4.9). The maximum lower bound on the minimum achievable slack bus voltage (i.e., the square root of the optimal objective values of (4.10) and (4.11)) is denoted as $\underline{V}_{slack}^{min}$.

No solution to the power flow equations exists if the lower bound from the semidefinite relaxation is greater than the specified slack bus voltage. That is,

$$\underline{V}_{slack}^{min} > V_0 \tag{4.12}$$

where V_0 is the specified slack bus voltage, is a sufficient but not necessary condition for insolvability of the power flow equations. Note that this formulation does not enforce any requirements on the rank of the $\mathbf{W}$ or $\mathbf{A}$ matrices in (4.10) and (4.11); the solution to the semidefinite relaxation is only used as a lower bound on (4.9).

The converse condition does not necessarily hold: the power flow equations may not have a solution even if

$$\underline{V}_{slack}^{min} \leq V_0 \tag{4.13}$$

Thus, (4.13) is a necessary, but not sufficient, condition for power flow solvability. However, satisfaction of (4.13) is expected to often predict the existence of a power flow solution.

If the $\mathbf{W}$ matrix in (4.10) has rank less than two or the corresponding $\mathbf{A}$ matrix in (4.11) has a nullspace with dimension less than or equal to two, a solution with slack bus voltage equal to $\underline{V}_{slack}^{min}$ (and PV bus voltage magnitudes scaled proportionally) can be obtained (see Section 3.3.5 for further details). If a solution with slack bus voltage equal to V_0 does not exist, the solution with lower slack bus voltage must disappear as the controlled voltages increase. The disappearance of a solution due to increasing controlled voltages does not typically occur. Thus, satisfaction of (4.13) by a solution to (4.10) with $\mathrm{rank}\,(\mathbf{W}) \leq 2$ or a solution to (4.11) with $\dim\,(\mathrm{null}\,(\mathbf{A})) \leq 2$ strongly suggests solution existence.

Note that the insolvability condition as formulated above does not consider systems with generator reactive power limits; generators are modeled as ideal voltage sources with no limits on reactive power output. However, more detailed generator models often include reactive power limits. When a generator reaches its upper reactive power limit, the voltage magnitude at the corresponding bus may decrease. (Upper limits on generator reactive power injections are the typical mechanisms of limit-induced bifurcations.) A modified form of the optimization problem (4.9)

bounds the effect of upper limits on generator reactive power injections. Specifically, change constraint (4.9d) from an equality to an inequality by enforcing

$$V_k \leq \alpha_k V_{\text{slack}} \qquad \forall\, k \in \mathcal{PV} \tag{4.14}$$

instead of (4.9d). This modification accommodates the possibility of reduced voltages, thus considering upper generator reactive power limits in the insolvability condition. The accompanying semidefinite relaxation of this modified problem is formed by changing the constraint (4.10d) to

$$\text{trace}\,(\mathbf{M}_k \mathbf{W}) \leq \alpha_k^2\ \text{trace}\,(\mathbf{M}_{\text{slack}} \mathbf{W}) \qquad \forall\, k \in \mathcal{PV} \tag{4.15a}$$

The corresponding change to the dual form (4.11) is to add the constraint

$$\mu_k \leq 0 \qquad \forall\, k \in \mathcal{PV} \tag{4.15b}$$

Satisfaction of the condition (4.12) using the minimum slack bus voltage obtained from this modified optimization problem is sufficient to guarantee power flow insolvability with upper limits on generator reactive power injections. Note that these modified optimization problems may be more conservative than for cases without considering generator reactive power limits.

4.3.2 Controlled Voltage Margin

The sufficient condition (4.12) is binary: the specified power flow equations either cannot have a solution or may have a solution. The sufficient condition can also be interpreted to give a measure of the *degree* of solvability. This section develops a measure of the distance to the power flow solvability boundary, which is defined as the set of solvable power injections where all solutions may vanish under small perturbations. Since operating a power system far from the power flow solvability boundary is desirable to ensure stability, a measure of the distance to the solvability boundary is useful. A measure of the distance to the solvability boundary also indicates how close insolvable power flow equations are to solvability.

This section introduces a controlled voltage margin measure σ for the distance to the power flow solvability boundary. The controlled voltage margin is defined as the ratio between the specified slack bus voltage and the lower bound on the minimum slack bus voltage $\underline{V}_{slack}^{min}$ obtained from the semidefinite relaxation.

$$\sigma = \frac{V_0}{\underline{V}_{slack}^{min}} \tag{4.16}$$

The margin σ is an upper (non-conservative) bound of the distance to the power flow solvability boundary. For solvable power flow equations, a decrease in the specified slack bus voltage by a factor greater than σ is guaranteed to result in power flow insolvability. For insolvable power flow equations, increasing the slack bus voltage magnitude (with proportional increases in PV bus voltage magnitudes) by at least a factor of $\frac{1}{\sigma}$ (without changing the power injections) is required for solvability.

The sufficient condition can be written in terms of the voltage margin: $\sigma < 1$ is a sufficient condition for power flow insolvability.

4.3.3 Power Injection Margin

The power injection margin developed in this section is a measure of how large of a change in the power injections in a certain profile is required for the power injections to be on the solvability boundary. This margin considers the profile where power injections are uniformly changed at each bus in order to take advantage of the quadratic nature of the optimization problem (4.9) in the sufficient condition. The quadratic property is

$$h\left(\eta\left(P + jQ\right)\right) = \eta\left(\underline{V}_{slack}^{min}\right)^2 \tag{4.17}$$

where P and Q are vectors of the active and reactive power injection at each bus, h is the function representing optimization problem (4.9) relating the minimum slack bus voltage to the power injections, and η is a scalar.

Equation (4.17) describes the linear relationship between the squared voltage magnitudes and the power injections. This relationship is evident from (4.9b) and (4.9c): scaling all voltages by $\sqrt{\eta}$ scales the active and reactive power injections by η.

To develop the power injection margin, uniformly scale the power injections until the sufficient condition (4.12) indicates that the power injections are (at least) on the solvability boundary.

$$\eta \left(\underline{V}_{slack}^{min}\right)^2 = (V_0)^2 \tag{4.18}$$

The power injection margin η corresponding to the condition in (4.18) gives an upper, non-conservative bound of the distance to the solvability boundary in the direction of uniformly increasing power injections. For a solvable set of power injections, the largest proportional increase in power injections at each bus while potentially maintaining solvability is a factor of η. For an insolvable set of power injections, a proportional change of all power injections by at least η is required for a solution to be possible.

Note that the power injection margin can be rewritten in terms of the voltage margin.

$$\eta = (\sigma)^2 \tag{4.19}$$

The sufficient condition for power flow insolvability can be rewritten in terms of the power injection margin: $\eta < 1$ is a sufficient condition for power flow insolvability.

4.3.4 Alternate Formulation for the Insolvability Condition Calculation

The optimization problem (4.9) used to evaluate the power flow insolvability condition introduces a degree of freedom in the controlled voltage magnitudes. This formulation naturally yields a voltage stability margin in terms of controlled voltages and a power injection margin is derived using the quadratic nature of the power flow equations. Next, an alternate formulation is developed that introduces a degree of freedom in the power injections. This alternate formulation naturally yields a power injection margin.

$$\max_{V,\delta,\eta} \quad \eta \qquad \text{subject to} \tag{4.20a}$$

$$V_k \sum_{i=1}^{n} V_i \left(\mathbf{G}_{ik}\cos\left(\delta_k-\delta_i\right)+\mathbf{B}_{ik}\sin\left(\delta_k-\delta_i\right)\right) = P_k\eta \qquad \forall\, k \in \{\mathcal{PQ},\, \mathcal{PV}\} \tag{4.20b}$$

$$V_k \sum_{i=1}^{n} V_i \left(\mathbf{G}_{ik}\sin\left(\delta_k-\delta_i\right)-\mathbf{B}_{ik}\cos\left(\delta_k-\delta_i\right)\right) = Q_k\eta \qquad \forall\, k \in \mathcal{PQ} \tag{4.20c}$$

$$V_k = \alpha_k V_0 \qquad \forall\, k \in \mathcal{PV} \tag{4.20d}$$

$$V_{slack} = V_0 \qquad \forall\, k \in \mathcal{S} \tag{4.20e}$$

where $\mathcal{S}$ indicates the slack bus. In this formulation, all voltage magnitudes are fixed since V_0 is a specified value. The variable η introduced in the power injection equations (4.20b) and (4.20c) provides a single degree of freedom along the uniform, constant-power-factor injection profile.

The non-convexity of (4.20) makes it difficult to calculate a global optimum. The semidefinite relaxation of (4.20) is therefore used to calculate an upper bound on the power injection margin. The primal form of the semidefinite relaxation of (4.20) is

$$\max_{\mathbf{W},\eta} \quad \eta \qquad \text{subject to} \tag{4.21a}$$

$$\text{trace}\left(\mathbf{Y}_k\mathbf{W}\right) = P_k\eta \qquad \forall\, k \in \{\mathcal{PQ},\, \mathcal{PV}\} \tag{4.21b}$$

$$\text{trace}\left(\bar{\mathbf{Y}}_k\mathbf{W}\right) = Q_k\eta \qquad \forall\, k \in \mathcal{PQ} \tag{4.21c}$$

$$\text{trace}\left(\mathbf{M}_k\mathbf{W}\right) = \alpha_k^2 V_0^2 \qquad \forall\, k \in \mathcal{PV} \tag{4.21d}$$

$$\text{trace}\left(\mathbf{M}_k\mathbf{W}\right) = V_0^2 \qquad \forall\, k \in \mathcal{S} \tag{4.21e}$$

$$\mathbf{W} \succeq 0 \tag{4.21f}$$

The dual form of the semidefinite relaxation of (4.20) is

$$\max_{\lambda,\gamma,\mu} \quad \sum_{k\in\{\mathcal{PV},\mathcal{S}\}} \left(V_k^2\mu_k\right) \qquad \text{subject to} \tag{4.22a}$$

$$1 + \sum_{k\in\{\mathcal{PQ},\mathcal{PV}\}} \left(P_k\lambda_k\right) + \sum_{k\in\mathcal{PQ}} \left(Q_k\gamma_k\right) = 0 \tag{4.22b}$$

$$\mathbf{A} = \left[\sum_{k\in\{\mathcal{PQ},\mathcal{PV}\}} \left(\mathbf{Y}_k\lambda_k + \bar{\mathbf{Y}}_k\gamma_k\right) + \sum_{k\in\{\mathcal{PV},\mathcal{S}\}} \left(\mathbf{M}_k\mu_k\right)\right] \succeq 0 \tag{4.22c}$$

where free variables λ_k, γ_k, and μ_k are the Lagrange multipliers associated with equality constraints (4.20b), (4.20c), and (4.20d)–(4.20e). The optimal solutions to (4.21) and (4.22) are equivalent to the power injection margin η developed in Section 4.3.3.

In contrast to the power injection margin defined in Section 4.3.3, which is specific to a uniform, constant-power-factor injection profile, this alternative formulation suggests a method for considering the impact of non-uniform power injection profiles. Specifically, a semidefinite relaxation can be written for any choice of the right hand side of the power injection constraints (4.20b) and (4.20c) that is a linear expression of active and reactive power injections, P_k and Q_k, the square of voltage magnitude, V_k^2, and the degree-of-freedom η. For instance, with nominal power injections P_{k0} and Q_{k0}, choosing the expressions

$$P_{k0} + \eta \tag{4.23a}$$

$$Q_{k0} + \tan(\phi_k)\,\eta \tag{4.23b}$$

for the right hand sides of the active power constraint (4.20b) and reactive power constraint (4.20c), respectively, yields the power injection margin for the injection profile with specified power factor angles ϕ_k.

Note, however, that alternate choices for the right hand sides of the constraints in (4.20) may not always yield feasible optimization problems. For instance, consider the choice of right hand sides where all buses except one are fixed at large values, with the one remaining bus allowing constant-power-factor changes in active and reactive power. It is possible that no admissible value of power injections at that bus yields a feasible optimization problem, and thus the optimization problem (4.20) cannot be evaluated. This is not a concern for the uniform, constant-power-factor power injection profile, which yields a feasible optimization problem as demonstrated by the proof in Section 4.2. Further, although alternate right-hand-side expressions allow for calculating the power injection margin for non-uniform injection profiles, the insolvability condition $\eta < 1$ is not applicable for all injection profiles (e.g., a right hand side specifying an injection profile with a non-uniform power factor angle ϕ_k as in (4.23)).

4.4 Numeric Examples

The sufficient condition for power flow insolvability is next applied to the IEEE 14 and 118-bus systems [68] using optimization codes YALMIP [64] and SeDuMi [59]. The power injections are uniformly increased at each bus at constant power factor until the sufficient condition indicates that no solutions exist. The sufficient condition results are compared to power flow solution attempts using a Newton-Raphson algorithm.

4.4.1 IEEE 14-Bus System Results

Results from applying the sufficient condition to the IEEE 14-bus system are given in Table 4.1. The specified slack bus voltage is $V_0 = 1.0600$ per unit.

To generate a sequence of study cases for which solvability may be examined, the originally specified active and reactive power injections are increased uniformly at each bus. The first column of Table 4.1 lists the multiple by which the injections are increased. No power flow solutions exist after a sufficiently large increase (approximately 4.060 for this example). Note that the injection multiplier given in the first column does not change at a constant rate but rather focuses on the region near power flow solution non-existence.

The second column indicates whether a Newton-Raphson solver converged to a solution at the corresponding loading. In order to increase the likelihood of convergence, the Newton-Raphson solver was initialized at each injection multiplier with the solution from the previous injection multiplier and a large number of Newton-Raphson iterations were allowed.

The third column provides the lower bound on the minimum slack bus voltage in per unit obtained from (4.11). In order to evaluate the sufficient condition for power flow insolvability at each injection multiplier, the value in this column is compared to the specified slack bus voltage of 1.06 per unit. If the value in the third column is greater than 1.06, the sufficient condition indicates that no power flow solutions exist. These results show agreement between Newton-Raphson convergence and the sufficient condition; a power flow solution was found for all injection multipliers where the sufficient condition indicated that a solution was possible (observe that both

Injection Multiplier	**NR Converged**	$\underline{V}_{slack}^{min}$
1.000	Yes	0.5261
4.000	Yes	1.0522
4.020	Yes	1.0548
4.040	Yes	1.0575
4.050	Yes	1.0588
4.055	Yes	1.0594
4.056	Yes	1.0595
4.057	Yes	1.0597
4.058	Yes	1.0598
4.059	**Yes**	**1.0599**
4.060	**No**	**1.0601**
4.061	No	1.0602
4.062	No	1.0603
5.000	No	1.1764

Table 4.1 Insolvability Condition Results For IEEE 14-Bus System

$\underline{V}_{slack}^{min}$ is just greater than 1.06 and no solution is found by the Newton-Raphson solver at an injection multiplier of 4.060).

The existence of a solution for all power injections that satisfy (4.13) is expected since the $\mathbf{A}$ matrix in (4.11b) has a nullspace with dimension two. This does not occur for all sets of power flow equations. In Section 4.4.2, the IEEE 118-bus system with $\dim(\text{null}(\mathbf{A})) = 4$ displays no solution for some power injections even though (4.13) was satisfied.

The insolvability condition considering the specified upper reactive power limits is next applied to the IEEE 14-bus system at a power injection multiplier of 4.061. Imposing upper limits on generator reactive power power outputs, the optimization problem modified using (4.14) yields $\underline{V}_{slack}^{min} = 1.0601$ (i.e., the same value as in Table 4.1). Since this value satisfies the insolvability

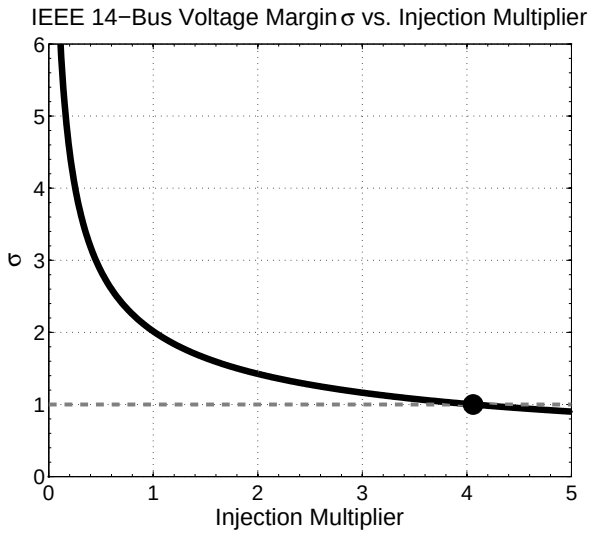

Figure 4.2 IEEE 14-Bus Voltage Margin

condition (4.12), the power flow equations with upper generator reactive power limits are insolvable. This is not surprising as optimization problem (4.9) minimizes the slack bus voltage with proportional scaling of the PV bus voltage magnitudes; further decreasing the PV bus voltage magnitudes is not likely to enable reduction of the slack bus voltage. In other words, imposing reactive power limits is not expected to improve power flow solvability.

The IEEE 14-bus system is next used to demonstrate the voltage and power injection margins. In Figure 4.2, the voltage margin σ is plotted versus the injection multiplier. The voltage margin decreases as power injections increase. The voltage margin crosses one at an injection multiplier of 4.0595, indicating that no power flow solution can exist for larger power injections. Beyond this point, the voltage margin provides the minimum increase in the slack bus voltage (with corresponding proportional voltage increases at all PV buses) required in order for a power flow solution to possibly exist.

Figure 4.3 shows the power versus voltage (P-V) curves for the high-voltage, stable solution to the IEEE 14-bus system. These curves, which were plotted using continuation techniques [105], illustrate how a solution voltage magnitude changes with proportional increases in power injections at all buses. The plots show the voltage at the arbitrarily selected PQ bus five. (Plotting the voltage

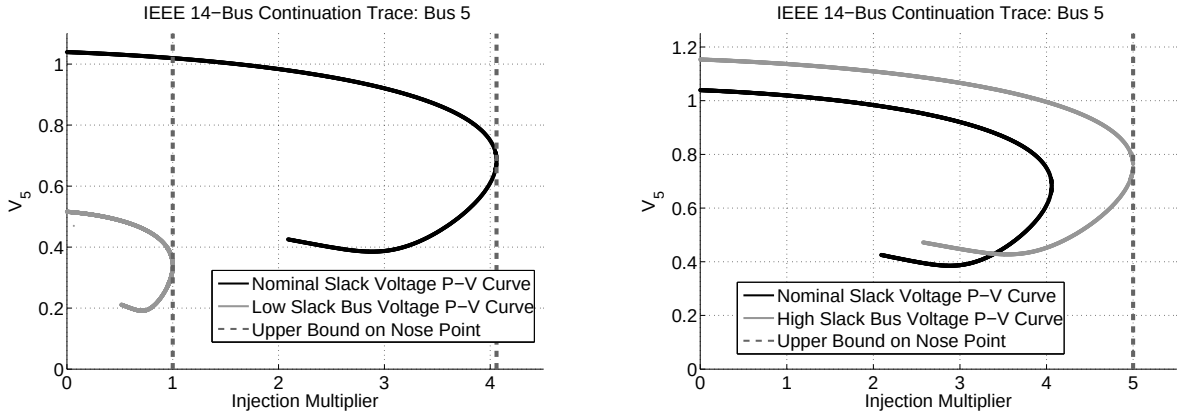

(a) Nominal and Low Slack Bus Voltage P-V Curves (b) Nominal and High Slack Bus Voltage P-V Curves

Figure 4.3 IEEE 14-Bus System P-V Curves

at a PQ bus is required since voltage magnitudes at slack and PV buses are fixed.) The P-V curve using the nominal slack and PV bus voltages is shown in black.

Evaluating the optimization problem (4.11) at an injection multiplier of one gives a $\underline{V}_{slack}^{min} = 0.5261$. The voltage margin is $\sigma = \frac{1.0600}{0.5261} = 2.0148$ per unit. Thus, no solution can exist if the slack bus voltage is reduced by more than a factor of 2.0148 (with all PV bus voltages reduced proportionally). The gray P-V curve in Figure 4.3a is obtained when the voltages are thus reduced. This curve shows that with these reduced voltages, the power injections with an injection multiplier equal to one yield a solution on the power flow solvability boundary; no solutions exist after any further increase in the injection multiplier. Thus, the voltage margin accurately indicates the distance to power flow insolvability.

The solution to the optimization problem (4.11) also enables determination of the power injection margin η. Solving (4.18) yields $\eta = \left(\frac{1.0600}{0.5261}\right)^2 = 4.0595$. Thus, the power injections can be increased uniformly by a factor of 4.0595 until the sufficient condition indicates that no power flow solutions are possible. The black P-V curve associated with the nominal voltages in Figure 4.3a corroborates this assertion: a power flow solution exists for all power injection multipliers less than 4.0595, but no solution exists beyond this power injection multiplier.

The voltage and power injection margins can also be used to investigate insolvable power injections. Consider desired operation at a power injection multiplier equal to five. Evaluating the optimization problem (4.11) at a power injection multiplier of five gives $\underline{V}_{slack}^{min} = 1.1764$. Note that (4.18) implies that knowledge of $\underline{V}_{slack}^{min}$ at a power injection multiplier of one allows the direct calculation $\underline{V}_{slack}^{min}$ at a power injection multiplier of five:

$$\underline{V}_{slack}^{min}\big|_{\text{Inj Mult}=5} = \sqrt{\eta}\,\underline{V}_{slack}^{min}\big|_{\text{Inj Mult}=1} = 1.1764 \tag{4.24}$$

The voltage margin at a power injection multiplier of five is $\sigma = \frac{1.06}{1.1764} = 0.9011$. $\sigma < 1$ indicates that there is no solution at a power injection multiplier of five. To potentially achieve a power flow solution, the slack bus voltage must increase by at least a factor of $\frac{1}{0.9011} = 1.1098$ (with corresponding proportional increases in all PV bus voltages). The gray P-V curve in Figure 4.3b has the voltages thus increased. Observe that increasing the voltages allows a solution on the power flow solvability boundary for an injection multiplier of five.

The power injection margin η can also be calculated at a power injection multiplier of five using (4.18).

$$\eta = \left(\frac{V_0}{\underline{V}_{slack}^{min}\big|_{\text{Inj Mult}=5}}\right)^2 = \left(\frac{1.0600}{1.1764}\right)^2 = 0.8119 \tag{4.25}$$

$\eta < 1$ implies that no solution exists at a power injection multiplier of five. The power injection margin also indicates that no solution can exist for power injection multipliers greater than $0.8119 \cdot 5 = 4.0595$. This corresponds to the "nose" point of the black (nominal) P-V curve in Figure 4.3b.

4.4.2 IEEE 118-Bus System Results

Results from applying the sufficient condition to the IEEE 118-bus system are given in Table 4.2. The data are arranged in the same manner as in Table 4.1. The specified slack bus voltage is $V_0 = 1.0350$ per unit.

Injection Multiplier	**NR Converged**	$\underline{V}_{slack}^{min}$
1.00	Yes	0.5724
1.50	Yes	0.7010
2.00	Yes	0.8095
2.50	Yes	0.9050
3.00	Yes	0.9914
3.15	Yes	1.0159
3.16	Yes	1.0175
3.17	Yes	1.0191
3.18	Yes	1.0207
3.19	No	1.0223
3.20	No	1.0239
3.21	No	1.0255
3.22	No	1.0271
3.23	No	1.0287
3.24	No	1.0303
3.25	No	1.0319
3.26	No	1.0335
3.27	No	1.0351
3.28	No	1.0366
3.29	No	1.0382
4.00	No	1.1448

Table 4.2 Insolvability Condition Results for IEEE 118-Bus System

The results can be categorized intro three regions: small power injections where the sufficient condition indicates that a solution is possible and a solution is indeed found using a Newton-Raphson solver, larger power injections where the sufficient condition indicates that a solution is

possible but no solutions are found, and yet larger power injections where the sufficient condition indicates that no solutions are possible and no solutions are found.

The dimension of the nullspace of the $\mathbf{A}$ matrix in (4.11b) for the IEEE 118-bus system is four. Therefore, the expectation that satisfaction of (4.13) will result in power flow solvability may not hold. Correspondingly, these results emphasize the fact that (4.12) is a *sufficient* condition for power flow insolvability. Specifically, a power flow solution is not found for injection multipliers greater than 3.18, even though $\underline{V}_{slack}^{min}$ is less than the specified slack bus voltage until an injection multiplier of 3.27. A continuation power flow indicates that the high-voltage solution bifurcates at a power injection multiplier of 3.185, so it is likely that no solutions exist after this point. No solutions are found at injection multipliers larger than 3.27 where the sufficient condition indicates that no solutions are possible. Chapter 7 analyzes non-zero relaxation gap solutions to the optimization problem (4.20) which result in failure to satisfy the insolvability condition for cases that appear to be insolvable.

The IEEE 118-bus system example is next used to demonstrate the voltage and power injection margins. In Figure 4.4, the voltage margin σ is plotted versus the injection multiplier. Similar to Figure 4.2, the voltage margin decreases as power injections increase. The voltage margin crosses

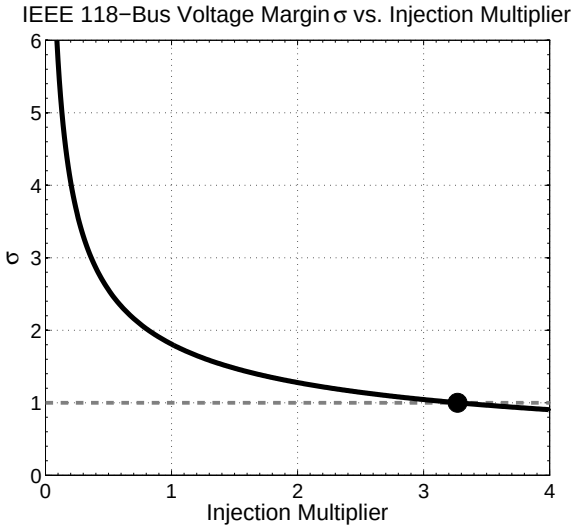

Figure 4.4 IEEE 118-Bus Voltage Margin

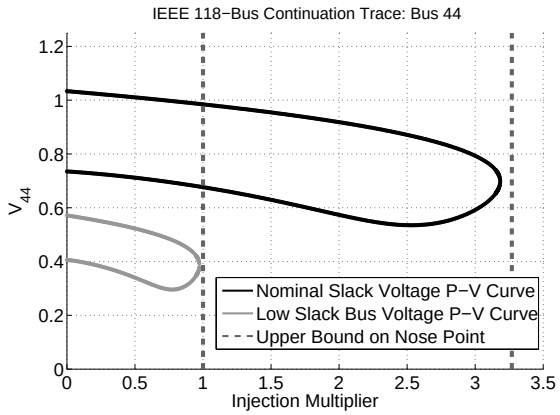

(a) Nominal and Low Slack Bus Voltage P-V Curves

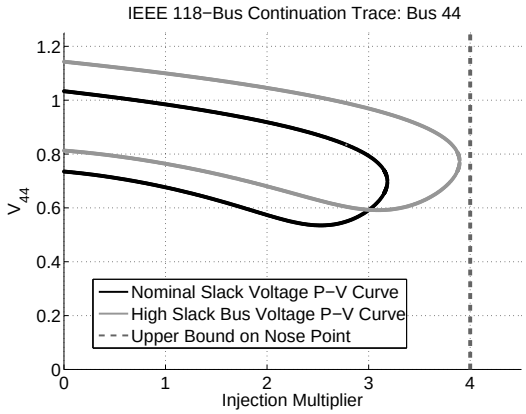

(b) Nominal and High Slack Bus Voltage P-V Curves

Figure 4.5 IEEE 118-Bus System P-V Curves

one at an injection multiplier of 3.2695, indicating that no power flow solution can exist for larger power injections. For larger power injections, the voltage margin provides the minimum increase in the slack bus voltage (with corresponding proportional voltage increases at all PV buses) that is required in order for a power flow solution to possibly exist.

Figure 4.5 shows the P-V curves for the high-voltage, stable solution to the IEEE 118-bus system. The plots provide the voltage at the arbitrarily selected PQ bus 44 (plotting the voltage at a PQ bus is required since the voltages at slack and PV buses are fixed). The P-V curve using the nominal slack and PV bus voltages is shown in black.

Evaluating the optimization problem (4.11) associated with the sufficient condition at an injection multiplier of one gives a $\underline{V}_{slack}^{min} = 0.5724$. The voltage margin is $\sigma = \frac{1.0350}{0.5724} = 1.8082$. Thus, no solution can exist if the slack bus voltage is reduced by more than a factor of 1.8082 (with all PV bus voltages reduced proportionally). The gray P-V curve in Figure 4.5a is obtained when the voltages are thus reduced. Although no solutions exist for the gray P-V curve at injection multipliers larger than one, there are also injection multipliers slightly less than one for which no solutions are found with continuation techniques. This reinforces the fact that the voltage margin is an *upper bound* on the distance to the solvability boundary.

The solution to the optimization problem (4.11) also enables determination of the power injection margin η. Solving (4.18) yields $\eta = \left(\frac{1.0350}{0.5724}\right)^2 = 3.2695$. Thus, the power injections can be increased uniformly by a factor of 3.2695 until the sufficient condition indicates that no power flow solutions are possible. This is also an upper bound on the distance to the solvability boundary: as indicated by the sufficient condition, the black P-V curve associated with the nominal voltages in Figure 4.5a has no solutions for power injection multipliers larger than 3.2695, but also appears to have no solutions for some values of power injection multipliers below 3.2695. (It is possible, but unlikely, that a P-V curve associated with a different solution may exist at injection multipliers between the "nose" of the P-V curve associated with the high-voltage solution at 3.1840 and the value of 3.2695 from the sufficient condition.)

The voltage and power injection margins can also be used to investigate insolvable power injections. Consider desired operation at a power injection multiplier equal to four. Evaluating the optimization problem (4.11) at a power injection multiplier of four gives $\underline{V}_{slack}^{min} = 1.1448$. Note that (4.18) implies that knowledge of $\underline{V}_{slack}^{min}$ at a power injection multiplier of one allows the direct calculation $\underline{V}_{slack}^{min}$ at a power injection multiplier of four:

$$\underline{V}_{slack}^{min}\big|_{\text{Inj Mult}=4} = \sqrt{\eta}\,\underline{V}_{slack}^{min}\big|_{\text{Inj Mult}=1} = 0.5724 \cdot \sqrt{4} = 1.1448\,\text{per unit}$$

The voltage margin at a power injection multiplier of four is $\sigma = \frac{1.0350}{1.1448} = 0.9041$. $\sigma < 1$ indicates that there is no solution at a power injection multiplier of four. To potentially achieve a power flow solution, the slack bus voltage must increase by at least a factor of $\frac{1}{0.1098} = 1.1061$ (with corresponding proportional increases in all PV bus voltages). The gray P-V curve in Figure 4.5b has the voltages thus increased. Since no solutions are evident from the P-V curve at an injection multiplier of four, it appears that this is not a large enough voltage increase to obtain solvability. This is a result of the fact that a *sufficient* condition for power flow insolvability is used to calculate the voltage margin; failing to satisfy the sufficient condition for power flow insolvability does not ensure the existence of a solution.

The power injection margin η can also be calculated at a power injection multiplier of four using (4.18).

$$\eta = \left(\frac{V_0}{\underline{V}_{slack}^{min}\big|_{\text{Inj Mult}=4}} \right)^2 = \left(\frac{1.0350}{1.1448} \right)^2 = 0.8174$$

$\eta < 1$ implies that no solution exists at a power injection multiplier of four. The power injection margin also indicates that no solution can exist for power injection multipliers greater than $0.8174 \cdot 4 = 3.2695$. The "nose" point of the black (nominal) P-V curve in Figure 4.3b is slightly lower than this upper limit on power flow solvability.

4.5 Conclusion

This chapter has presented a sufficient condition for identifying power flow insolvability. This condition requires evaluation of an optimization problem. This optimization problem is proven to be feasible for lossless power systems; practical power systems are also expected to yield a feasible optimization problem. To quantify the degree of solvability, this chapter developed controlled voltage and power injection margins from the sufficient condition that provide upper bounds on the distance to the power flow solvability boundary. Finally, the sufficient condition, voltage margin, and power injection margin are applied to the IEEE 14 and 118-bus systems. Although this chapter provides a sufficient condition for power flow *insolvability*, the majority of evaluated power systems yielded results similar to the IEEE 14-bus system where a power flow solution was found with a Newton-Raphson algorithm up to the point identified by the sufficient condition as insolvable.

Note that the work in this chapter models generators as ideal voltage sources capable of injecting any amount of reactive power; the sufficient condition has only limited incorporation of reactive power limited generators. Extension of this research to consider reactive power limited generators is presented in Chapter 5.

Also note that although the methods proposed in this chapter are suitable for off-line planning studies with contingencies, computational challenges for semidefinite program solvers may preclude the on-line calculation of voltage stability margins in very large-scale systems. Specifically, the positive semidefinite constraint on a matrix with size $2n \times 2n$, where n is the number of buses in

the system, controls the solution time of (4.11). For locations with known voltage stability issues, a small, more localized system model could be used to apply the proposed methods in an on-line environment. Further, exploiting power system sparsity using the matrix decomposition techniques detailed in Chapter 3 enables significantly faster solution of the semidefinite optimization problem for larger systems.

Finally note that Chapter 7 analyzes the IEEE 14 and 118-bus results to investigate the causes of non-zero relaxation gap solutions (i.e., solutions with $\dim(\text{null}(\mathbf{A})) > 2$) and the subsequent failure to satisfy the insolvability condition for some cases that do not appear to have a solution.

Chapter 5

A Sufficient Condition for Power Flow Insolvability Considering Reactive Power Limited Generators with Applications to Voltage Stability Margins

5.1 Introduction

As shown in the previous chapter, it is possible to specify a set of power injections for which no valid corresponding voltage profile exists. This results in insolvability of the power flow equations. It is also possible that no power flow solutions have reactive power injections that can be supported by the generators. That is, enforcing reactive power limits may result in power flow insolvability within the generators' capabilities [29–31].

This chapter presents two sufficient conditions that, when satisfied, rigorously classify a specified case as insolvable within the generators' reactive power capabilities. The first condition uses mixed-integer semidefinite programming and yields a voltage stability margin that characterizes a distance to the power flow solvability boundary [18]. The second condition uses real algebraic geometry and sum-of-squares programming [67] to generate infeasibility certificates which prove power flow insolvability.

See Section 1.2 and Chapter 4 and for an introduction and literature review concerning power flow insolvability conditions and voltage stability margins. (Relevant references include [20–26, 28].) Note that much of the existing literature models generators as ideal voltage sources with no limits on reactive power output. However, reactive power limits are relevant to power flow solvability since non-existence of power flow solutions may result from limit-induced bifurcations [29–31]. Power flow equations identified as solvable under the conditions proposed in many

of the references in Section 1.2 and Chapter 4 may not have any solutions within the generators' reactive power capabilities.

Recognizing the importance of reactive power limits, common industry practice determines static voltage stability margins using repeated power flow calculations to find the "nose point" of a power versus voltage ("P-V") curve while monitoring "reactive margins" on generators (i.e., the margin between the generator's reactive power output at a given operating point and its maximum reactive output). Descriptions of relevant industry standards can be found in such works as [32–34].

Chapter 4 presents a sufficient condition for power flow insolvability that yields voltage stability margins. A semidefinite program is used to evaluate this sufficient condition. In contrast to existing Newton-based methods whose conditions for convergence are inherently local in nature, the semidefinite program in Chapter 4 provides a global solution to the optimization problem that is formulated from the originally specified power flow equations. However, the method proposed in Chapter 4 has only a rudimentary incorporation of limits on generator reactive power outputs.

This chapter presents two sufficient conditions under which the power flow equations are guaranteed to be insolvable within the generators' reactive power limits. The first condition is an extension of the work in Chapter 4 that uses mixed-integer semidefinite programming (i.e., optimization problems with both integer and semidefinite matrix constraints) to model reactive power limited generators. The ability to achieve a global optimum enables the guarantee of solution non-existence upon satisfaction of a sufficient condition.

The computation for the first condition provides a power injection margin to the power flow solvability boundary. This margin is a non-conservative bound. Thus, for an insolvable set of specified values, a change in power injections by *at least* the amount indicated by the power injection margin is required for the power flow equations to be *potentially* solvable. More precisely, the margin identifies the shortest distance (as measured by the change in power injections in the direction of a specified injection profile) to a point at which the sufficient condition for power flow insolvability fails to be satisfied.

Current mixed-integer semidefinite programming solvers are relatively immature, and unlike algorithms for semidefinite programs, solvers are not assured to run in polynomial time. However,

this is an active area of research, and future availability of more capable algorithms is anticipated. Existing tools [63, 64] can solve the proposed formulation for small power system models, and Section 5.3.3 discusses potential modifications that improve the computational tractability of the proposed formulation with respect to solution algorithms in the literature [65, 66].

The second sufficient condition for power flow insolvability uses the concept of infeasibility certificates from the field of real algebraic geometry [67]. Infeasibility certificates for polynomial equations are calculated using sum-of-squares decompositions that are themselves computed with semidefinite optimization programs. Specifically, infeasibility certificates use the Positivstellensatz theorem, which states that there exists an algebraic identity to certify the non-existence of real solutions to every infeasible system of polynomial equalities and inequalities [67]. This theorem does not require any assumptions about the system of polynomials. Since the power flow equations can be expressed as a system of polynomial equalities, infeasibility certificates can be directly applied to power flow problems. Further, this chapter formulates limits on generator reactive power outputs as a system of polynomial equalities and inequalities and thus provides a means for extending the theory of infeasibility certificates to power flow problems with these limits.

The organization of this chapter is as follows. Section 5.2 reviews the power flow equations with an emphasis on their polynomial representation and the behavior of reactive power limited generators. Section 5.3 then describes the first sufficient condition for power flow insolvability and defines a power injection margin. Section 5.4 first provides an overview of infeasibility certificates and sum-of-squares programming and then describes the second proposed sufficient condition. Numeric examples using standard test systems are provided in Section 5.5. The work described in this chapter is published as [106].

5.2 The Power Flow Equations Considering Reactive Power Limited Generators

With a rectangular representation for complex voltages ($V_i = V_{di} + jV_{qi}$) and rectangular "active/reactive" representation of complex power ($P_i + jQ_i$), the power flow equations are formulated as polynomial equalities. The power flow equations at bus i are

$$P_i = f_{Pi}\left(V_d,\, V_q\right) = V_{di} \sum_{k=1}^{n} \left(\mathbf{G}_{ik} V_{dk} - \mathbf{B}_{ik} V_{qk}\right) + V_{qi} \sum_{k=1}^{n} \left(\mathbf{B}_{ik} V_{dk} + \mathbf{G}_{ik} V_{qk}\right) \tag{5.1a}$$

$$Q_i = f_{Qi}\left(V_d,\, V_q\right) = V_{di} \sum_{k=1}^{n} \left(-\mathbf{B}_{ik} V_{dk} - \mathbf{G}_{ik} V_{qk}\right) + V_{qi} \sum_{k=1}^{n} \left(\mathbf{G}_{ik} V_{dk} - \mathbf{B}_{ik} V_{qk}\right) \tag{5.1b}$$

where $\mathbf{Y} = \mathbf{G} + j\mathbf{B}$ is the network admittance matrix and n is the number of buses in the system.

The rectangular voltage components must additionally satisfy the voltage magnitude equation, which is also a polynomial equality.

$$V_i^2 = f_{Vi}\left(V_d,\, V_q\right) = V_{di}^2 + V_{qi}^2 \tag{5.1c}$$

Using the voltage at the slack bus $V_{slack} = V_{d,slack} + jV_{q,slack}$ as an angle reference, $V_{q,slack} = 0$.

To represent typical behavior of equipment in the power system, each bus is classified as PQ, PV, or slack according to the constraints imposed. PQ buses, which typically correspond to loads and are denoted by the set $\mathcal{PQ}$, treat P_i and Q_i as specified quantities and enforce the active power (5.1a) and reactive power (5.1b) equations at that bus. PV buses, which typically correspond to generators and are denoted by the set $\mathcal{PV}$, specify a voltage magnitude V_i and active power injection P_i and enforce the active power and voltage magnitude equations (5.1a) and (5.1c). The associated reactive power Q_i may be computed as an "output quantity" via (5.1b). Finally, a single slack bus is selected with specified V_{di} and V_{qi} (typically chosen such that the reference angle is $0°$). The set $\mathcal{S}$ denotes the slack bus. The active power P_i and reactive power Q_i at the slack bus are determined from (5.1a) and (5.1b); network-wide conservation of complex power is thereby satisfied.

Additionally, generator reactive power outputs must be within specified limits. If a generator's reactive power output is between the upper and lower limits, the generator maintains a constant voltage magnitude at the bus (i.e., the bus behaves like a PV bus). If a generator's reactive power output reaches its upper limit, the reactive power output is fixed at the upper limit and the bus voltage magnitude is allowed to decrease (i.e., the bus behaves like a PQ bus with reactive power injection determined by the upper limit). If the generator's reactive power output reaches its lower

limit, the reactive power output is fixed at the lower limit and the voltage magnitude is allowed to increase (i.e., the bus behaves like a PQ bus with reactive power injection determined by the lower limit). Figure 5.1 shows the reactive power versus voltage magnitude characteristic for this generator model with a voltage setpoint of V^*, lower reactive power limit of Q^{min}, and upper reactive power limit of Q^{max}.

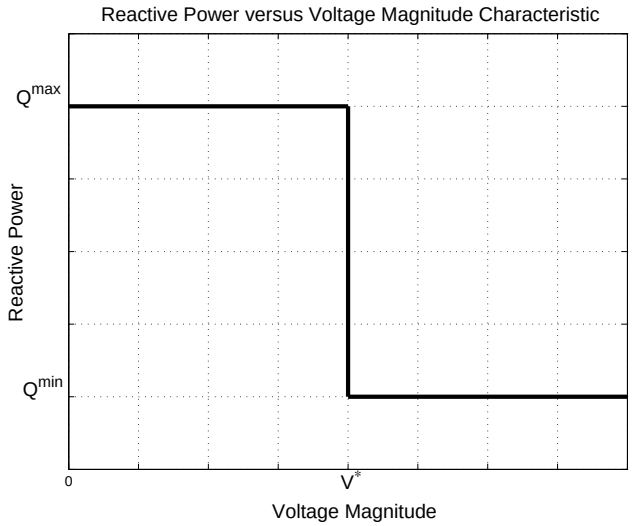

Figure 5.1 Reactive Power versus Voltage Magnitude Characteristic (Reproduction of Figure 1.1)

5.3 A Sufficient Condition for Power Flow Insolvability Using Mixed-Integer Semidefinite Programming

This section first presents a voltage stability margin for the power flow equations using the model of reactive power limited generators described in the previous section. Reactive power limits are formulated as a mixed-integer semidefinite program. The resulting voltage stability margin is then used to provide the first sufficient condition for power flow insolvability with consideration of reactive power limited generators. This section also discusses computational considerations associated with the mixed-integer semidefinite programming formulation.

5.3.1 Mixed-Integer Semidefinite Programming Formulation for a Voltage Stability Margin

This section first formulates a mixed-integer semidefinite program to calculate a voltage stability margin that incorporates generator reactive power limits. To write the semidefinite relaxation, first define the vector of voltage coordinates

$$x = \begin{bmatrix} V_{d1} & V_{d2} & \dots & V_{dn} & V_{q1} & V_{q2} & \dots & V_{qn} \end{bmatrix} \tag{5.2}$$

Then define the rank one matrix

$$\mathbf{W} = xx^T \tag{5.3}$$

The matrices $\mathbf{Y}_k$, $\bar{\mathbf{Y}}_k$, and $\mathbf{M}_k$ employed in the formulation are defined in Chapter 2. The active and reactive power injections at bus i are given by $\mathrm{trace}\,(\mathbf{Y}_i\mathbf{W})$ and $\mathrm{trace}\left(\bar{\mathbf{Y}}_i\mathbf{W}\right)$. The square of the voltage magnitude at bus i is given by $\mathrm{trace}\,(\mathbf{M}_i\mathbf{W})$.

Replacement of the non-convex rank constraint (5.3) by the less stringent constraint $\mathbf{W} \succeq 0$, where $\succeq 0$ indicates the corresponding matrix is positive semidefinite, yields the convex semidefinite relaxation. This relaxation gives a lower bound for the globally optimal solution of the rank constrained problem. Further, a solution to the semidefinite relaxation has zero relaxation gap if and only if the rank condition (5.4) is satisfied (i.e., the relaxation is "tight").

$$\mathrm{rank}\,(\mathbf{W}) \leq 2 \tag{5.4}$$

For a zero relaxation gap solution, a unique rank one matrix $\mathbf{W}$ can be recovered by enforcing the known voltage angle at the slack bus [7].

The work described in Chapter 4 uses the semidefinite relaxation to define margins to the power flow solvability boundary. The additional flexibility provided by mixed-integer programming is used to extend this work to model reactive power limited generators. The mixed-integer semidefinite programming formulation is given in (5.5).

$$\max_{\mathbf{W},\,\psi_U,\,\psi_L,\,\eta} \quad \eta \qquad \text{subject to} \tag{5.5a}$$

$$\text{trace}\left(\mathbf{Y}_k\mathbf{W}\right) = P_k\,\eta \qquad \forall k \in \{\mathcal{PQ},\,\mathcal{PV}\} \tag{5.5b}$$

$$\text{trace}\left(\bar{\mathbf{Y}}_k\mathbf{W}\right) = Q_{Dk}\,\eta \qquad \forall k \in \mathcal{PQ} \tag{5.5c}$$

$$\left.\begin{aligned}&\text{trace}\left(\bar{\mathbf{Y}}_k\mathbf{W}\right) \geq Q_k^{max}\psi_{Uk} + Q_k^{min}\left(1-\psi_{Uk}\right)\\&\text{trace}\left(\bar{\mathbf{Y}}_k\mathbf{W}\right) \leq Q_k^{min}\psi_{Lk} + Q_k^{max}\left(1-\psi_{Lk}\right)\end{aligned}\right\} \qquad \forall k \in \{\mathcal{PV},\,\mathcal{S}\} \tag{5.5d}$$

$$\left.\begin{aligned}&\text{trace}\left(\mathbf{M}_k\mathbf{W}\right) \geq \left(V_k^*\right)^2\left(1-\psi_{Uk}\right)\\&\text{trace}\left(\mathbf{M}_k\mathbf{W}\right) \leq \left(V_k^*\right)^2\left(1-\psi_{Lk}\right) + d\psi_{Lk}\end{aligned}\right\} \qquad \forall k \in \{\mathcal{PV},\,\mathcal{S}\} \tag{5.5e}$$

$$\psi_{Lk} + \psi_{Uk} \leq 1 \qquad \forall k \in \{\mathcal{PV},\,\mathcal{S}\} \tag{5.5f}$$

$$\sum_{k\in\{\mathcal{PV},\,\mathcal{S}\}} \left(\psi_{Lk} + \psi_{Uk}\right) \leq n_g - 1 \tag{5.5g}$$

$$\mathbf{W} \succeq 0 \tag{5.5h}$$

$$\psi_{Uk} \in \{0,\,1\} \qquad \psi_{Lk} \in \{0,\,1\} \qquad \forall k \in \{\mathcal{PV},\,\mathcal{S}\} \tag{5.5i}$$

where d is a large scalar such that the upper limit of (5.5e) is non-binding when $\psi_{Lk} = 1$, and the scalar n_g is the number of generators (i.e., the number of slack and PV buses). Let η^{max} be a globally optimal solution to (5.5).

Generator reactive power and voltage magnitude limits are enforced by equations (5.5d), (5.5e), (5.5f), and (5.5g). When the binary variable ψ_{Uk} is equal to one, the upper reactive power limit of the generator at bus k is binding. Accordingly, (5.5d) fixes the reactive power output at the upper limit and (5.5e) sets the lower voltage magnitude limit to zero. When the binary variable ψ_{Lk} is equal to one, the lower reactive power limit of the generator at bus k is binding. Accordingly, (5.5d) fixes the generator reactive power output at the lower limit and (5.5e) removes the upper voltage magnitude limit. When both $\psi_{Uk} = 0$ and $\psi_{Lk} = 0$, (5.5d) constrains the reactive power output within the upper and lower limits and (5.5e) fixes the voltage magnitude to the specified value V_k^*. Consistency in the reactive power limits is enforced by (5.5f); a generator's reactive

power output cannot simultaneously be at both the upper and lower limits. Finally, reactive power balance is enforced by (5.5g).

Note that the formulation (5.5) gives a power injection margin in the specific direction of a uniform, constant-power-factor injection profile; however, the formulation can be extended to consider the impact of non-uniform power injection profiles. Specifically, a semidefinite relaxation can be written for any choice of the right hand side of the power injection constraints (5.5b) and (5.5c) that is a linear expression of active and reactive power injections P_k and Q_k, the square of voltage magnitude $(V_k^*)^2$, and the degree-of-freedom η. For instance, with nominal power injections P_{k0} and Q_{k0}, choosing the expressions

$$P_{k0} + \eta \tag{5.6a}$$

$$Q_{k0} + \tan(\phi_k)\,\eta \tag{5.6b}$$

for the right hand sides of the active power constraint (5.5b) and reactive power constraint (5.5c), respectively, yields an additive power injection margin for the injection profile with specified power factor angles ϕ_k.

Although alternate right-hand-side expressions allow for calculating the power injection margin for non-uniform injection profiles, the insolvability condition that is described next is not applicable for all injection profiles (e.g., a right hand side specifying an injection profile with a non-uniform power factor angle ϕ_k as in (5.6)).

5.3.2 Optimality Considerations and a Sufficient Condition for Power Flow Insolvability

The solution to (5.5), η^{max}, is a voltage stability margin to the power flow solvability boundary with consideration of generator reactive power limits. In contrast to traditional iterative methods that may only obtain a locally optimal solution, the formulation (5.5) yields a globally optimal voltage stability margin.

It is important to note that η^{max} is, in general, a non-conservative bound. Thus, for an insolvable set of specified values, η^{max} indicates the *least* factor by which the power injections must change

in the specified profile for the power flow equations to be *potentially* solvable. For a solvable set of specified values, η^{max} indicates the *greatest* factor by which the power injections can change while the power flow equations remain *potentially* solvable.

The non-conservativeness of the bound given by η^{max} is a result of the possibility that a solution to (5.5) does not satisfy the rank condition of the semidefinite programming relaxation (5.4) (i.e., the solution to (5.5) exhibits non-zero relaxation gap). If a solution to (5.5) satisfies the rank condition and thus exhibits zero relaxation gap, a power flow solution can be obtained [7]. This power flow solution is the furthest possible point (i.e., the "nose point") of a P-V curve constructed with consideration of generator reactive power limits. Since (5.5) can be solved to global optimality, a solution satisfying the rank condition is guaranteed to locate the furthest possible point on the P-V curve. (This is an advantage over traditional iterative approaches which are not guaranteed to locate the furthest possible point.) For solutions satisfying the rank condition (5.4), the voltage stability margin η^{max} provides the exact distance to the power flow solvability boundary rather than a non-conservative bound.

A globally optimal η^{max} provides a sufficient but not necessary insolvability condition for the power flow equations with generator reactive power limits. Specifically, since η^{max} is a measure of the distance to the power flow solvability boundary,

$$\eta^{max} < 1 \tag{5.7}$$

is a sufficient but not necessary condition indicating that the specified set of power flow equations has no solution. Conversely,

$$\eta^{max} \geq 1 \tag{5.8}$$

is a necessary but not sufficient condition for power flow solvability. The conditions (5.7) and (5.8) hold regardless of the rank properties of the solution to (5.5) (i.e., the semidefinite relaxation need not be "tight").

Note that unlike previous work in Chapter 4 which develops power injection margins using a provably feasible optimization problem, the formulation in (5.5) does not have a feasibility proof.

That is, it may be possible to specify a set of power flow equations for which the optimization problem (5.5) has an empty feasibility set; the formulation (5.5) can fail when an injection profile is specified that does not have a value of η such that the power injections have a valid corresponding voltage profile (i.e., the power flow equations are insolvable for any choice of η in (5.5)).

5.3.3 Computational Considerations

Computational challenges exist in solving mixed-integer semidefinite programs. Without considering the integer constraints, the computational requirements of a semidefinite relaxation of the power flow equations scales with square of the number of buses. The computational advances described in Chapter 3 that exploit power system sparsity in semidefinite program relaxations can be applied to ameliorate this challenge. Thus, each semidefinite program evaluation internal to the mixed-integer semidefinite program solver can be performed significantly more quickly.

The integer constraints introduce added difficulty, and mixed-integer semidefinite programming algorithms are not as mature as, for instance, mixed-integer linear programming algorithms. The existing mixed-integer semidefinite programming solvers BARON [63] and YALMIP [64] are suited for small problems. For instance, YALMIP's branch-and-bound solver is capable of calculating the voltage stability margin using (5.5) for IEEE test systems [68] with sizes up to 57 buses.

The algorithms described in [65] and [66] claim to be capable of solving large mixed-integer semidefinite programs. The algorithm proposed in [65] is limited by the need to symbolically invert certain submatrices of the positive semidefinite constrained matrix, which is computationally intractable for large matrices. However, this limitation may be overcome for power systems applications by exploiting the sparsity inherent to power system models. Specifically, the matrix completion techniques described in Chapter 3 create a block-diagonal positive-semidefinite-constrained matrix; since each block can be separately inverted, the algorithm described in [65] may be computationally tractable for large power systems.

An additional technique for improving the computational tractability of the proposed method employs a semidefinite relaxation of the integer constraints (5.5i). This relaxation uses the fact that

the binary constraint $\psi \in \{0,\, 1\}$ is equivalent to the quadratic constraint $\psi^2 - \psi = 0$. Define the constant matrix $\mathbf{N}$ as

$$\mathbf{N} = \begin{bmatrix} 0 & -\frac{1}{2} \\ -\frac{1}{2} & 1 \end{bmatrix} \tag{5.9}$$

If the 2×2 symmetric matrix $\mathbf{R}$ is rank one and $\mathbf{R}^{11} = 1$, then $\mathbf{R}^{22} = \left(\mathbf{R}^{12}\right)^2$, where superscript cd indicates the $(c,\, d)$ entry of the corresponding matrix. Then the equation $\mathrm{trace}\,(\mathbf{NR}) = \mathbf{R}^{22} - \mathbf{R}^{12} = 0$ implements the quadratic constraint $\left(\mathbf{R}^{12}\right)^2 - \mathbf{R}^{12} = 0$. For reactive power limited generator bus i, semidefinite relaxations of the quadratic equations (i.e., replacing the requirement $\mathrm{rank}\,(\mathbf{R}) = 1$ with the less stringent $\mathbf{R} \succeq 0$) are then implemented with the constraints given in (5.10), which replace the binary-constraints (5.5i).

$$\mathrm{trace}\,(\mathbf{NR}_{Ui}) = 0 \qquad \mathrm{trace}\,(\mathbf{NR}_{Li}) = 0 \tag{5.10a}$$

$$\mathbf{R}_{Ui}^{11} = 1 \qquad \mathbf{R}_{Li}^{11} = 1 \tag{5.10b}$$

$$\mathbf{R}_{Ui}^{12} = \psi_{Ui} \qquad \mathbf{R}_{Li}^{12} = \psi_{Li} \tag{5.10c}$$

$$\mathbf{R}_{Ui} \succeq 0 \qquad \mathbf{R}_{Ui} \succeq 0 \tag{5.10d}$$

The positive semidefinite constraint (5.10d) relaxes the rank one requirement on the $\mathbf{R}_{Ui}$ and $\mathbf{R}_{Li}$ matrices. See reference [107] for further discussion on this relaxation technique.

Semidefinite relaxation of the integer constraints using (5.10) yields an upper bound, denoted as $\bar{\eta}^{max}$, on the distance to the power flow solvability boundary considering reactive power limited generators. Accordingly, the sufficient condition for power flow insolvability (5.7) holds with this relaxation (i.e., $\bar{\eta}^{max} \leq 1$ is a sufficient condition for power flow insolvability). If the solution to the relaxed problem has rank one $\mathbf{R}_{Li}$ and $\mathbf{R}_{Ui}$ matrices for all reactive power limited generator buses, the semidefinite relaxation of the integer constraints is "tight." With additional satisfaction of the rank condition for $\mathbf{W}$ (5.4), the proposed formulation gives the exact distance to the power flow solvability boundary.

Unlike the semidefinite relaxation of the power flow equations, this relaxation of the integer constraints is typically not "tight" and, as will be shown in Section 5.5, may substantially overestimate the distance to the power flow solvability boundary. This section therefore proposes the following method for obtaining a lower bound on the distance to the power flow solvability boundary. First, calculate $\bar{\eta}^{max}$ with relaxed integer constraints from (5.10). Then, using the solution to the relaxed problem, set all values of ψ_{Ui} and ψ_{Li} that are over a specified threshold to one with the remainder set to zero. Solve the semidefinite program (5.5) with the specified values for ψ_{Ui} and ψ_{Li}. If the resulting solution has non-zero relaxation gap (i.e., the solution satisfies (5.4)), the solution provides a lower bound, denoted as $\underline{\eta}^{max}$, on the distance to the power flow solvability boundary considering reactive power limited generators. If the rank condition (5.4) is not satisfied, the solution does not provide a bound on the distance to the power flow solvability boundary.

5.4 A Sufficient Condition for Power Flow Insolvability Using Infeasibility Certificates

The second sufficient condition for power flow insolvability uses real algebraic geometry and sum-of-squares programming to develop infeasibility certificates. After providing an overview of infeasibility certificate theory, this section formulates reactive power limits as a system of polynomial inequalities and equalities. This enables application of the Positivstellensatz theorem, which states that there exists an algebraic identity to certify the non-existence of real solutions to every infeasible system of polynomial equalities and inequalities [67].

5.4.1 Overview of Infeasibility Certificate Theory

This section first introduces the theory used in constructing infeasibility certificates, specifically the Positivstellensatz theorem and the relationship between sum-of-squares and semidefinite programming. See [67] for a more detailed overview of this material.

Notation and several definitions are required for understanding the infeasibility certificate theory. This theory applies to a ring of multivariate polynomials with real coefficients, which is

denoted as $\mathbb{R}[x]$ for the variables $\{x_1, \ldots, x_n\}$. Some polynomials have a sum-of-squares decomposition. These polynomials can be written as

$$p(x) = \sum_i q_i^2(x), \qquad q_i \in \mathbb{R}[x] \tag{5.11}$$

Note that this decomposition is not necessarily unique. Polynomials with sum-of-squares decompositions have the important property that they are non-negative for all values of x.

Polynomials with sum-of-squares decompositions can always be written in the form of a semidefinite program [67]. Define the vector z using monomials of x.

$$z = \begin{bmatrix} 1 & x_1 & x_2 & \ldots & x_n & x_1^2 & \ldots & x_1 x_n & x_2^2 & \ldots \end{bmatrix}^T \tag{5.12}$$

Then any polynomial with a sum-of-squares decomposition can be written as

$$p(x) = z^T \mathbf{Q} z \tag{5.13}$$

where $\mathbf{Q} \succeq 0$. Thus, sum-of-squares decompositions can be calculated using semidefinite optimization techniques.

Two definitions necessary for creating infeasibility certificates are next introduced. First, the *ideal* of a set of multivariate polynomials $\{f_1, \ldots, f_m\}$ is defined as

$$\text{ideal}(f_1, \ldots, f_m) = \left\{ f \mid f = \sum_{i=1}^{m} t_i f_i, \qquad t_i \in \mathbb{R}[x] \right\} \tag{5.14}$$

Note that every polynomial in $\text{ideal}(f_1, \ldots, f_m)$ is zero at the zeros of the polynomials $f_1, \ldots, f_m$. That is, $f_1(x_0) = 0, \ldots, f_m(x_0) = 0$ implies that any polynomial in $\text{ideal}(f_1, \ldots, f_m)$ is zero when evaluated at x_0.

Next define the *cone* of the set of multivariate polynomials $\{g_1, \ldots, g_r\}$ as

$$\text{cone}(g_1, \ldots, g_r) = \left\{ g \mid g = s_0 + \sum_i s_i g_i + \sum_{\{i,j\}} s_{ij} g_i g_j + \sum_{\{i,j,k\}} s_{ijk} g_i g_j g_k + \cdots \right\} \tag{5.15}$$

where the terms s_0, s_{ij}, s_{ijk}, ... are sum-of-squares polynomials. Note that every polynomial in $\text{cone}(g_1, \ldots, g_r)$ is non-negative if $g_k(x) \geq 0 \; \forall k$.

The Positivstellensatz theorem can then be written as follows. The set of polynomial equations

$$f_i(x) = 0 \qquad i = 1, \ldots, m \tag{5.16a}$$

$$g_k(x) \geq 0 \qquad k = 1, \ldots, r \tag{5.16b}$$

is infeasible in $\mathbb{R}^n$ (i.e., the equations admit no real solution) if and only if there exist polynomials

$$F(x) \in \text{ideal}(f_1, \ldots, f_m)$$
$$G(x) \in \text{cone}(g_1, \ldots, g_r)$$

such that $F(x) + G(x) = -1$ for all x.

Since F is in $\text{ideal}(f_1, \ldots, f_m)$, $F(x_0) = 0$ for any solution x_0 to the equations $f_i(x_0) = 0, \quad i = 1, \ldots, m$. Since G is in $\text{cone}(g_1, \ldots, g_r)$, $G(y_0) \geq 0$ for any point y_0 in the feasible set of $g_k(y_0) \geq 0, \quad k = 1, \ldots, r$. Thus, $F(x_0) + G(x_0)$ must be non-negative for any x_0 that satisfies (5.16). However, existence of such an x_0 contradicts the fact that $F(x) + G(x) = -1$ for all x. Thus, no valid x_0 exists and the set of equations (5.16) is infeasible.

5.4.2 Infeasibility Certificates for the Power Flow Equations

This section next applies infeasibility certificate theory to the power flow equations. In order to apply infeasibility certificate theory to power flow equations with reactive power limited generators, the reactive power versus voltage magnitude characteristic shown in Figure 5.1 is formulated as a system of polynomial equalities and inequalities. Infeasibility certificates are then generated for both this polynomial system and the power flow equations without reactive power limited generators.

5.4.2.1 Polynomial Formulation of the Power Flow Equations

In order to generate infeasibility certificates, the power flow equations with reactive power limited generators are represented as a system of polynomial inequalities and equalities. The power

flow equations without consideration of reactive power limited generators are polynomial equalities in terms of the voltage components V_d and V_q as shown in (5.1). The reactive power limit characteristic shown in Figure 5.1 is next formulated as a set of polynomial equalities and inequalities in the form of (5.16). Reactive power limits at the generator bus i are written as

$$f_{Vi} = (V_i^*)^2 - V_i^- + V_i^+ \tag{5.17a}$$

$$Q_i^{max} - f_{Qi} = x_i \tag{5.17b}$$

$$V_i^- x_i = 0 \tag{5.17c}$$

$$V_i^+ \left(Q_i^{max} - Q_i^{min} - x_i\right) = 0 \tag{5.17d}$$

$$Q_i^{max} - Q_i^{min} - x_i \geq 0 \tag{5.17e}$$

$$V_i^+ \geq 0, \quad V_i^- \geq 0, \quad x_i \geq 0 \tag{5.17f}$$

where the polynomial functions $f_{Qi}(V_d, V_q)$ and $f_{Vi}(V_d, V_q)$ are defined in (5.1b) and (5.1c), respectively.

The variable x_i represents the distance to the upper reactive power limit for the generator bus i (i.e., x_i is a "slack variable" for this limit). With x_i constrained to be non-negative in (5.17f), the reactive power generation at bus i is maintained within its upper limit. Similarly, the distance to the lower reactive power limit is $Q_i^{max} - Q_i^{min} - x_i$, which is constrained to be non-negative in (5.17e). Reactive power generation is thus greater than or equal to the lower limit. With equality constraints (5.17a) and (5.17c), the non-negative variable V_i^- allows the voltage magnitude at bus i to decrease when the reactive power generation is at its upper limit. Similarly, with equality constraints (5.17a) and (5.17d), the non-negative variable V_i^+ allows the voltage magnitude at bus i to increase when the reactive power generation is at its lower limit. Thus, the set of equations (5.17) models the reactive power versus voltage magnitude characteristic shown in Figure 5.1.

5.4.2.2 Infeasibility Certificates for the Power Flow Equations Without Considering Reactive Power Limits

With a polynomial formulation, infeasibility can be verified using the Positivstellensatz theorem. This section first considers the case without reactive power limits on generators (i.e., generators are modeled as ideal voltage sources with fixed voltage V_i^* for any reactive power output). For this case, the power flow equations are entirely in the form of polynomial equalities. An infeasibility certificate is found if a polynomial $F(V_d, V_q)$ in the ideal formed by the power flow equations (5.1) satisfies

$$F(V_d, V_q) = -1 \tag{5.18}$$

A polynomial in the ideal of the power flow equations has the form

$$F(V_d, V_q) = \tau V_{q,slack} + \sum_{i \in \{\mathcal{PV}, \mathcal{PQ}\}} \lambda_i \left(f_{Pi} - P_i\right) + \sum_{i \in \mathcal{PQ}} \gamma_i \left(f_{Qi} - Q_i\right) + \sum_{i \in \{\mathcal{S}, \mathcal{PV}\}} \mu_i \left(f_{Vi} - V_i^2\right) \tag{5.19}$$

where $V_{q,slack}$ is the q-component of the slack bus voltage and τ, λ, γ, and μ are polynomials (which are not necessarily sum of squares) associated with the slack bus angle, active power injection, reactive power injection, and squared voltage magnitude equations, respectively.

Using the Positivstellensatz theorem, the power flow equations are insolvable if there exist polynomials τ, λ, γ, and μ such that $F(V_d, V_q) = -1$. This condition is evaluated by attempting to find a sum-of-squares decomposition for the polynomial $-F(V_d, V_q) - 1$ using semidefinite programming. If such a decomposition exists, the power flow equations are proven insolvable.

This can be understood using the fact that the polynomial $-F(V_d, V_q) - 1$ is negative for any values of V_d and V_q that are solutions to the power flow equations (5.1); conversely, a sum-of-squares decomposition is non-negative for all values of V_d and V_q. Thus, $-F(V_d, V_q) - 1$ being a sum of squares provides a sufficient condition for the power flow equations to be insolvable.

Note that the theory used to develop this result does not provide any information on the necessary degree of the unknown polynomials τ, λ, γ, and μ. A need for high-degree polynomials may make this method computationally intractable, and there are examples of polynomial equations for

which high degrees are necessary to prove infeasibility [108]. Fortunately, numerical experience suggests that low-degree choices for τ, λ, γ, and μ often suffice for proving insolvability of the power flow equations. For instance, infeasibility certificates were generated using constant (degree zero) polynomials for the numeric examples shown in the Section 5.5.

5.4.2.3 Infeasibility Certificates for the Power Flow Equations Considering Reactive Power Limits

To find infeasibility certificates for the power flow equations with reactive power limited generators (5.1a), (5.1b), and (5.17), form the following polynomial.

$$\begin{aligned} H\left(V_d, V_q, x, V^+, V^-\right) = \; & \tau V_{q,slack} + \sum_{i\in\{\mathcal{PV},\mathcal{PQ}\}} \lambda_i \left(f_{Pi} - P_i\right) + \sum_{i\in\mathcal{PQ}} \gamma_i \left(f_{Qi} - Q_i\right) \\ & + \sum_{i\in\{\mathcal{S},\mathcal{PV}\}} \Big\{ \psi_{1i}\left((V_i^*)^2 - V_i^- + V_i^+ - f_{Vi}\right) + \psi_{2i}\left(Q_i^{max} - f_{Qi} - x_i\right) + \psi_{3i} V_i^- x_i \\ & \quad + \psi_{4i}\left(Q_i^{max} - Q_i^{min} - x_i\right) V_i^+ + s_{1i}\left(Q_i^{max} - Q_i^{min} - x_i\right) + s_{2i} V_i^+ + s_{3i} V_i^- + s_{4i} x_i \Big\} \end{aligned} \tag{5.20}$$

where ψ_{1i}, ψ_{2i}, ψ_{3i}, and ψ_{4i} are polynomials and s_{1i}, s_{2i}, s_{3i}, and s_{4i} are sum-of-squares polynomials. If the polynomials τ, λ, γ, and ψ and sum-of-squares polynomials s can be chosen such that $-H\left(V_d, V_q, x, V^+, V^-\right) - 1$ is a sum of squares, the power flow equations with consideration of reactive power limits on generators are insolvable.

As shown in (5.20), H is a quadratic function of the variables x, V^+, and V^- used to model the reactive power limits as well as the voltage components V_d and V_q. For an n-bus system with n_g reactive power limited generators and constant (degree zero) polynomials chosen for τ, λ, γ, ψ, and s, the number of monomials used in a sum-of-squares decomposition of H (i.e., the number of entries in z for the form (5.13)) is equal to $2n + 3n_g + 1$. Since the number of entries in the positive semidefinite matrix $\mathbf{Q}$ in (5.13) scales as the square of the number of monomials in z, a naïve implementation for creating infeasibility certificates becomes computationally intractable

for moderate size systems. However, pre-processing the sum-of-squares program with the Newton Polytope method [109] decreases the number of monomials required in the decomposition, thus reducing the computational burden of the sum-of-squares program. While this method improves computational tractability, further computational advances may be necessary for practical application to large-scale systems.

Experience with the IEEE test systems demonstrates that infeasibility certificates are not found with either degree zero or degree one polynomials when both upper and lower limits on generator reactive power outputs limits are modeled. Since the number of monomials required increases combinatorially with the degree chosen for the polynomials, choices of higher degree polynomials are not computationally tractable. However, infeasibility certificates are found by neglecting lower reactive power limits on generator outputs. If lower limits on reactive power outputs are not considered, (5.17) is simplified by eliminating equations (5.17d) and (5.17e) as well as V_i^+ in (5.17a) and (5.17f), with corresponding changes to (5.20). Since lower limits on reactive power outputs are rarely responsible for power flow insolvability through limit-induced bifurcations, neglecting the lower limits is an acceptable approximation for the large majority of cases.

5.5 Examples

This section next applies the mixed-integer semidefinite programming and the infeasibility certificate formulations to test systems using optimization codes YALMIP [64] and SeDuMi [59]. Consider a power injection profile where the active and reactive injections at both PQ and PV buses are uniformly increased at constant power factor as in (5.5).

This section first considers application to the IEEE 14-bus system [68]. The power injection margin calculated from (5.5) is $\eta^{max} = 1.3522$. Since the solution obtained from (5.5) satisfies the condition $\mathrm{rank}\,(\mathbf{W}) \leq 2$, the condition (5.8) indicates that a power flow solution exists for power injection changes in the direction of the specified profile up to an injection multiplier of 1.3522. The insolvability condition (5.7) indicates that no solutions exist for power injection multipliers greater than 1.3522.

Although the IEEE 14-bus system is small enough to find a global optimum to (5.5) with branch-and-bound techniques, this test case can also illustrate the use of the relaxations proposed in Section 5.3.3. With all $\mathbf{R}_{Ui}$ matrices being rank two, the relaxation of the integer constraints is not "tight." The resulting upper bound $\bar{\eta}^{max}$ of 5.3589 is well above the actual maximum value of 1.3522. In an attempt to obtain a lower bound $\underline{\eta}^{max}$, set to one all integer variables ψ_{Ui} and ψ_{Li} that are above a threshold of 0.5, with the remainder set to zero. (For this case, all $\psi_{Ui} = 1$ and $\psi_{Li} = 0$ except for the variables corresponding to the slack bus.) The solution to the resulting semidefinite optimization satisfies the rank condition (5.4) and therefore provides a lower bound $\underline{\eta}^{max}$ of 1.3522. Thus, the lower bound $\underline{\eta}^{max}$ for this case is equal to the actual value of η^{max}.

Considering only upper reactive power limits for computational tractability, an infeasibility certificate is found using (5.20) with constant (degree zero) polynomials for an injection multiplier of 1.36. This infeasibility certificate proves power flow insolvability for this power injection profile. Note that the infeasibility certificates do not directly provide a measure of the distance to the power flow solvability boundary. However, a measure can be calculated using binary search over loading cases in the direction of the specified power injection profile (uniform power injection changes for these examples).

In Figure 5.2, these results are verified by tracing the P-V curve while enforcing generator reactive power limits for the IEEE 14-bus system. When a generator reaches a reactive power limit, the bus is converted to a PQ bus with reactive power injection determined by the binding reactive power limit. The "nose point" of the P-V curve for this system occurs when all generators, including the generator at the slack bus, reach upper reactive power limits. Without the ability to enforce reactive power balance, the power flow solution disappears in a limit-induced bifurcation at a power injection multiplier of 1.3522, thus verifying both of the proposed sufficient conditions for power flow insolvability.

Table 5.5 shows the results of the proposed sufficient conditions for several of the IEEE test systems considering reactive power limited generators. The columns of Table 5.5 show 1.) the system name, 2.) the nose point identified by tracing the P-V curve of the high-voltage, stable

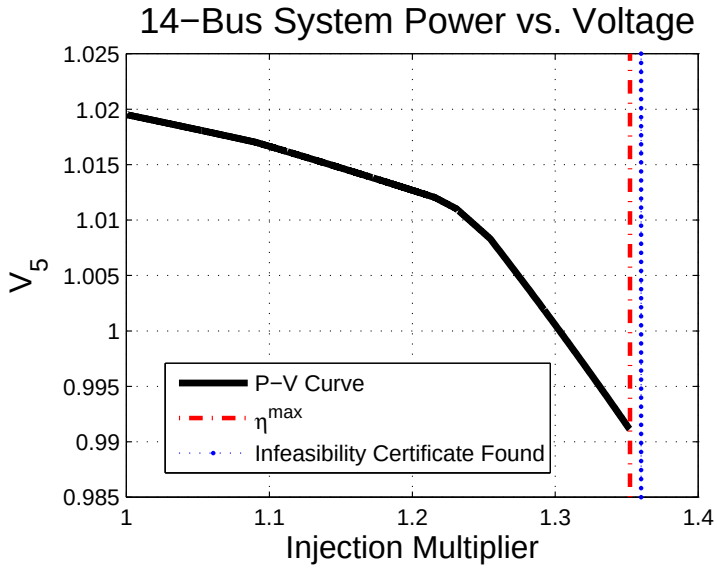

Figure 5.2 IEEE 14-Bus Power Injection Margin with Generator Reactive Power Limits

System	Trace Nose Point	η^{max}	$\bar{\eta}^{max}$	$\underline{\eta}^{max}$	Infeasibility Certificate
14-bus	1.3522	1.3522	5.3589	1.3522	1.36
30-bus	2.8609	2.8609	3.3218	N/A	2.86
57-bus	1.6486	1.6486	4.4261	1.6486	1.65

Table 5.1 Stability Margins For IEEE Test Systems Considering Reactive Power Limited Generators

power flow solution, 3.) the value of η^{max} for a global solution to (5.5) calculated using branch-and-bound techniques, 4.) an upper bound $\bar{\eta}^{max}$ resulting from relaxing the integer constraints with (5.10), 5.) a lower bound $\underline{\eta}^{max}$ resulting from the technique described in Section 5.3.3, and 6.) the smallest power injection multiplier for which an infeasibility certificate is found using constant (degree zero) polynomials and only upper limits on reactive power generation. A case for which no lower bound $\underline{\eta}^{max}$ could be estimated (i.e., the solution did not satisfy the rank condition (5.4)) is denoted with "N/A" in the fifth column of Table 5.5.

Note that the only method with a guarantee of the actual distance to the power flow solvability boundary is a global solution to the mixed-integer semidefinite programming formulation (5.5)

that satisfies the rank condition (5.4). (The rank condition is satisfied by solutions to the IEEE 14, 30, and 57-bus systems.) The remaining methods provide upper bounds ($\bar{\eta}^{max}$, η^{max} with a solution that does not satisfy the rank condition (5.4), and infeasibility certificates) and lower bounds (tracing the P-V curve and $\underline{\eta}^{max}$ with a solution that satisfies the rank condition (5.4)) on the actual distance to the power flow solvability boundary.

The results in Table 5.5 verify the proposed sufficient conditions for power flow insolvability. The voltage margin η^{max} from (5.5) matches the nose points of the P-V curves. Although the upper bound $\bar{\eta}^{max}$ does not give a result close to the nose point, the lower bound $\underline{\eta}^{max}$, when calculable, matches the actual value η^{max}. Finally, infeasibility certificates identify the nose point for each test case.

Infeasibility certificates can also be found without considering reactive power limits on generators. As shown in Chapter 4 for the IEEE 118-bus system, there may be loadings for which no power flow solution is found but the sufficient conditions for power flow insolvability are not satisfied. Using (5.19), the smallest injection multiplier certified infeasible with constant (degree zero) polynomials is equal to the power injection margin calculated using the semidefinite-programming-based sufficient condition for power flow insolvability described in Chapter 4. (Specifically, while the nose point resulting from a continuation trace of the high-voltage, stable solution is at an injection multiplier of 3.18, both the sufficient condition for insolvability from Chapter 4 and a degree-zero infeasibility certificate are first satisfied at an injection multiplier of 3.27.) This suggests the possibility of a deeper connection between the infeasibility certificates with degree-zero polynomials and the semidefinite-programming-based sufficient condition for power flow insolvability, at least for cases without reactive power limited generators. (Note that computational limitations preclude use of higher-order polynomials, which may more closely identify the nose point.)

5.6 Conclusion

This chapter has presented two sufficient conditions for power flow insolvability considering reactive power limited generators. The first condition formulates a mixed-integer semidefinite program to determine a global voltage stability margin. This margin gives a bound on the distance to the power flow solvability boundary and can be applied to both solvable and insolvable sets of power injections. For solutions that satisfy a rank condition, the proposed formulation gives the exact distance to the solvability boundary (i.e., a guarantee of the "nose point" of the P-V curve). The margin gives a sufficient condition for power flow insolvability with consideration of reactive power limited generators.

The second sufficient condition creates infeasibility certificates to prove power flow insolvability. Writing the power flow equations, including reactive power limits on generators, as a system of polynomial equalities and inequalities allows for application of the Positivstellensatz theorem from the field of real algebraic geometry. If a specified polynomial can be written in sum-of-squares form, which is determined using semidefinite programming, the power flow equations are proven insolvable.

Both sufficient conditions, along with several approximations to improve computational tractability, are applied to IEEE test systems. The results show that the sufficient conditions are capable of identifying the distance to the power flow solvability boundary with consideration of reactive power limited generators.

Chapter 6

Multiple Solutions to the Power Flow Equations

6.1 Introduction

The previous two chapters considered conditions for non-existence of solutions to the power flow equations. Next, this chapter investigates questions related to multiple solutions to the power flow equations. These solutions correspond to the equilibrium points of the underlying differential equations that govern power system dynamic behavior; it is well known that large numbers of such solutions can exist [110]. Power systems are typically operated at the high-voltage, stable solution, for which numerous solution techniques have been developed (e.g., Newton-Raphson, Gauss-Seidel, etc.). However, other solutions are also of interest. For instance, multiple solutions, particularly those exhibiting low-voltage magnitude, are important to power system stability assessment and bifurcation analysis [36–40].

A direct approach to finding multiple power flow solutions simply initializes Newton-Raphson iterations [9] over a range of carefully selected candidate initial conditions. However, this approach does not guarantee obtaining all power flow solutions. In another approach, Salam et al. [42] apply the homotophy method of Chow et al. [43] to the power flow problem. This method can reliably find all solutions, but has a computational complexity that grows exponentially with system size. It is not computationally tractable for large systems.

Ma and Thorp published a continuation-based algorithm that they claimed would reliably find all solutions to the power flow equations [44, 45]. Since the computational complexity of this algorithm scales with the number of actual rather than possible solutions, it is computationally tractable for large systems. A similar algorithm is used to find all type-1 power flow solutions [46].

Type-1 solutions are those where the Jacobian of the power flow equations has a single eigenvalue with positive real part. Type-1 solutions are closely related to voltage instability phenomena [47].

The completeness proof of Ma and Thorp's continuation-based algorithm (i.e., the claim that the algorithm will find all power flow solutions for all systems) is shown to be flawed in the appendix of the thesis of reference [48]. That thesis, however, does not provide a counterexample to the completeness claim. In Section 6.2, this chapter provides a five-bus system counterexample to the completeness claim; the continuation-based algorithm fails to find all solutions to the power flow equations for this system. Since this system contains a type-1 solution, the continuation-based algorithm also fails to obtain every type-1 solution. This work is published as [111].

Since other methods for finding all solutions to the power flow equations are not computationally tractable for large systems, current literature offers no method for reliably computing all solutions to the power flow equations for practically sized systems. Other methods for calculating multiple power flow solutions are therefore worthy of research. In Section 6.3, this chapter next describes a method for calculating multiple solutions using the semidefinite relaxation of the power flow equations. This method modifies the constraints and the objective function of the OPF problem to find a solution with desired voltage magnitude characteristics. Specifically, the objective function is chosen to be a linear function of squared voltage magnitudes. In the two test cases examined, this method was successful in finding all of the power flow solutions. Although not all choices of objective functions yielded physically meaningful solutions, objective functions capable of finding all solutions for the two test systems were identified. This work is published as [83].

6.2 Counterexample to a Continuation-Based Algorithm for Finding All Power Flow Solutions

This section presents a five-bus system counterexample to the claim that the continuation-based algorithm will reliably find all solutions to the power flow equations. All ten solutions to the five-bus system were calculated using a homotopy method [42].

Results obtained from applying the continuation-based algorithm to the five-bus system show that there are three groups of solutions that, while connected by continuation traces to all other solutions within the group, are not connected to solutions outside of the group. Thus, the continuation-based algorithm fails to find all solutions. Further, since a type-1 solution exists for this system, the five-bus system also provides an example where the continuation-based algorithm fails to find every type-1 solution. Finally, in the specific context of the five-bus system, this section illustrates a flaw (originally identified in [48]) in the proof for completeness of the continuation-based algorithm [45].

6.2.1 Overview of the Continuation-Based Algorithm

The continuation-based algorithm [44,45] modifies the power flow equations by adding a scalar parameter α to the active or reactive power equation of a single bus. This modification eliminates the Jacobian singularity typically encountered at the "nose" of the power versus voltage (P-V) curve of the unmodified power flow equations. The algorithm starts from a single power flow solution obtained using traditional methods (e.g., Newton-Raphson). A continuation trace is created by incrementally solving the modified power flow equations after taking a small step in a direction dictated by the Jacobian of the modified power flow equations [112]. Solutions to the power flow equations are obtained when $\alpha = 0$. The continuation trace terminates when the trace returns to its starting point. Existing literature claims that all solutions are connected by these continuation traces [44, 45]. Thus, if continuation traces are started from each solution for each parameter (i.e., each solution/parameter pair) all solutions will be obtained; at most $\frac{ns}{2}$ continuation traces are required to find all solutions, where n is the number of buses and s is the number of solutions.

6.2.2 Five-Bus System Counterexample

The five-bus system given in Figure 6.1 provides a counterexample to the claim that the continuation-based algorithm finds all solutions to the power flow equations for all power systems. Line values are given in per unit impedance and power injections are given in MW. The system uses a 100 MVA base.

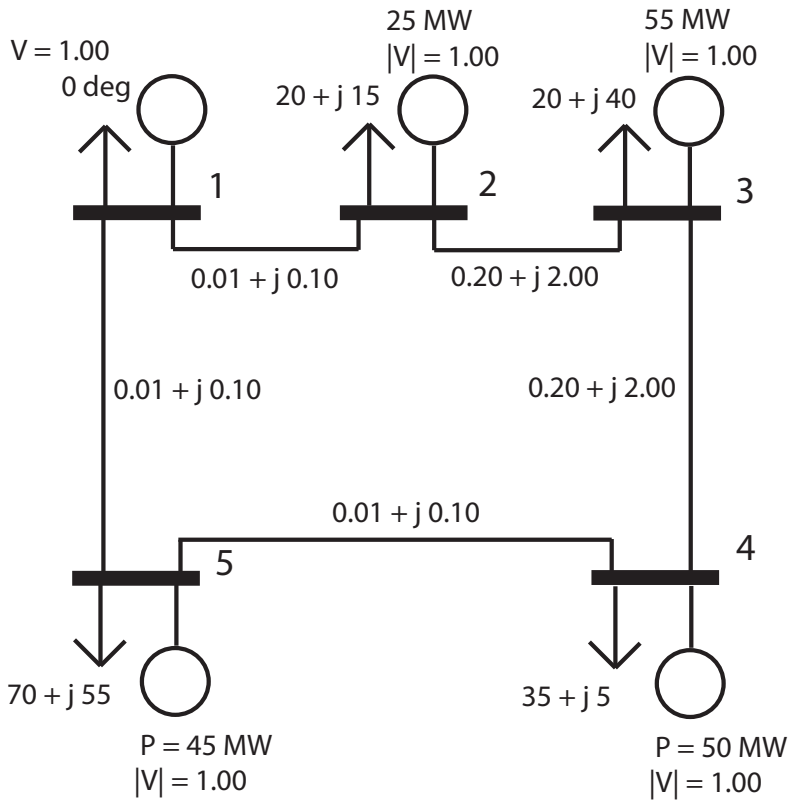

Figure 6.1 Five-Bus System Counterexample

It is expected that the algorithm may fail to find all solutions for systems with non-radial, weakly connected regions that have strong voltage support. In this example, bus three is weakly connected (i.e., connected via high impedance lines) to the rest of the network. Since they consist of PV buses, both bus three and the rest of the network (including the slack bus at bus one) have strong voltage support.

The ten solutions to the power flow equations for the five-bus system are given in Table 6.1. Since the system contains only slack and PV buses, the voltage magnitude is specified at each bus (all voltage magnitudes are 1.000 per unit). δ_i is the voltage angle at bus i in degrees.

The continuation traces for this system using active power parameters and starting from solution one are shown in Figure 6.2. These continuation traces only contain solutions one and two. The continuation traces started from solution two are identical to those in Figure 6.2 and also only contain solutions one and two. These continuation traces do not find solutions three though ten.

Thus, solutions one and two are disconnected from the eight other solutions. Similarly, continuation traces started from solutions three and four only find solutions three and four, and continuation traces started from any of the remaining solutions five through ten only find solutions five through ten. The continuation-based algorithm therefore fails to find all solutions.

The eigenvalues of the power flow Jacobian were evaluated at each solution. With a single eigenvalue that has positive real part, solution two is the only type-1 solution. This solution cannot be reached from continuation traces that start from solutions three through ten. Thus, the five-bus system also provides a counterexample to the claim in reference [46] that the continuation-based algorithm can reliably find every type-1 solution.

Solution	δ_1	δ_2	δ_3	δ_4	δ_5
1	0	1.286	22.061	2.194	0.372
2	0	0.166	171.198	0.028	-0.710
3	0	-169.906	-148.192	-167.129	-168.909
4	0	-168.702	3.182	-167.131	-167.912
5	0	2.187	45.923	46.616	-143.973
6	0	-168.657	-172.863	44.012	-145.341
7	0	-171.391	-99.227	50.716	-141.807
8	0	-0.897	-168.405	44.388	-145.144
9	0	-169.370	-10.988	165.903	-25.378
10	0	-169.282	-160.897	166.147	-22.898

Table 6.1 All Solutions to the Five-Bus System

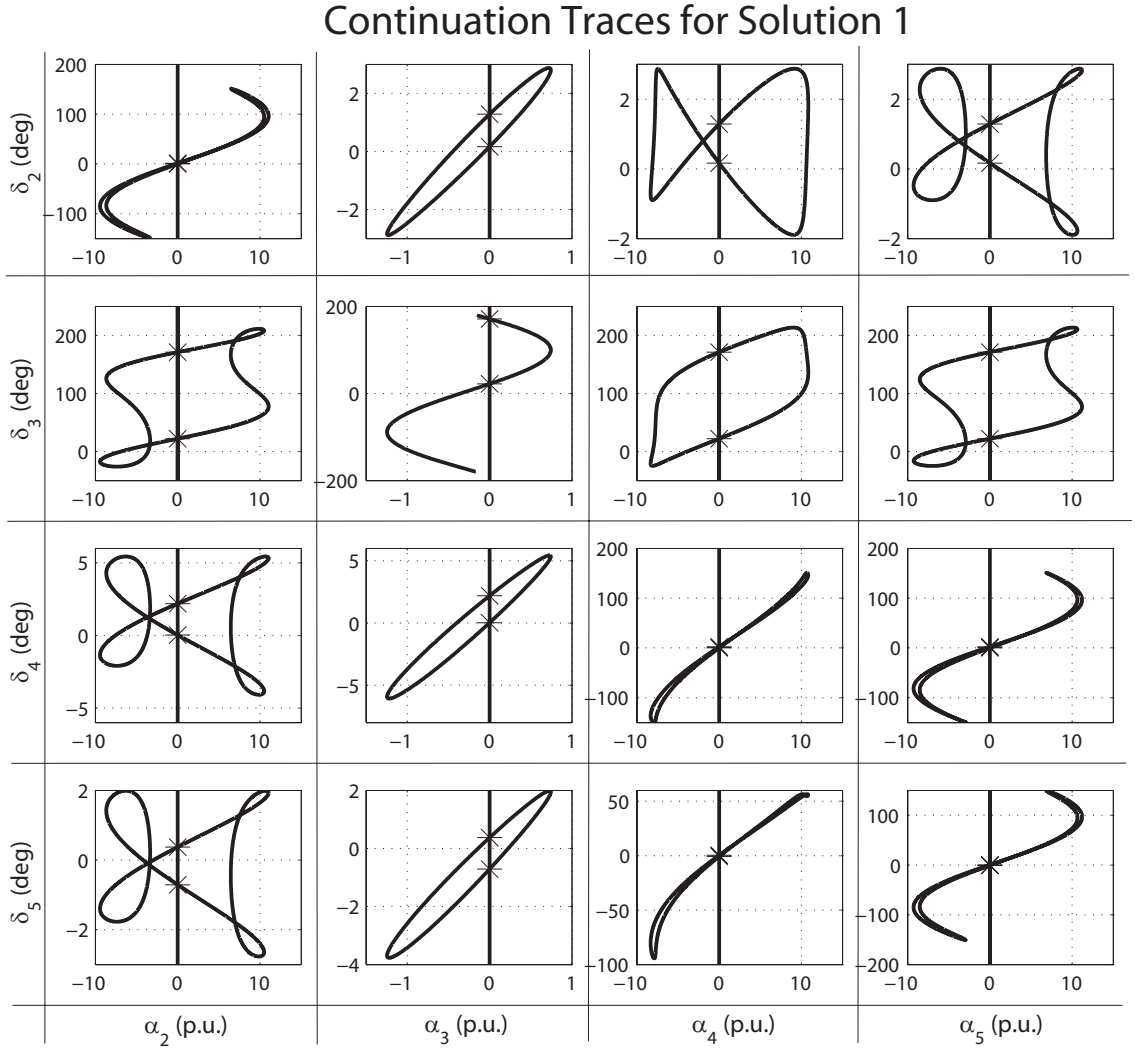

Figure 6.2 Continuation Traces for Solution 1

6.2.3 Completeness Proof Flaw

Reference [45] contains a completeness proof that claims to show that this continuation-based method will find all power flow solutions. This section concludes by illustrating a flaw in this proof. The proof assigns binary labels b of length equal to $n-1$ to each solution, where n is the number of buses in the system. b_i represents the i^{th} bit of b corresponding to bus i. This section

focuses on the binary labels for PV buses since the five-bus example system does not have PQ buses; a description of binary labels for PQ buses is contained in Section 3 of [45].

To calculate the value of b_i corresponding to PV bus i, first consider the active power injection equation

$$V_i^2 \operatorname{Re}(\mathbf{Y}_{ii}) + V_i \sum_{\substack{k=1,\ldots,n \\ k \neq i}} (V_k |\mathbf{Y}_{ik}| \cos(\delta_i - \delta_k - \theta_{ik})) - P_i = 0 \tag{6.1}$$

where $\mathbf{Y}_{ik}$ is the (i,k) element of the bus admittance matrix, θ_{ik} is the angle of $\mathbf{Y}_{ik}$, and P_i is the active power injection at bus i. V_i and δ_i are the voltage magnitude and angle, respectively, at bus i.

Combine the cosine terms to rewrite (6.1) as

$$V_i^2 \operatorname{Re}(\mathbf{Y}_{ii}) + V_i A_i \cos(\delta_i - \Lambda_i) - P_i = 0 \tag{6.2}$$

Then assign $b_i = 0$ if δ_i is to the left of Λ_i (equivalently, $\sin(\delta_i - \Lambda_i) > 0$). Otherwise assign $b_i = 1$.

Reference [45] asserts that each solution produces a unique binary label. The completeness proof in reference [45] requires unique binary labels in order to form a reversible map from each solution to a binary cube (each solution point is the sole occupant of one of the corners of the binary cube). However, as shown in Table 6.2, solutions six and ten and solutions seven and nine for the five-bus example system have identical binary labels. Note that non-unique binary labels are also possible for systems with PQ buses. (See [48] for an example three-bus system.) Since each solution does not necessary produces a unique binary label, the assertion in reference [45] that "every solution point is connected to exactly another solution point from every dimension of the binary cube" is not true for all systems, and the completeness proof fails.

Theorem 4 in reference [45] claims that 2^{n-1} is an upper bound to the number of power flow solutions for an n-bus system. This theorem relies on the binary label uniqueness and is therefore potentially flawed. Indeed, Baillieul and Brynes [35] identified six solutions to a three-bus system, which is greater than the claimed upper bound of $2^{3-1} = 4$ solutions.

Solution	Bus 2	Bus 3	Bus 4	Bus 5
1	1	1	1	1
2	1	0	1	1
3	0	1	1	0
4	0	0	1	0
5	1	1	0	0
6	**0**	**1**	**0**	**0**
7	*0*	*0*	*0*	*0*
8	1	0	0	0
9	*0*	*0*	*0*	*0*
10	**0**	**1**	**0**	**0**

Table 6.2 Binary Labels for Solutions to the Five-Bus System

6.3 Calculating Multiple Power Flow Solutions Using Semidefinite Programming

The counterexample in the previous section indicates that current literature offers no computationally tractable method for reliably computing all solutions to the power flow equations. Other methods for calculating multiple power flow solutions therefore deserve additional research. This section investigates application of semidefinite programming to the problem of finding multiple power flow solutions. Five and seven-bus example systems whose modest dimension allow for identification of all solutions using a homotopy method [42] are used as test cases. A semidefinite relaxation of the power flow equations is used to replicate these solutions. (See Section 1.2 for an overview of the power flow equations and Section 1.5 for a description of the semidefinite relaxation of the power flow equations.) Two variants of the semidefinite programming relaxation were attempted: one modifying constraints, the other modifying the objective function. The constraint modification proved wholly unsuccessful. Objective modification had varying success as will be described in more detail.

6.3.1 Example Systems

The five and seven-bus systems shown in Figures 6.3 and 6.4 are used to demonstrate both approaches. Load demand, generation injections, and voltage magnitudes in Figures 6.3 and 6.4 are given in per unit. Network values in Figures 6.3 and 6.4 are given as per unit impedances. All power flow solutions for these systems have been calculated using a homotopy method [42], and are summarized in Tables 6.3 and 6.4.

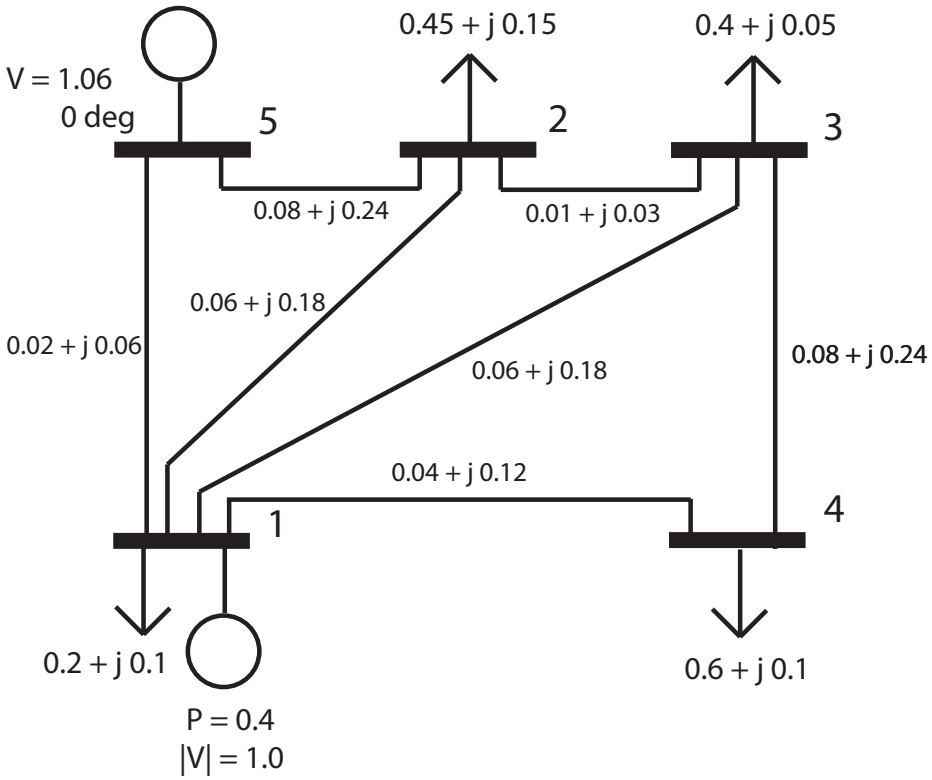

Figure 6.3 Five-Bus Example System

	Solution				
	1	2	3	4	5
V_1	1.0000	1.0000	1.0000	1.0000	1.0000
V_2	0.9805	0.5012	0.3770	0.7933	0.0626
V_3	0.9771	0.5879	0.4108	0.7403	0.2160
V_4	0.9662	0.8317	0.0666	0.0580	0.6982
V_5	1.0600	1.0600	1.0600	1.0600	1.0600
δ_1	-2.0675	-138.9679	-128.5864	-12.1469	-126.6253
δ_2	-4.5358	-129.8511	-116.8370	-12.6793	-159.5293
δ_3	-4.8535	-134.8640	-124.1731	-13.8795	-144.7963
δ_4	-5.6925	-141.6605	-185.7340	-71.5017	-133.4401
δ_5	0.0000	0.0000	0.0000	0.0000	0.0000
	Solution				
	6	7	8	9	10
V_1	1.0000	1.0000	1.0000	1.0000	1.0000
V_2	0.1972	0.0563	0.0342	0.1968	0.0884
V_3	0.0301	0.0496	0.1846	0.0369	0.1658
V_4	0.6289	0.6327	0.6865	0.0814	0.0756
V_5	1.0600	1.0600	1.0600	1.0600	1.0600
δ_1	-16.5040	-18.0976	-16.9090	-22.5210	-119.8826
δ_2	-26.0422	-61.1266	-69.0465	-30.6818	-141.8399
δ_3	-81.8652	-80.6706	-37.7869	-85.9455	-144.7567
δ_4	-23.4519	-25.4435	-23.8729	-79.4189	-178.4992
δ_5	0.0000	0.0000	0.0000	0.0000	0.0000

Table 6.3 The Ten Solutions for the Five-Bus System

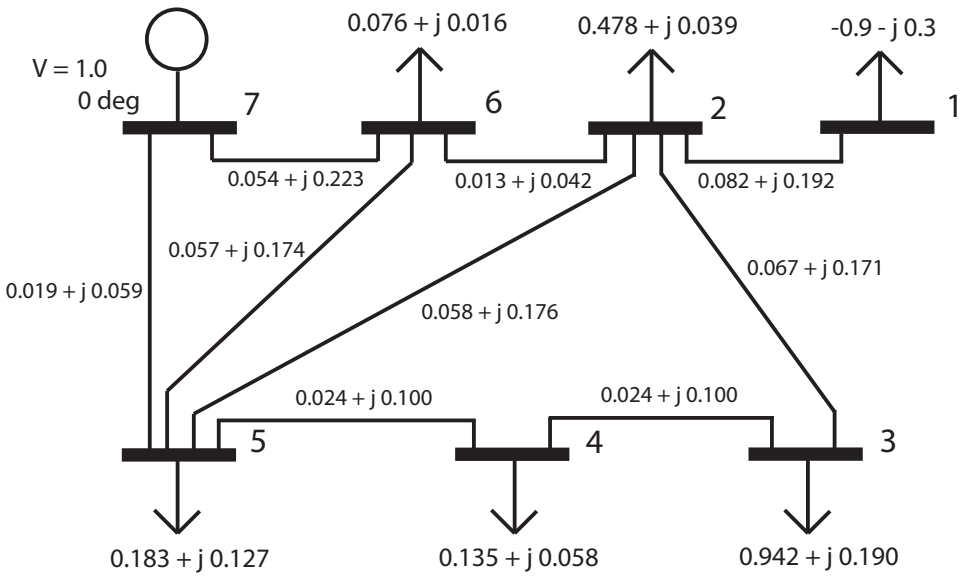

Figure 6.4 Seven-Bus Example System

	Solution			
	1	2	3	4
V_1	1.0758	0.7312	0.2880	0.3435
V_2	0.9635	0.5876	0.5415	0.4332
V_3	0.9041	0.1745	0.5430	0.2497
V_4	0.9278	0.4122	0.6458	0.4359
V_5	0.9638	0.7229	0.7750	0.6879
V_6	0.9675	0.6638	0.6402	0.5496
V_7	1.0000	1.0000	1.0000	1.0000
δ_1	5.2859	14.9576	101.8188	88.3361
δ_2	-2.9342	-5.2212	-6.2931	-6.8346
δ_3	-8.4439	-52.6775	-19.8095	-44.2797
δ_4	-5.7500	-14.2056	-11.2462	-16.1362
δ_5	-2.4463	-3.2056	-3.8617	-3.9193
δ_6	-2.5918	-4.3031	-5.0158	-5.3138
δ_7	0.0000	0.0000	0.0000	0.0000

Table 6.4 The Four Solutions for the Seven-Bus System

6.3.2 Modifying the Constraints

The first approach to finding multiple solutions seeks to differentiate among possible solutions by imposing an inequality constraint on slack bus active power while minimizing slack bus active power injection:

$$\min_{\mathbf{W}} \quad \text{trace}\,(\mathbf{Y}_{slack}\mathbf{W}) \qquad \text{subject to} \tag{6.3a}$$

$$\text{trace}\,(\mathbf{Y}_{slack}\mathbf{W}) \geq \xi \tag{6.3b}$$

$$\text{trace}\,(\mathbf{Y}_k\mathbf{W}) = P_k \qquad \forall\, k \in \{\mathcal{PQ},\, \mathcal{PV}\} \tag{6.3c}$$

$$\text{trace}(\bar{\mathbf{Y}}_k\mathbf{W}) = Q_k \qquad \forall\, k \in \mathcal{PQ} \tag{6.3d}$$

$$\text{trace}\,(\mathbf{M}_k\mathbf{W}) = V_k^2 \qquad \forall\, k \in \{\mathcal{S},\, \mathcal{PV}\} \tag{6.3e}$$

$$\mathbf{W} \succeq 0 \tag{6.3f}$$

where ξ is a specified scalar parameter.

The power flow solution having least power generated by the slack bus corresponds to the solution with lowest losses. This base solution (i.e., the solution to (6.3) with $\xi = -\infty$) is found with no inequality constraint. Imposing a minimum slack bus power constraint greater than the slack bus power in the base solution, such that (6.3b) is a binding constraint, forces the optimization problem to another solution with higher losses. However, in all such cases examined, the solution to the semidefinite relaxation has a non-zero relaxation gap and fails to yield a physically meaningful solution to the power flow equations.

An alternate formulation examined selects slack bus active power generation as an objective to be maximized. The solution with highest losses for the five-bus system, solution three in Table 6.3, is obtained via semidefinite programming in this way. Other examples, including the seven-bus system, identifies only non-zero relaxation gap solutions with this objective function.

Constraining the voltage magnitudes at PQ buses to be below the base solution also fails; imposing such voltage constraints yields only non-zero relaxation gap solutions.

6.3.3 Modifying the Objective Function

Next considered is an objective function based on bus voltage magnitudes:

$$\min_{\mathbf{W}} \sum_{i=1}^{n} c_i \operatorname{trace}(\mathbf{M}_i \mathbf{W}) \qquad \text{subject to} \tag{6.4a}$$

$$\operatorname{trace}(\mathbf{Y}_k \mathbf{W}) = P_k \qquad \forall\, k \in \{\mathcal{PQ},\, \mathcal{PV}\} \tag{6.4b}$$

$$\operatorname{trace}(\bar{\mathbf{Y}}_k \mathbf{W}) = Q_k \qquad \forall\, k \in \mathcal{PQ} \tag{6.4c}$$

$$\operatorname{trace}(\mathbf{M}_k \mathbf{W}) = V_k^2 \qquad \forall\, k \in \{\mathcal{S},\, \mathcal{PV}\} \tag{6.4d}$$

$$\mathbf{W} \succeq 0 \tag{6.4e}$$

where c is a specified vector of weights; that is, the objective function in (6.4a) is a weighted sum of squared voltage magnitudes. Appropriate choices of the weights in c favored different solutions based on their voltage magnitude characteristics.

This method identified all of the ten solutions in the five-bus system, as summarized in Table 6.5, and all of the four solutions in the seven-bus system, as summarized in Table 6.6. Solutions above the line in Tables 6.5 and 6.6 were found using heuristically determined weights c. Similar heuristically determined weights were identified that were expected to find the remaining solutions (solutions three, five, and ten for the five-bus system and solution four in the seven-bus system); however, the semidefinite relaxation for these heuristically determined weights had non-zero relaxation gap solutions. Alternatively, testing a variety of randomly generated weights yielded the combinations below the lines in Tables 6.5 and 6.6 that found the remaining solutions.

Non-zero relaxation gap solutions can be used to estimate approximate, candidate solutions. As a heuristic, the closest rank one matrices to these non-zero relaxation gap solutions were used as initial conditions for a Newton-Raphson power flow solver. With this approach, some but not all of the non-zero relaxation gap solutions resulted in convergence to power flow solutions for the five and seven-bus systems.

Solution	c_1	c_2	c_3	c_4	c_5
1	0	-1	-1	-1	0
2	0	1	-1	0	0
4	0	0	0	1	0
6	0	0	1	0	0
7	0	1	1	0	0
8	0	1	0	0	0
9	0	0	1	1	0
3	0	0.65	-0.70	0.90	0
5	0	0.70	-0.10	-0.15	0
10	0	0.45	-0.25	0.50	0

Table 6.5 Combinations of Weights c and Corresponding Solutions for Five-Bus System

Solution	c_1	c_2	c_3	c_4	c_5	c_6	c_7
1	-1	-1	-1	-1	-1	-1	0
2	0	0	1	0	0	0	0
3	1	0	0	0	0	0	0
4	0.30	-0.20	0.35	0.45	-0.40	0.05	0

Table 6.6 Combinations of Weights c and Corresponding Solutions for Seven-Bus System

6.4 Conclusion

This chapter has first presented a five-bus system counterexample to the claim in existing literature that a continuation-based algorithm is capable of finding all solutions to the power flow equations for all systems. Since other methods for finding all solutions to the power flow equations are not computationally tractable for large systems, current literature offers no method for reliably computing all solutions to the power flow equations for practically sized systems.

A flaw in the proof used to justify this claim has been demonstrated using the five-bus system. Furthermore, the five-bus system was used to show that the continuation-based algorithm is not

capable of reliably finding every type-1 solution (i.e., a solution where the power flow Jacobian has a single eigenvalue with positive real part). The five-bus system has a non-radial, weakly connected region that has strong voltage support. The continuation-based algorithm may fail for other systems with similar structure.

This counterexample indicates the need for further research in finding multiple solutions to the power flow equations. For this purpose, this chapter formulates families of semidefinite relaxations of the power flow equations by modifying the constraints and objective function. In the test cases examined, the modified objective approach was successful in finding all of the power flow solutions. Although not all objective functions yielded physically meaningful solutions, objective functions capable of finding all solutions were identified. However, the proposed method is not guaranteed to find all power flow solutions. Further research is necessary for both the proposed method (e.g., determining a systematic approach for identifying objective functions that result in physically meaningful solutions) and other methods for reliably calculating all power flow solutions.

Chapter 7

Investigation of Non-Zero Relaxation Gap Solutions

7.1 Introduction

This dissertation has investigated applications of a semidefinite relaxation of the power flow equations. When this relaxation is "tight" (i.e., satisfies a rank condition for obtaining a zero relaxation gap solution), a globally optimal solution is recoverable. However, this relaxation is not tight for all practical problems of interest, resulting in non-zero relaxation gap solutions. This chapter investigates non-zero relaxation gap solutions using three applications of the semidefinite relaxation of the power flow equations: the optimal power flow problem (i.e., work from Chapters 2 and 3), a formulation used to determine voltage stability margins (i.e., work from Chapters 4 and 5), and a formulation for determining multiple solutions to the power flow equations (i.e., work from Chapter 6).

The first application of the semidefinite relaxation is to the optimal power flow (OPF) problem. This problem seeks decision variable values to yield an optimal operating point for an electric power system in terms of a specified objective and subject to a wide range of engineering inequality constraints (e.g., active and reactive power generation, bus voltage magnitudes, transmission line and transformer flows, etc.) and network equality constraints (i.e., the power flow equations). Total generation cost is the typical objective; other objectives, such as loss minimization, may be considered. See Chapters 1 and 3 for a more detailed overview of the OPF problem.

Although the semidefinite relaxation yields zero relaxation gap solutions (i.e., the relaxation is "tight") for many OPF problems, there are practical OPF problems which have non-zero relaxation

gap solutions. (See Chapter 2 and references [76, 77].) Such solutions to the semidefinite relaxation provide lower bounds on the optimal objective value but do not give physically meaningful solutions to the original engineering quantities of interest in the OPF problem. Existing literature studies cases for which the semidefinite relaxation of the OPF problem is tight by providing sufficient conditions for zero relaxation gap solutions. These conditions include highly limiting requirements on power injection and voltage magnitude limits and either radial networks (typical only of distribution system models) or unrealistically dense placement of controllable phase shifting transformers [69–72]. Research explaining why the semidefinite relaxation of the OPF problem may yield solutions with non-zero relaxation gap is limited to [76, 77], which present test OPF problems with locally optimal solutions in the feasible space.

The second application of the semidefinite relaxation involves evaluation of a sufficient condition for power flow insolvability, which yields voltage stability margins to the power flow solvability boundary. (See Chapters 4 and 5.) Since the sufficient condition for power flow insolvability uses the semidefinite relaxation to provide a lower bound on the objective value, zero relaxation gap solutions are not required. However, for cases with non-zero relaxation gap solutions, the sufficient condition for power flow insolvability may not be satisfied even if the power flow equations are indeed insolvable. That is, the sufficient condition is not also a necessary condition for insolvability. For non-zero relaxation gap solutions, the voltage stability margins resulting from this sufficient condition overestimate the actual distance to the power flow solvability boundary.

The third application of the semidefinite relaxation is a formulation for finding multiple solutions to the power flow equations. (See Chapter 6.) This application requires that the solution to the semidefinite relaxation has zero relaxation gap; solutions with non-zero relaxation gap are not physically meaningful, although they may yield good initial guesses for a traditional power flow solution method (e.g., Newton-Raphson iteration).

All three of these applications of the semidefinite relaxation of the power flow equations would benefit from understanding the causes of non-zero relaxation gap solutions. One cause of non-zero relaxation gap solutions is a disconnected feasible space with components near a global optimum.

This cause of non-zero relaxation gap solutions can be considered using the geometry of the feasible space of the semidefinite relaxation. The semidefinite relaxation forms a convex space that contains the entire feasible space defined by the power flow equations. Nearby disconnected components may result in the semidefinite relaxation finding a solution "between" the disconnected components of the feasible space defined by the power flow equations which is nonetheless in feasible space of the semidefinite program. This chapter expands on the two-bus test system from [76] and provides an additional three-bus example system with disconnected feasible space that yields a non-zero relaxation gap solution. Existing work in this area also includes an archive of test cases with local optima [77]. For these systems, the semidefinite relaxation of the OPF problem has limited success in obtaining zero relaxation gap solutions to cases with local optima; eight of the ten test cases with local optima yield non-zero relaxation gap solutions for some choice of parameters.

Non-zero relaxation gap solutions may also result from other types of non-convexity. For instance, the semidefinite relaxation of the OPF problem yields a non-zero relaxation gap solution to a five-bus example from [49], which has connected but non-convex feasible space.

Using insights from these small systems, this chapter next studies larger systems that yield non-zero relaxation gap solutions. Using the rank one matrix closest to the non-zero relaxation gap solution, this chapter evaluates the active and reactive power "mismatches" to the injections specified at load (PQ) buses. For the cases studied, this analysis shows that small subsets of the network have large mismatches while the mismatches at the majority of the buses are insignificant. For some systems with non-zero relaxation gap solutions, minor perturbations in specified system data result in zero relaxation gap solutions. In other words, small problematic subsets of the network may cause non-zero relaxation gap solutions. Perturbations to these subsets of the network resulted in zero relaxation gap solutions. However, these perturbations were determined heuristically by examining the power injection mismatches and could only be determined for some systems; no robust method of identifying all such modifications has yet been identified.

Further analysis shows that radially connecting a small system with non-zero relaxation gap solution to a larger system with zero relaxation gap solution results in the solution to the merged

system having non-zero relaxation gap. This also suggests that non-zero relaxation gap solutions to large system models may be due to non-convexity in a small subset of the system.

In addition to OPF problems, this chapter also investigates non-zero relaxation gap solutions associated with the sufficient condition for power flow insolvability presented in Chapter 4. When the solution to the semidefinite program used to evaluate this condition has non-zero relaxation gap, the condition may not indicate insolvability for some cases that nonetheless do not appear to have a solution, and voltage stability margins calculated from this condition overestimate the apparent distance to the power flow solvability boundary. Non-zero relaxation gap solutions occur when there exist many power flow solutions near the power flow solvability boundary (i.e., the "nose point" of the power versus voltage (P-V) curve); conversely, solutions with zero relaxation gap occur when only two solutions bifurcate near the power flow solvability boundary. This is illustrated with examples from the IEEE 14 and 118-bus systems.

The semidefinite formulation used in Chapter 6 to find multiple power flow solutions provides another viewpoint on non-zero relaxation gap solutions. This formulation specifies an objective function in terms of squared voltage magnitudes. Non-zero relaxation gap solutions result when an objective function is chosen such that multiple power flow solutions have similar objective function values (i.e., nearby disconnected components of the feasible space defined by the power flow equations). This is illustrated with the five-bus example system used in Chapter 6.

This chapter is organized as follows. Section 7.2 discusses non-zero relaxation gap solutions to the semidefinite relaxation of the OPF problem. Section 7.3 next provides examples of non-zero relaxation gap solutions to the semidefinite programming formulation used to evaluate a sufficient condition for power flow insolvability. Section 7.4 then describes non-zero relaxation gap solutions to the semidefinite programming formulation used to find multiple solutions to the power flow equations. Section 7.5 gives concluding comments. The OPF analysis in Section 7.2 is submitted for publication as [113].

7.2 Non-Zero Relaxation Gap Solutions to OPF Problems

As shown in Chapters 2 and 3, the semidefinite relaxation of the power flow equations yields non-zero relaxation gap solutions for some OPF problems. This section first explores non-zero relaxation gap solutions to small example systems for which the feasible spaces can be conveniently visualized. This section then analyzes non-zero relaxation gap solutions to large OPF problems.

7.2.1 Feasible Space Exploration

The semidefinite relaxation does not yield zero relaxation gap solutions for all practical OPF problems. (See Chapters 1 and 3 for overviews of the OPF problem with both classical and semidefinite relaxation formulations.) A non-zero relaxation gap solution provides a lower bound on the optimal objective value of the OPF problem, but does not yield a physically meaningful solution (i.e., a non-zero relaxation gap solution does not provide a voltage profile that satisfies the power flow equations). One explanation for non-zero relaxation gap solutions is non-convexity due to a disconnected feasible space. This source of non-convexity is first explored using the two-bus example system from [76], which is reproduced as Figure 7.1.

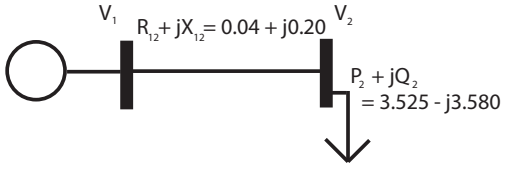

Figure 7.1 Two-Bus System from [76]

The line in this system has impedance $R + jX = 0.04 + j0.20$ per unit, with no line-flow limit. The load demand at bus 2 is $P_{D2} + jQ_{D2} = 3.525 - j3.580$ per unit using a 100 MVA base. There are no limits on active and reactive power injections at bus 1. The voltage magnitude at bus 1 is constrained to the range $[0.95, 1.05]$ per unit. The voltage magnitude at bus 2 has a lower bound of 0.95 per unit and an upper bound of V_2^{max}. The objective function minimizes the cost of a \$1/MWh active power generation at bus 1.

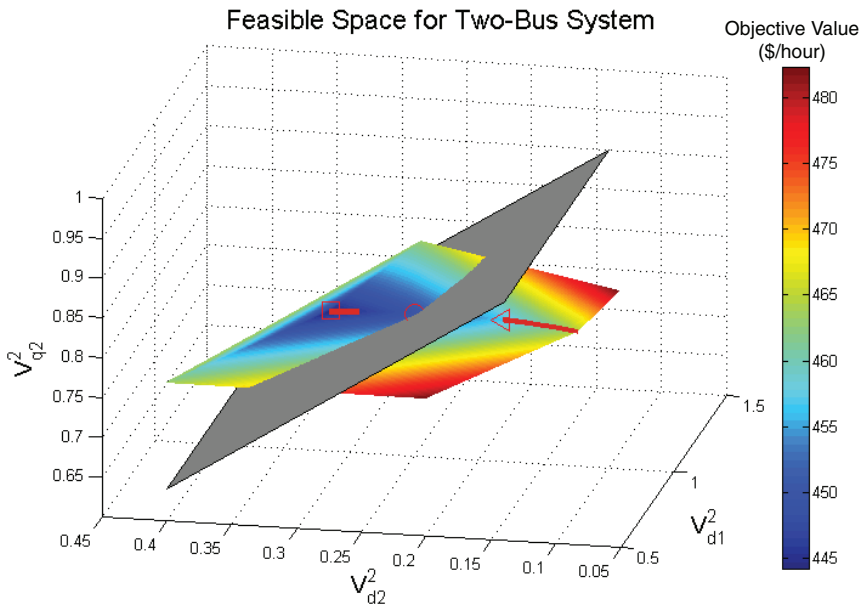

Figure 7.2 Feasible Space for Two-Bus System

Using bus 1 as the angle reference, $V_{q1} = 0$. First consider the case where the upper voltage magnitude limit at bus 2, V_2^{max}, is 1.05 per unit. In Figure 7.2, the entire feasible space for the non-relaxed problem (i.e., the squares of the three non-zero voltage components, V_{d1}^2, V_{d2}^2, V_{q2}^2) is plotted as the red line. The semidefinite relaxation has six degrees of freedom corresponding to the entries in the upper triangle of the $\mathbf{W}$ matrix. The conic shape in Figure 7.2 results from projecting this six-dimensional feasible space into three dimensions. The colors of the conic shape represent the objective value for each point in the space of the semidefinite relaxation.

Figure 7.2 shows that both the semidefinite relaxation and the non-relaxed feasible spaces share a global minimum, which is marked with a square in the figure. Consequentially, the semidefinite relaxation has a zero relaxation gap solution. (The optimal objective value is \$444.08 per hour.)

Next consider the case where $V_2^{max} = 1.02$ per unit. This limit is illustrated by the gray plane cutting through Figure 7.2. This tighter limit reduces the feasible space to the region that is to the right of this plane. The global minimum in the space of the semidefinite relaxation (circle with objective value \$449.82 per hour) does not match the minimum of the non-relaxed problem

(triangle with objective value $456.55 per hour). Accordingly, the solution to the semidefinite relaxation has non-zero relaxation gap.

This example illustrates how non-zero relaxation gap solutions result when the non-relaxed space has components that are nearby but disconnected from the component of the feasible space containing the global optimum. The semidefinite relaxation of the OPF problem finds a solution that is not in the feasible space of the non-relaxed problem but is in the feasible space of the semidefinite program. That is, the semidefinite relaxation has an optimal solution "between" the disconnected components of the feasible space defined by the power flow equations.

A three-bus system adopted from the system used in Chapter 2 provides another example of a case where the semidefinite relaxation has a non-zero relaxation gap solution due to a disconnected

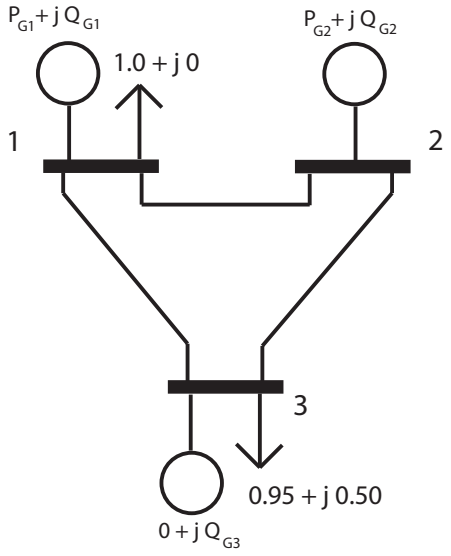

Figure 7.3 Three-Bus System

From Bus	To Bus	Resistance	Reactance	Shunt Susceptance
1	3	0.065	0.62	0.45
2	3	0.025	0.75	0.70
1	2	0.042	0.90	0.30

Table 7.1 Line Parameters for Three-Bus System (per unit)

feasible space. Figure 7.3 shows the diagram for this system. Bus 1 has an active power load of 1.0 per unit using a 100 MVA base. The generators at buses 1 and 2 are constrained to inject positive active power, but have no other limits on active or reactive power generation. The generator at bus 3 is a synchronous condenser which outputs zero active power and has no limit on reactive power output. The line parameters are given in Table 7.1. The line connecting buses 2 and 3 has an apparent-power line-flow limit of 1.0 per unit. This example uses cost functions of \$3/MWh for active power generation at bus 1 and \$1/MWh for active power generation at bus 2.

Voltage magnitudes at each bus are fixed to 1.0 per unit. With fixed voltage magnitudes and bus 1 providing an angle reference, this system has two degrees of freedom in the voltage angles at buses 2 and 3 (δ_2 and δ_3), which are related to the rectangular voltage components as $\tan \delta_2 = \frac{V_{q2}}{V_{d2}}$ and $\tan \delta_3 = \frac{V_{q3}}{V_{d3}}$. In Figure 7.4, the feasible space for the non-relaxed problem is visualized in a two-dimensional space of the voltage angles δ_2 and δ_3. The optimal solution to the non-relaxed problem, which is obtained using exhaustive search of the feasible space, has objective value of \$235.19 per hour and is marked with a square in Figure 7.4. The space of voltage angles used for Figure 7.4 does not allow for easily representing the feasible space of the semidefinite relaxation.

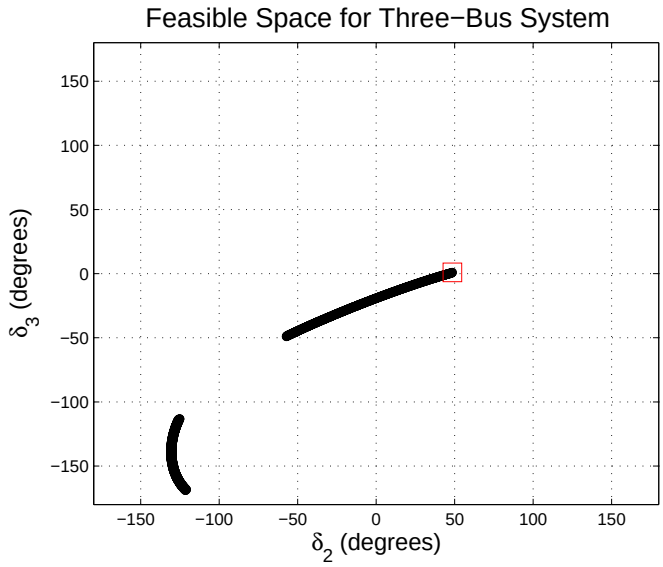

Figure 7.4 Feasible Space for Three-Bus System

With an apparent-power line-flow limit of 1.0 per unit for the line between buses 2 and 3, the semidefinite relaxation yields a solution with objective value of \$234.62 per hour, which is 0.24% smaller than the result obtained using exhaustive search. A non-zero relaxation gap solution results from the non-convexity associated with the disconnected feasible space evident in Figure 7.4.

OPF problems with disconnected feasible spaces may still have zero relaxation gap solutions (i.e., a disconnected feasible space is not sufficient for obtaining a non-zero relaxation gap solution). For instance, a less stringent but still binding apparent-power line-flow limit of 1.05 per unit between buses 2 and 3 yields a disconnected feasible space with a zero relaxation gap solution.

In addition to a disconnected feasible space, other sources of non-convexity may result in non-zero relaxation gap solutions. This is next illustrated with a five-bus example system from [49] (reproduced as Figure 7.5), which has a connected but non-convex feasible space. All buses in this system are constrained to have 1.0 per unit voltage magnitude. All line flows are unconstrained, and the line reactances are specified in Figure 7.5. (The system is lossless since all line resistances are set to zero.) The generators at buses 1 and 2 have non-negative active power generation, and the generators at buses 3, 4, and 5 are synchronous condensers with zero active power generation. There are no limits on reactive power injection for any generator. The load demand at bus 3 is allowed to be any non-negative value $P_{D3} \geq 0$. Equations describing the feasible space for the corresponding OPF problem in terms of the voltage angles are given in [49]. Since the network is lossless, system-wide active power balance imposes the equality

$$P_{D3} = P_{G1} + P_{G2} \tag{7.1}$$

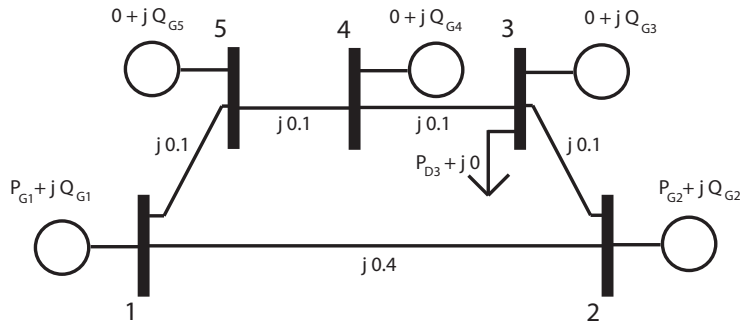

Figure 7.5 Five-Bus System from [49]

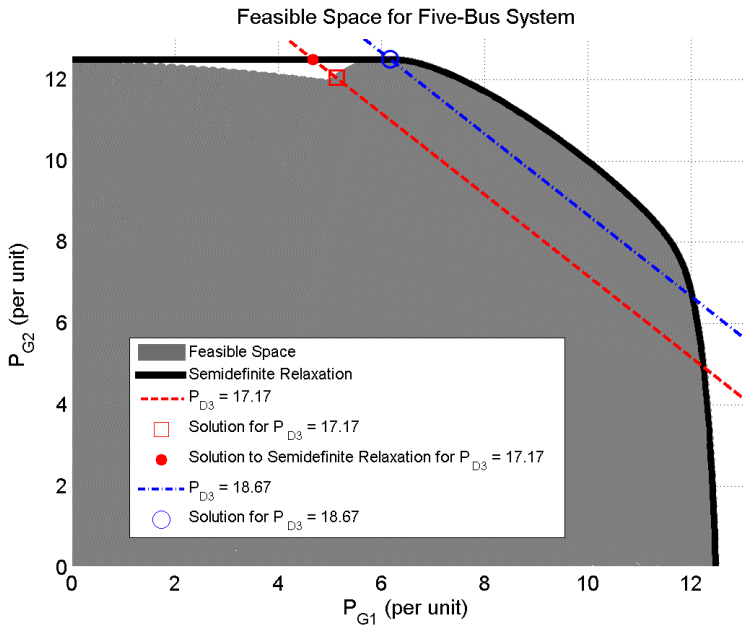

Figure 7.6 Feasible Space for Five-Bus System

Figure 7.6 shows the feasible space of active power injections in the P_{G2} vs. P_{G1} plane. This feasible space is connected but non-convex. Projecting the semidefinite relaxation into this space yields the region enclosed by the solid black line in Figure 7.6. The semidefinite relaxation is tight when viewed in this space for the boundary points on the right side of the feasible space.

To illustrate a case where the non-convexity results in a non-zero relaxation gap solution, consider a load demand $P_{D3} = 17.17$ per unit. All combinations of P_{G1} and P_{G2} that satisfy the equality (7.1) resulting from this load demand are on the red dashed line in Figure 7.6. Consider the case where the generator at bus 1 is more expensive than the generator at bus 2 such that the optimal solution occurs when P_{G1} is minimized.

The globally optimal solution to the OPF problem is located at the red square in Figure 7.6, while the solution to the semidefinite relaxation is located at the red dot. Thus, the semidefinite relaxation yields a non-zero relaxation gap solution for these values of P_{D3} and generator costs. Even though the feasible space with specified P_{D3}, which consists of the one-dimensional intersection between the red dashed line from (7.1) and the gray region in Figure 7.6, is connected and convex, the non-convexity of the gray region in Figure 7.6 still results in a non-zero relaxation

gap solution. Note that non-zero relaxation gap solutions still occur when the lines have small resistances (e.g., 1×10^{-3} per unit).

7.2.2 Non-Zero Relaxation Gap Solutions to Large OPF Problems

With increased understanding of how non-convexity affects the tightness of the semidefinite relaxation for small OPF problems, this chapter next studies non-zero relaxation gap solutions to larger OPF problems. Solving the semidefinite relaxation for large-scale OPF problems requires exploitation of power system sparsity as presented in Chapter 3.

First proposed in Chapter 3, one metric for the relaxation gap is based on the mismatch between the calculated and specified active and reactive power injections at PQ buses. To recover a candidate voltage profile, form the closest rank one matrix to the solution's $\mathbf{W}$ matrix using the eigenvector associated with the largest eigenvalue of $\mathbf{W}$. If the solution has zero relaxation gap, the matrix $\mathbf{W}$ is rank one and the resulting voltage profile will satisfy the power injection equality constraints at the PQ buses. Conversely, the closest rank one matrix to a solution with non-zero relaxation gap will typically not yield a voltage profile that satisfies the power injection equality constraints at PQ buses. Thus, the mismatch between the calculated and specified power injections at PQ buses provides a measure for satisfaction of the rank condition

$$\operatorname{rank}(\mathbf{W}) \leq 2 \tag{7.2}$$

This section specifically considers non-zero relaxation gap solutions to the IEEE 300-bus [68] and Polish 3012-bus [55] systems. Figures 7.7a and 7.7b (reproductions of Figures 3.5a and 3.5b) show the mismatch between the specified and calculated active and reactive power injections at PQ buses for the IEEE 300-bus and Polish 3012-bus systems, respectively, sorted in order of increasing active power mismatch. (Note that minimum resistances of 1×10^{-4} per unit are enforced in accordance with [7].) The large power mismatches indicate non-zero relaxation gap solutions for these systems.

The voltage profile obtained from the closest rank one matrix to $\mathbf{W}$ yields small mismatches for the majority of buses, but a few buses display large mismatches in both active and reactive

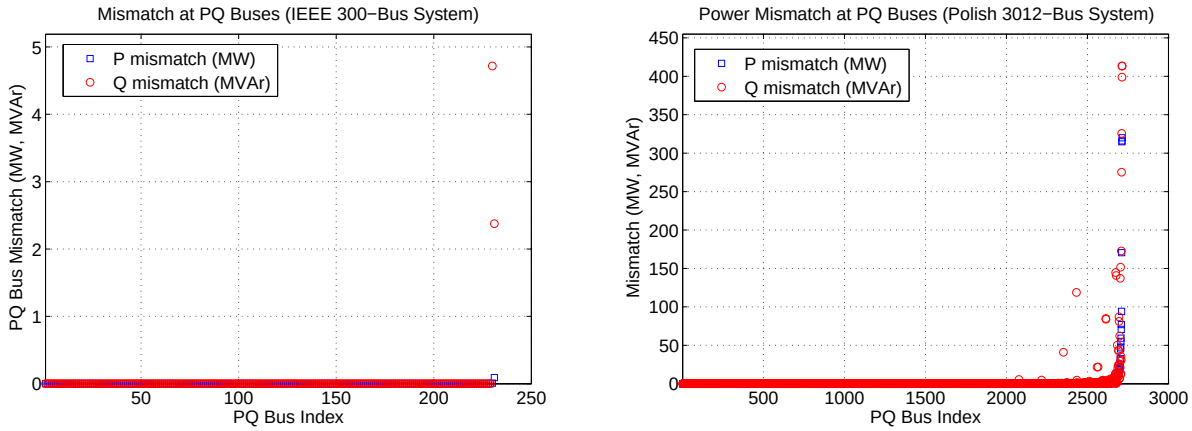

(a) Power Mismatch for IEEE 300-Bus System

(b) Power Mismatch for Polish 3012-Bus System

Figure 7.7 Active and Reactive Power Mismatch at PQ Buses (Reproduction of Figure 3.5)

power injections. These results suggest that there are small subsections of the network that are responsible for the non-zero relaxation gap solutions to these systems.

To further investigate this phenomenon, this section creates new systems by radially connecting the two and three-bus systems shown in Figures 7.1 and 7.3 to IEEE test systems [68]. The OPF problems for the IEEE test systems have zero relaxation gap solutions, while, as shown in Section 7.2.1, non-convexities in the two and three-bus systems result in non-zero relaxation gap solutions. The semidefinite relaxations of the connected OPF problems have non-zero relaxation gap solutions. That is, non-convexities introduced in a small subset of an OPF problem may result in a non-zero relaxation gap solution to a problem for which the semidefinite relaxation is otherwise tight.

For example, consider a 15-bus system resulting from radial connection of bus 2 from the two-bus system in Figure 7.1 to bus 1 of the IEEE 14-bus system [68] using the same line impedance as in the two-bus system. If no reactive power limits are enforced for the generator at bus 1, the resulting 15-bus system has non-convexity due to a disconnected feasible space in the same manner as shown in Figure 7.2. Accordingly, the semidefinite relaxation has a non-zero relaxation gap solution. Connections of the two-bus system to other generator buses in the IEEE 14 and 30-bus systems also result in non-zero relaxation gap solutions. Similar test cases resulting from

radial connection of the three-bus system in Figure 7.3 to the IEEE 14 and 30-bus systems also exhibit non-zero relaxation gap solutions.

These results support the conjecture that non-convexity associated with small subsets of the IEEE 300-bus and Polish 3012-bus systems are responsible for non-zero relaxation gap solutions. Since large systems have many opportunities to have such non-convex subsections, the semidefinite relaxations of large problems are likely to have non-zero relaxation gap solutions. (Limited access to large-scale system models precludes empirical evaluation of this conjecture. See Section 3.3.3 for relaxation gap analysis using the few publicly available large models.)

However, non-zero relaxation gap solutions with non-convexities that are limited to small regions of the network may provide close initial points for local search algorithms. Further, small perturbations to OPF problems may yield zero relaxation gap solutions. This section next provides such perturbations for the test systems used in Section 7.2.1.

For the two-bus system in Figure 7.1, changing the line reactance from 0.20 per unit to 0.215 per unit (a 7.5% increase) results in non-zero relaxation gap solutions for any value of $V_2^{max} \geq V_2^{min} = 0.95$ per unit. The feasible space for the two-bus system with a line reactance of 0.215 per unit and $V_2^{max} = 1.05$ per unit is shown in Figure 7.8. Since the power flow

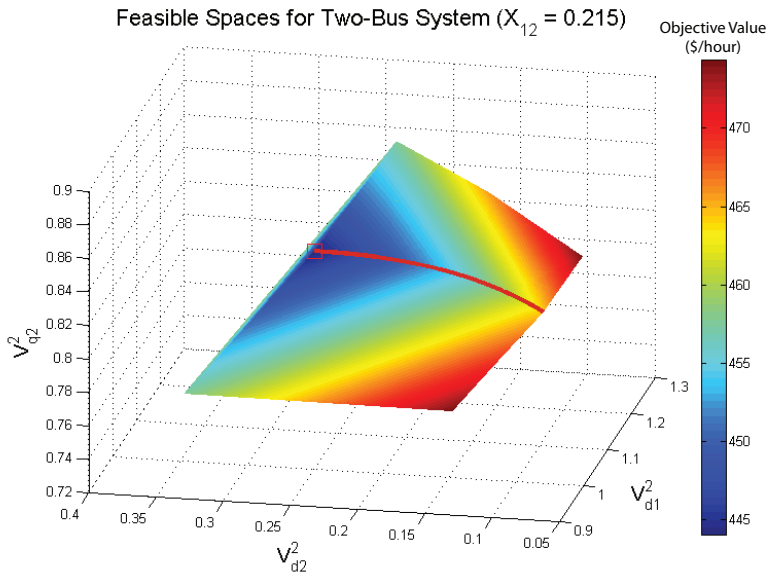

Figure 7.8 Feasible Space for Two-Bus System with $X_{12} = 0.215$ per unit

equations for this problem form a connected feasible space, any valid choice of V_2^{max} will result in the semidefinite relaxation finding a zero relaxation gap solution to this problem.

As mentioned previously for the three-bus system in Figure 7.3, replacing the apparent-power line-flow limit of 1.0 per unit with a less stringent but still binding limit of 1.05 per unit (a 5% increase) yields a zero relaxation gap solution.

For the five-bus system in Figure 7.5, changing the load demand P_{D3} from 17.17 per unit to any value greater than 18.67 per unit (an 8.7% increase) results in a zero relaxation gap solution. (The OPF problem is infeasible for values of P_{D3} greater than 20 per unit. The semidefinite relaxation yields non-zero relaxation gap solutions for any positive value of P_{D3} smaller than 18.67 per unit, which is shown using the blue dashed line in Figure 7.5.)

Similar perturbations may be capable of yielding tight semidefinite relaxations for large OPF problems with non-zero relaxation gap solutions that result from non-convexities that are isolated to small subsections of the network. Perturbations that yield zero relaxation gap solutions for the IEEE 300-bus system include increasing the upper bounds on voltage magnitudes at buses 23 and 7023 from 1.06 to 1.08 per unit (a 1.9% increase) and either changing the reactance of the line between buses 9533 and 9053 from 0.75 to 0.1875 per unit (a 75% decrease) or reducing the linear cost term for the generator at bus 9053 from \$40/MWh to \$38/MWh (a 5% decrease). (Note that, in accordance with [7], minimum resistances of 1×10^{-4} per unit are enforced on all lines.) The solutions to these perturbed systems have maximum active and reactive power mismatches less than 0.1 MW/MVAr at all PQ buses, which is the default Newton solution tolerance used by the commercial power flow solution package PSS/E [89].

These perturbations were obtained heuristically by iteratively changing constraint and cost parameters near buses with large mismatches (i.e., the buses corresponding to large values in Figures 7.7a and 7.7b). There is no guarantee that this approach is valid for all systems. For instance, no perturbations that yield a zero relaxation gap solution for the Polish 3012-bus system were obtained.

Future work includes developing a method for identifying subsections of the network whose non-convexity results in non-zero relaxation gap solutions. Moving beyond the heuristic approach

used in this chapter, additional future work includes developing a systematic method for obtaining the smallest perturbations to OPF problems necessary to yield zero relaxation gap solutions. Such a method would allow power system engineers to identify a globally optimal solution to a "nearby" OPF problem for systems with non-zero relaxation gap solutions. There is always some uncertainty associated with power system parameters (e.g., forecast errors in load demands and measurement inexactness for line parameters). Global solution to a nearby OPF problem within the limits of these uncertainties would be particularly valuable.

7.3 Non-Zero Relaxation Gap Solutions When Evaluating a Power Flow Insolvability Condition

This chapter next explores non-zero relaxation gap solutions to the semidefinite programming formulation used in Chapter 4 to prove insolvability of the power flow equations. Byproducts of this formulation are voltage stability margins describing the distance to the power flow solvability boundary. The power flow insolvability condition is valid regardless of whether the solution to the semidefinite program has a zero relaxation gap solution; however, solutions with non-zero relaxation gap may not indicate power flow insolvability even when no solution exists. Voltage stability margins corresponding to these cases may overestimate the distance to the power flow solvability boundary.

This section first reviews the formulation used to evaluate the power flow insolvability condition and then shows how non-convexity associated with a disconnected feasible space (i.e., multiple power flow solutions bifurcating near the power flow solvability boundary) result in non-zero relaxation gap solutions.

7.3.1 A Semidefinite Formulation for a Power Flow Insolvability Condition

A semidefinite programming formulation used to evaluate a sufficient condition for power flow insolvability is next reviewed. Satisfaction of this condition guarantees that no power flow solutions exist. This formulation determines the distance to the power flow solvability boundary (i.e.,

the "nose point" of a power versus voltage (P-V) curve). See Chapter 4 for further discussion on this formulation.

To write this formulation, define a feasible space that is the semidefinite relaxation of the power flow equations with one additional degree of freedom in the variable η. The optimal value of η indicates the distance to the power flow solvability boundary in the direction of a uniformly changing, constant-power-factor injection profile.

$$\max_{\mathbf{W},\,\eta} \quad \eta \qquad \text{subject to} \tag{7.3a}$$

$$\operatorname{trace}\left(\mathbf{Y}_k \mathbf{W}\right) = P_k \eta \qquad \forall\, k \in \{\mathcal{PQ},\, \mathcal{PV}\} \tag{7.3b}$$

$$\operatorname{trace}(\bar{\mathbf{Y}}_k \mathbf{W}) = Q_k \eta \qquad \forall\, k \in \mathcal{PQ} \tag{7.3c}$$

$$\operatorname{trace}\left(\mathbf{M}_k \mathbf{W}\right) = V_k^2 \qquad \forall\, k \in \{\mathcal{S},\, \mathcal{PV}\} \tag{7.3d}$$

$$\mathbf{W} \succeq 0 \tag{7.3e}$$

A solution to (7.3) has zero relaxation gap if $\mathbf{W}$ satisfies the rank condition (7.2).

Let η^{max} be the globally optimal solution to (7.3). Since $\eta = 1$ corresponds to the specified injections P_k and Q_k, the condition

$$\eta^{max} \geq 1 \tag{7.4}$$

is a necessary for power flow solvability. Conversely,

$$\eta^{max} < 1 \tag{7.5}$$

is a sufficient condition for power flow insolvability since the specified injections P_k and Q_k corresponding to $\eta = 1$ cannot be achieved. Thus, η^{max} indicates the factor by which the power injections may be uniformly increased at constant power factor while maintaining the possibility of power flow solvability.

7.3.2 Non-Zero Relaxation Gap Solutions to the Power Flow Insolvability Condition Formulation

The semidefinite formulation (7.3) identifies the distance to the nose point of the P-V curve associated with a constant-power-factor, uniform change in power injections. When multiple power flow solutions bifurcate at or near the nose point, non-convexity associated with the disconnected feasible space of the power flow equations results in non-zero relaxation gap solutions to (7.3).

This observation is illustrated with the IEEE 14 and 118-bus systems. The IEEE 14-bus system has only a single pair of solutions bifurcating near the nose point and therefore (7.3) yields a zero relaxation gap solution. Conversely, the IEEE 118-bus system has many solutions bifurcating near the nose point and therefore (7.3) yields a non-zero relaxation gap solution.

Figure 7.9a shows the P-V curve for the high-voltage solution to the IEEE 14-bus system. The horizontal axis shows the factor by which the active and reactive power injections are uniformly changed. The vertical axis shows the voltage magnitude at an arbitrarily selected PQ bus.

With the solution to (7.3) having $\eta^{max} = 4.059$, no power flow solutions exist after this injection multiplier (marked with a red line in Figure 7.9a). Since the solution has zero relaxation gap, this value of η^{max} matches the nose point of the P-V curve. That is, η^{max} does not overestimate the distance to the power flow solvability boundary.

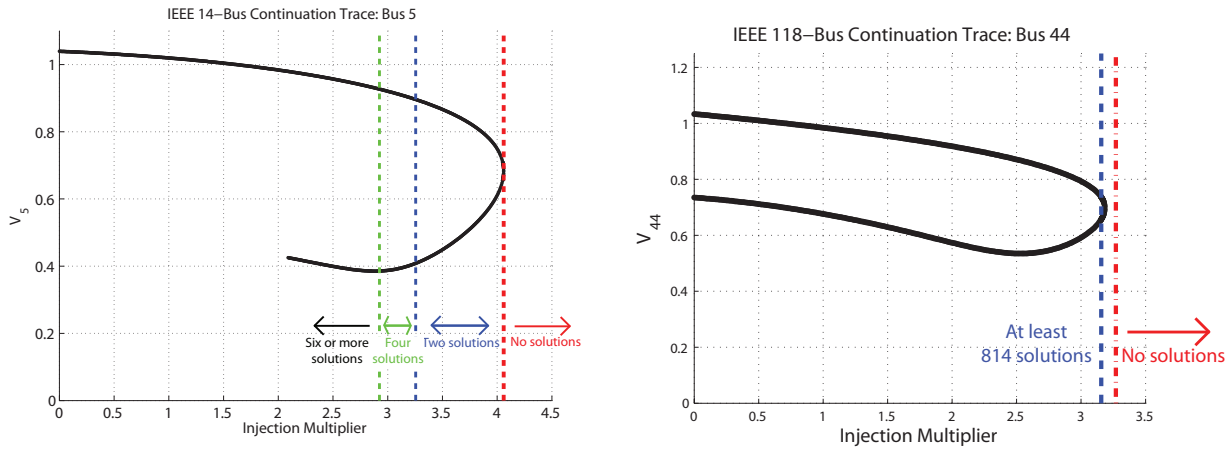

(a) P-V Curve for IEEE 14-Bus System

(b) P-V Curve for IEEE 118-Bus System

Figure 7.9 P-V Curves for IEEE Test Systems

As determined using a continuation method [44], the number of solutions for various ranges of the injection multiplier are labeled. (As shown in Chapter 6, the continuation method [44] does not find all power flow solutions to all systems. However, it is a computationally tractable method that is typically able to find many power flow solutions.) The continuation method finds only two solutions for injection multipliers near the nose point. No other solutions are found until an injection multiplier of 3.255. This suggests that there is not a source of non-convexity near the nose point (i.e., no nearby disconnected components of the feasible space due to multiple power flow solutions).

Next consider the IEEE 118-bus system. The P-V curve associated with the high-voltage solution for this system is shown in Figure 7.9b. Solving (7.3) yields $\eta^{max} = 3.270$, which guarantees that no power flow solutions exist after an injection multiplier of 3.270. Since the solution has non-zero relaxation gap, there may be a region for which no solutions exist but the sufficient condition for power flow insolvability (7.5) is not satisfied. That is, η^{max} may overestimate the distance to the power flow solvability boundary. Such a region appears evident in Figure 7.9b between the red line at an injection multiplier of 3.270 and the nose point of the P-V curve at an injection multiplier of 3.184.

At the blue line in Figure 7.9b, which is located near the nose point at an injection multiplier of 3.156, a continuation method [44] finds 814 power flow solutions. The non-convexity associated with these solutions bifurcating near the nose point results in a non-zero relaxation gap solution to (7.3) and the apparent overestimate of the distance to the power flow solvability boundary.

7.4 Non-Zero Relaxation Gap When Finding Multiple Power Flow Solutions

The previous section focuses on non-zero relaxation gap solutions to a formulation for determining when the power flow equations are insolvable. Next, this section considers the question of determining multiple power flow solutions. Solutions to the power flow equations correspond to the equilibrium points of the underlying differential equations that govern power system dynamic behavior; it is well known that large numbers of such solutions can exist [110]. Locating multiple solutions to the power flow equations, particularly those exhibiting low-voltage magnitude, is

important to power system stability assessment [37–40]. With the counterexample presented in Chapter 6, current literature offers no computationally tractable method for reliably calculating all power flow solutions.

This section investigates non-zero relaxation gap solutions to the semidefinite programming formulation used in Chapter 6 that attempts to calculate multiple power flow solutions. This formulation minimizes an objective function of squared voltage magnitudes over a semidefinite relaxation of the power flow equations. A power flow solution is identified when the semidefinite formulation has a zero relaxation gap solution. This section first reviews this formulation and then illustrates examples of non-zero relaxation gap solutions.

7.4.1 A Semidefinite Formulation for Calculating Multiple Power Flow Solutions

The formulation for finding multiple power flow solutions defines a feasible space using the semidefinite relaxation of the power flow equations (see Section 1.5). This feasible space convexly connects the disconnected power flow solutions. Multiple solutions are obtained by varying desired voltage magnitude properties specified using the objective function. Specifically, a weighting vector c is defined for squared voltage magnitudes. The semidefinite formulation is

$$\min_{\mathbf{W}} \quad \sum_{i=1}^{n} c_i \text{trace}\left(\mathbf{M}_i \mathbf{W}\right) \qquad \text{subject to} \tag{7.6a}$$

$$\text{trace}\left(\mathbf{Y}_k \mathbf{W}\right) = P_k \qquad \forall\, k \in \{\mathcal{PQ},\, \mathcal{PV}\} \tag{7.6b}$$

$$\text{trace}(\bar{\mathbf{Y}}_k \mathbf{W}) = Q_k \qquad \forall\, k \in \mathcal{PQ} \tag{7.6c}$$

$$\text{trace}\left(\mathbf{M}_k \mathbf{W}\right) = V_k^2 \qquad \forall\, k \in \{\mathcal{S},\, \mathcal{PV}\} \tag{7.6d}$$

$$\mathbf{W} \succeq 0 \tag{7.6e}$$

A solution to (7.6) has zero relaxation gap if $\mathbf{W}$ satisfies the rank condition (7.2). See Section 6.3 for further discussion on this formulation.

7.4.2 Non-Zero Relaxation Gap Solutions to the Multiple Power Flow Solution Formulation

Many values of c result in zero relaxation gap solutions to (7.6) and therefore yield power flow solutions. For instance, values of c exist for obtaining all power flow solutions to five and seven-bus test cases in Chapter 6. However, some values of c result in non-zero relaxation gap solutions and therefore do not solve the power flow equations. The power flow equations have the non-convexity of a disconnected feasible space (i.e., solutions to the power flow equations consist of a set of disconnected points). Non-zero relaxation gap solutions to the semidefinite formulation (7.6) are attributable to the non-convexity of the disconnected feasible space.

Non-zero relaxation gap solutions to (7.6) occur when multiple power flow solutions have similar objective value. Consider, for instance, the five-bus system in Figure 6.3 which is used as an example system in Chapter 6. All ten solutions to this system are calculated using a homotopy method in [42].

Two values of c for which (7.6) yields different zero relaxation gap solutions are $\bar{c} = \begin{bmatrix} 0 & -1 & 0.4 & 0.4 & 0 \end{bmatrix}^T$, which yields solution 4 in Table 6.3, and $\tilde{c} = \begin{bmatrix} 0 & -1 & 0 & 0 & 0 \end{bmatrix}^T$, which yields solution one in Table 6.3. Figure 7.10 shows the objective values of each of the ten

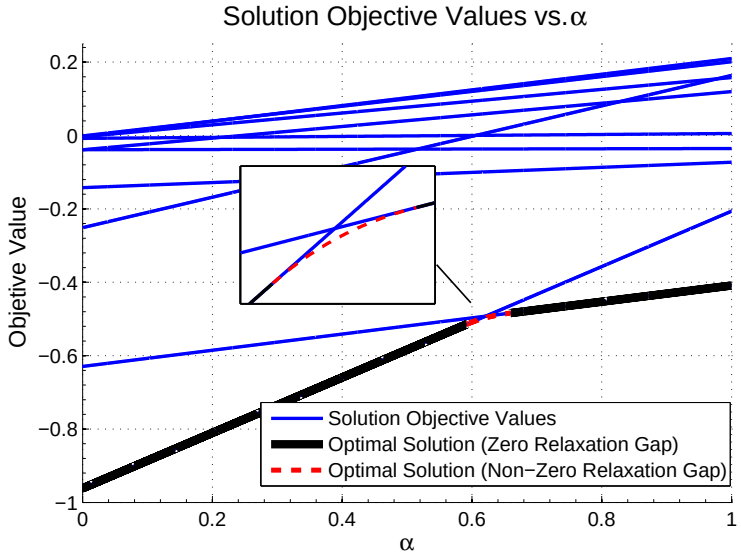

Figure 7.10 Objective Value of Solutions to Five-Bus System

solutions as the objective function is linearly varied between $\bar{c}$ and $\tilde{c}$ using the scalar parameter $\alpha \in [0,\, 1]$.

$$c = \bar{c}\alpha + (1 - \alpha)\tilde{c} \tag{7.7}$$

Many values of c yield zero relaxation gap solutions; however, values of c corresponding to the range $0.592 \leq \alpha \leq 0.659$ result in non-zero relaxation gap solutions. For these values of c, there are two power flow solutions with similar objective values. The non-convexity associated with these disconnected feasible spaces results in non-zero relaxation gap solutions to (7.6).

The five-bus system in Figure 6.3 contains two buses with fixed voltage magnitudes (the slack bus and a single PV bus). Linear functions of the squares of voltage magnitudes thus have three degrees of freedom: one for each of the three PQ bus voltages (buses 2, 3, and 4). These coefficients can be visualized as a vector $\hat{c} = \begin{bmatrix} c_2 & c_3 & c_4 \end{bmatrix}^T$ in $\mathbb{R}^3$.

Multiplying $\hat{c}$ by a positive scalar changes the optimal objective value but does not affect the optimal value of $\mathbf{W}$ (i.e., the power flow solution when $\mathbf{W}$ satisfies the rank condition (7.2)). Since only the power flow solutions (but not the objective function values) are of interest to finding multiple solutions, the vector $\hat{c}$ can be normalized to unit length without loss of generality.

To investigate how choices of $\hat{c}$ affect which power flow solution, if any, is obtained by (7.6), Figure 7.11 shows the solutions for many vectors $\hat{c}$, normalized to unit length, as a sphere in $\mathbb{R}^3$. Each solution is assigned a separate color, with all points in the plot (corresponding to values of $\hat{c}$) that find the same solution colored the same. Choices of $\hat{c}$ that do not result in physically meaningful solutions (i.e., the relaxation (7.6) yields a solution with non-zero relaxation gap) are colored white to differentiate these points from power flow solutions.

Figure 7.11 corroborates the results of Figure 7.10 in that regions for which choices of $\hat{c}$ that yield the same zero relaxation gap solution are separated by regions with non-zero relaxation gap solutions. That is, the non-convexity associated with a disconnected feasible space results in non-zero relaxation gap solutions whenever components of the disconnected feasible space have similar objective values.

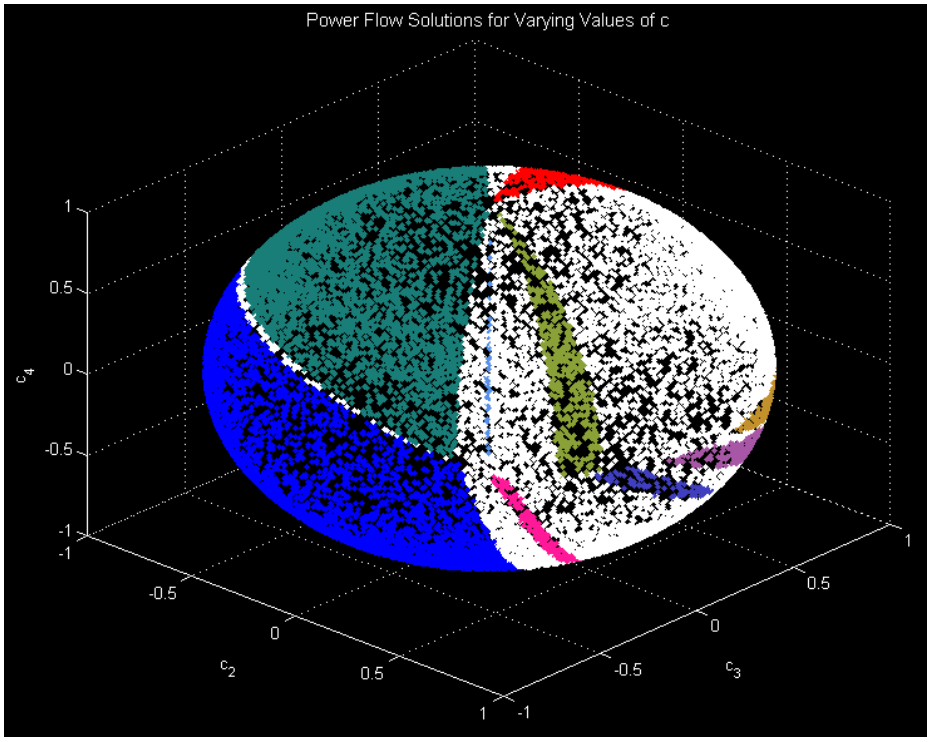

Figure 7.11 Power Flow Solutions Obtained for Varying Values of $\hat{c}$

7.5 Conclusion

Although the semidefinite relaxation of the power flow equations is often "tight" for many applications, practical problems may have non-zero relaxation gap solutions. This chapter investigates non-convexities associated with non-zero relaxation gap solutions for a variety of example problems. Specifically, this chapter considers a semidefinite programming relaxation for the optimal power flow (OPF) problem, a semidefinite formulation used in evaluating a sufficient condition for power flow insolvability and in determining voltage stability margins, and a semidefinite formulation for finding multiple power flow solutions.

Non-convexity associated with a disconnected feasible space may result in non-zero relaxation gap solutions for each of these semidefinite formulations. Illustrative examples are provided along with visualizations of the relevant feasible spaces. OPF problems for two and three-bus systems with disconnected feasible spaces exhibit non-zero relaxation gap solutions. A semidefinite formulation used to evaluate a sufficient condition for power flow insolvability has non-zero relaxation

gap solutions when many power flow solutions bifurcate at or near the power flow solvability boundary (i.e, the "nose point" of the power versus voltage curve). Multiple power flow solutions with similar objective values result in non-zero relaxation gap solutions to a semidefinite formulation for finding multiple power flow solutions.

This chapter also presents a five-bus system with connected but non-convex feasible space. An OPF problem associated with this system has non-zero relaxation gap, which demonstrates that a disconnected feasible space is not necessary for non-zero relaxation gap solutions.

Non-zero relaxation gap solutions for large OPF problems are also studied. Specifically, the IEEE 300-bus and Polish 3012-bus systems are found to exhibit non-zero relaxation gap solutions as evidenced by matrices that have rank greater than two. The closest rank one matrices to these non-zero relaxation gap solutions satisfy the power injection equations at the majority of PQ buses; mismatch at a small number of PQ buses suggests that the non-convexities causing the non-zero relaxation gaps are isolated to a few small subsections of the network. This is supported by non-zero relaxation gap solutions to example cases created by radially connecting small test systems with non-zero relaxation gap solutions to IEEE test cases for which the semidefinite relaxation is tight. Non-convexity introduced in a small subsection of the network is sufficient to cause non-zero relaxation gap solutions. Further, for many cases where the semidefinite relaxation is not tight, heuristically determined perturbations to small subsections of the network often result in problems with zero relaxation gap solutions.

Chapter 8

Conclusion and Future Work

This chapter summarizes the contributions of this dissertation and outlines plans for future work in applying semidefinite programming and other techniques used in this dissertation to problems in power systems engineering.

8.1 Conclusion

Motivated by the need to improve both power system economics and relibility, this dissertation has detailed applications of a semidefinite programming relaxation of the power flow equations to power systems problems. As discussed in the introduction, semidefinite program solvers can reliably find a globally optimal solution in polynomial time, and semidefinite relaxations have been successfully applied to a variety of computationally difficult problems in many fields. The literature to date details limited success in applying the semidefinite relaxation of the power flow equations to the optimal power flow problem. There are many opportunities to further apply semidefinite programming to problems in electric power systems engineering.

This dissertation first investigates application of the semidefinite relaxation of the power flow equations to the OPF problem. Chapter 2 describes practical cases where the relaxation fails to be tight (i.e., the solution to the semidefinite program has a non-zero relaxation gap and therefore is not physically meaningful). Chapter 2 first discusses cases with negative Lagrange multipliers for active power constraints (i.e., locational marginal prices (LMPs)). Existing literature classifies cases with negative Lagrange multipliers for active power constraints as abnormal and indicates that the semidefinite relaxation may fail to provide physically meaningful solutions for such

cases [7]. Chapter 2 discusses and provides a practical example of an OPF problem whose solution exhibits negative Lagrange multipliers. Failure to yield zero relaxation gap solutions for cases with negative Lagrange multipliers for active power constraints is thus an important limitation of the semidefinite relaxation of the power flow equations. Next, Chapter 2 provides a three-bus example system with apparent power ("MVA") line-flow constraints that fails to yield a zero relaxation gap solution even though all Lagrange multipliers for active power constraints are positive and all Lagrange multipliers for reactive power constraints are non-negative. These examples show that the semidefinite programming relaxation does not provide physically meaningful solutions for all practical OPF problems.

Chapter 3 provides modeling and computational contributions for solving semidefinite relaxations of large-scale OPF problems. While existing semidefinite relaxations, such as the formulation presented in Chapter 2, suffice for many small test systems, practical power systems often require additional modeling considerations. The first modeling consideration in Chapter 3 involves limiting line flows on parallel lines and transformers (i.e., branch elements that share both terminal buses) while incorporating the possibilities of non-zero phase shifts and off-nominal voltage ratios. A second modeling contribution of the proposed formulation is the possibility of multiple generators at the same bus. Multiple generators at the same bus are modeled by analogy to the "equal marginal cost" criterion of the economic dispatch problem. The formulation presented in Chapter 3 considers generators with both quadratic and piecewise-linear cost functions. Another contribution is an approximate representation of ZIP loads, which have constant impedance, constant current, and constant power components, in the semidefinite relaxation of the power flow equations. An analysis of this method details the worst case error in the approximation.

Chapter 3 continues by discussing computational improvements in solving the semidefinite relaxation of the OPF problem. The semidefinite relaxation is computationally limited by a $2n \times 2n$ positive semidefinite matrix constraint, where n is the number of buses in the system. Existing literature discusses matrix decomposition preprocessing of the semidefinite relaxation using the

sparsity inherent in practical large-scale power system models [7, 81, 82]. Solver speed is significantly increased by decomposing the constraint on the large $2n \times 2n$ matrix into positive semidefinite constraints on many smaller matrices. Equality constraints enforce consistency between terms in different matrices that represent the same term in the $2n \times 2n$ matrix.

Both the size of the matrices and the number of equality constraints affect the solver time; smaller matrices and fewer equality constraints speed computation. Existing OPF literature does not recognize the potential trade-off between the size of the matrices and the number of equality constraints in a semidefinite relaxation of the OPF problem. It may be computationally advantageous to combine some matrices in order to trade-off larger matrices for a reduction in the number of equality constraints. Chapter 3 proposes a heuristic method for combining matrices that reduces solver times by factors of 2.3 and 3.0 for the IEEE 300-bus and Polish 3012-bus test systems, respectively, as compared to existing matrix decompositions in the OPF literature.

These computational advances in exploiting power system sparsity allow for analysis of the relaxation gap properties for solutions to large OPF problems. Using two proposed measures of rank condition satisfaction, Chapter 3 details an analysis of non-zero relaxation gap solutions to the IEEE 300-bus and the Polish 3012-bus systems. This analysis shows a small number of buses with large active and reactive power mismatch, while the majority of buses have small mismatch. These results suggest that non-convexities in small subsections of the network are responsible for non-zero relaxation gap solutions.

An additional computational contribution in Chapter 3 is a method for recovering an optimal voltage profile from the solution to a decomposed semidefinite relaxation. This method relies on linear calculations that enforce consistency between terms that refer to the same voltage along with a reference angle constraint and a single binding constraint in the OPF problem.

Chapter 3 also proposes a modification to an existing matrix decomposition [82] that enables application to general power system models. The decomposition described in [82] requires that the absolute value of the imaginary part of the admittance matrix is positive definite. This condition is not satisfied by all practical power system models, particularly those with large capacitive

shunt elements. Since only the sparsity pattern of this matrix is required for the matrix decomposition, construction of a different, positive definite matrix with the same sparsity pattern extends the applicability of the matrix decomposition method to general power systems.

Finally, Chapter 3 describes a sufficient condition test for global optimality of a candidate OPF solution using the Karush-Kuhn-Tucker (KKT) conditions for optimality of the semidefinite relaxation of the OPF problem. A candidate solution obtained from a mature OPF solution algorithm that satisfies the KKT conditions of complementarity and feasibility is guaranteed to be globally optimal. However, satisfaction of these conditions is not necessary for global optimality. This approach pairs the speed advantage of existing solvers with the global solution advantage of the semidefinite relaxation.

This dissertation next investigates techniques for improving power system reliability. Chapter 4 discusses a sufficient condition, calculated using a semidefinite program, for the insolvability of the power flow equations. A proof of the feasibility of this semidefinite program ensures that the sufficient condition can be calculated for lossless power systems; the proof further argues that the semidefinite program is also feasible for practical power systems (i.e., systems with small active power losses).

As a byproduct of this sufficient condition, two voltage stability margins are developed that give measures of the distance to the power flow solvability boundary. The two voltage stability margins are 1.) a controlled voltage margin, which gives an upper bound on the factor by which the controllable voltages must be uniformly changed such that the solution is at the power flow solvability boundary, and 2.) a power injection margin, which gives an upper bound on the factor by which all power injections must be uniformly changed at constant power factor in order for the solution to be at the power flow solvability boundary. The insolvability condition and both voltage stability margins are demonstrated using the IEEE 14 and 118-bus test systems.

The sufficient condition and voltage stability margins described in Chapter 4 model generators as ideal voltage sources with no limits on reactive power outputs. More detailed generator models

consider reactive power limits, which may result in voltage collapse through limit-induced bifurcations. Chapter 5 provides two formulations that extend the work in Chapter 4 to consider reactive power limited generators.

The first of these formulations uses mixed-integer semidefinite programming (i.e., an optimization problem with both positive semidefinite matrix constraints and integer constraints) to model reactive power limited generators. Although current mixed-integer semidefinite programming solvers are relatively immature and not assured to run in polynomial time, this is an active area of research and more capable algorithms will likely become available. Existing tools are sufficient for small power system models and Chapter 5 discusses potential modifications that improve the computational tractability of the proposed formulation with respect to solution algorithms in the literature.

The second formulation in Chapter 5 uses the concept of infeasibility certificates from the field of real algebraic geometry. Using the Positivstellensatz theorem, infeasibility certificates for polynomial equations are calculated with sum-of-squares decompositions that are themselves computed with semidefinite optimization programs. Formulating the power flow equations with reactive power limited generators as a system of polynomials allows for the application of infeasibility certificate theory.

Questions regarding multiple power flow solutions are then addressed in Chapter 6. This chapter first presents a five-bus system counterexample to a claim in the literature about the ability of a continuation-based method to find all solutions to any power system model. Since other methods for finding all solutions to the power flow equations are not computationally tractable for large systems, there is presently no method for reliably computing all solutions to the power flow equations for practically sized systems. Other methods for calculating multiple power flow solutions therefore deserve further research attention.

Chapter 6 then proposes a method for finding multiple power flow solutions using the semidefinite relaxation of the power flow equations. With the choice of an objective function based on squared voltage magnitudes and appropriately selected constraints, the semidefinite relaxation of the power flow equations can be used to find power flow solutions with desired voltage magnitude

characteristics. It is important to note that this method does not yield physically meaningful solutions (i.e., the semidefinite relaxation is not tight) for all objective function choices; however, all solutions to the two test cases investigated in Chapter 6 were obtainable with some objective function choice.

Finally, by illustrating the feasible spaces for power system optimization problems and their semidefinite relaxations, Chapter 7 investigates examples of non-zero relaxation gap solutions. Three specific applications of the semidefinite relaxation of the power flow equations are considered: the optimal power flow problem, a formulation used to determine voltage stability margins, and a formulation for determining multiple solutions to the power flow equations. Visualizing the feasible spaces of both the original, rank-constrained problems and of the semidefinite relaxation illustrates examples of non-convexities that result in non-zero relaxation gap solutions. Studied non-convexities include both disconnected and connected but non-convex feasible spaces. This analysis includes a discussion of non-zero relaxation gap solutions to large OPF problems.

Open source MATLAB code implementing these contributions is under review for public release as part of MATPOWER [55]. Publicly available code will speed research progress by eliminating the need for researchers to independently implement these semidefinite formulations and will quickly distribute the contributions of this dissertation. This code includes `sdp_opf`, which implements the semidefinite relaxation of the OPF problem with the modeling and computational advances described in Chapter 3; `testGlobalOpt`, which is a computationally efficient implementation of the sufficient condition test for global optimality described in Section 3.4; `insolvablepf`, which evaluates the sufficient condition for power flow insolvability and calculates the voltage stability margins described in Chapter 4 while exploiting power system sparsity for computational efficiency; `pfcondition_limitQ`, which implements the mixed-integer semidefinite programming formulation that evaluates a sufficient condition for power flow insolvability and calculates a voltage stability margin with consideration of reactive power limited generators; and `insolvablepfsos_limitQ` and `insolvablepfsos`, which prove power flow insolvability using sum-of-squares programming to generate infeasibility certificates with and without considering reactive power limited generators, respectively.

8.2 Publications

Several publications have resulted from the research detailed in this dissertation. Work from Chapter 2 and Section 6.3 is published as

[83] B. C. Lesieutre, **D. K. Molzahn**, A. R. Borden, and C. L. DeMarco, "Examining the Limits of the Application of Semidefinite Programming to Power Flow Problems," in *49^{th} Annual Allerton Conference on Communication, Control, and Computing, 2011*, September 28-30 2011.

Work from Sections 3.2 and 3.3 is accepted for publication as

[94] **D. K. Molzahn**, J. T. Holzer, B. C. Lesieutre, and C. L. DeMarco, "Implementation of a Large-Scale Optimal Power Flow Solver Based on Semidefinite Programming," To appear in *IEEE Transactions on Power Systems*.

Work from Section 3.2.4 is submitted for publication as

[95] **D. K. Molzahn**, B. C. Lesieutre, and C. L. DeMarco, "Approximate Representation of ZIP Loads in a Semidefinite Relaxation of the OPF Problem," Submitted to *IEEE Transactions on Power Systems (Letters)*.

Work from Section 3.4 is accepted for publication as

[96] **D. K. Molzahn**, B. C. Lesieutre, and C. L. DeMarco, "A Sufficient Condition for Global Optimality of Solutions to the Optimal Power Flow Problem," To appear in *IEEE Transactions on Power Systems (Letters)*.

Work from Chapter 4 is published, with an extended version available as a technical report, as

[101] **D. K. Molzahn**, B. C. Lesieutre, and C. L. DeMarco, "A Sufficient Condition for Power Flow Insolvability with Applications to Voltage Stability Margins," *IEEE Transactions on Power Systems*, vol. 28, no. 3, pp. 2592-2601, August 2013.

[102] **D. K. Molzahn**, B. C. Lesieutre, and C. L. DeMarco, "A Sufficient Condition for Power Flow Insolvability with Applications to Voltage Stability Margins," University of Wisconsin-Madison Department of Electrical and Computer Engineering, Tech. Rep. ECE-12-01, 2012, [Online]. Available: `http://arxiv.org/abs/1204.6285`.

Work from Chapter 5 is accepted for publication as

[106] **D. K. Molzahn**, V. Dawar, B. C. Lesieutre, and C. L. DeMarco, "Sufficient Conditions for Power Flow Insolvability Considering Reactive Power Limited Generators with Applications to Voltage Stability Margins," To appear in *Bulk Power System Dynamics and Control - IX. Optimization, Security and Control of the Emerging Power Grid, 2013 IREP Symposium*, August 25-30 2013.

Work from Section 6.2 is published as

[111] **D. K. Molzahn**, B. C. Lesieutre, and H. Chen, "Counterexample to a Continuation-Based Algorithm for Finding All Power Flow Solutions," *IEEE Transactions on Power Systems (Letters)*, vol. 28, no. 1, pp. 564-564, February 2013.

Work from Chapter 7 is submitted for publication as

[113] **D. K. Molzahn**, B. C. Lesieutre, and C. L. DeMarco, "Investigation of Non-Zero Duality Gap Solutions to a Semidefinite Relaxation of the Power Flow Equations," Submitted to *47th Hawaii International Conference on System Sciences (HICSS), 2014*, 6-9 January 2014.

8.3 Future Work

This work opens several avenues for further investigation. The first involves extension of the modeling capabilities of the semidefinite relaxation. Significant research attention in developing and analyzing semidefinite relaxations has focused on distribution networks. The radial topology common to distribution networks has interesting properties in convex relaxations of the power flow equations. For instance, several sufficient conditions for zero relaxation gap solutions to convex relaxations of the OPF problem require radial network topologies [69–75] along with other restrictions. In addition, increasing prevalence of distributed generators and other active control devices connected to distribution systems makes development of OPF techniques for these systems necessary for efficient operation of future power systems [114].

Most existing semidefinite formulations assume balanced networks where phenomena are identical in each phase after accounting for the angle offset (e.g., voltage magnitudes for each phase of a three-phase system are identical with the voltage angles offset by $120°$). While this is a realistic assumption for typical steady-state transmission system operation, it is often not an accurate representation of distribution systems, which can have substantial imbalance between phases. Distribution networks also typically have much higher resistance to reactance (R to X) ratios than transmission networks. These differences require specialized algorithms for distribution network analysis. See, e.g., [114–119] for power flow and optimal power flow algorithms specialized for distribution networks.

Extending the semidefinite relaxation of the power flow equations to networks with phase imbalances is necessary for realistic analysis of many distribution systems. Existing work in this area includes [120], which proposes a semidefinite relaxation for the three-phase OPF problem, and [121], which focuses on microgrid applications of this semidefinite relaxation with the possibility of distributed computations. One important open question is determining whether the findings of existing literature regarding semidefinite relaxations of balanced radial networks apply to

imbalanced radial networks with high R to X ratios. That is, ascertaining if semidefinite relaxations of distribution networks with phase imbalance have the similar properties as distribution networks with balanced phases.

Extension of the semidefinite relaxation to imbalanced networks would also enable leveraging the techniques for voltage stability analysis developed in this dissertation. Power flow insolvability and voltage stability margins for imbalanced systems would help engineers ensure distribution system reliability and exploit the capabilities of distributed generation resources. This work would supplement continuation-based methods for voltage stability analysis of imbalanced distribution networks [122].

Further, distribution networks may be operated with different goals than transmission networks; for instance, improving power quality by minimizing harmonic distortions [119] and/or phase imbalances. Another question of interest is whether the semidefinite relaxation can be used to achieve these alternative operating goals.

Other avenues for future research involve further applications of the theories used in Chapter 5. This chapter uses the Positivstellensatz theorem from the field of real algebraic geometry to generate infeasibility certificates for the power flow equations with consideration of reactive power limited generators. This work exploits the fact that the power flow equations are polynomial in the rectangular voltage components V_d and V_q.

With the wealth of tools for analyzing polynomial equalities and inequalities, real algebraic geometry has significant potential for further application to the power flow equations. For instance, future advances in calculating only the real solutions of polynomial equations may enable development of a computationally tractable method for reliably finding all power flow solutions to large systems.

Chapter 5 also applies mixed-integer semidefinite programming to calculate a voltage stability margin with consideration of reactive power limited generators. Mixed-integer semidefinite programming can be directly applied to power systems problems that currently use mixed-integer programming (e.g., the unit commitment problem where a power system dispatch is optimized over time with the ability to commit and decommit generators [123] and the optimal transmission

switching problem where a generation dispatch and transmission topology is determined to meet a given load [124]). Existing work in this area includes the application of mixed-integer semidefinite programming to the transmission expansion problem [125].

To be computationally feasible for realistic system models, future work also includes investigating the application of large-scale mixed-integer semidefinite program algorithms, such as [65] and [66], to power system problems. (See Section 5.3.3.)

Future research also seeks to combine the optimal power flow and voltage stability margins into one optimization problem in order to investigate the potential trade-off between low cost and stable power system operation. The power injection margins developed in Chapters 4 and 5 are calculated using an optimization problem, which enables integration into an optimal power flow problem. Voltage stability margins in the directions of prespecified injection profiles could be considered as part of a multiobjective optimization problem. A multiobjective formulation would explore the pareto front of the optimization problem to study the trade-off between minimizing operating cost and improving the voltage stability margin. Operating point perturbations that significantly improve voltage stability margins with small increases in generation costs would be particularly valuable.

Future work can also build on Chapter 7's investigation of non-zero relaxation gap solutions. For several large systems with non-zero relaxation gap solutions, this chapter showed that the closest rank one matrix satisfies the power injection equations at the majority of load buses; mismatch at a small number of load buses suggests that the non-convexity causing the non-zero relaxation gap solution is isolated to a few small subsections of the network. This is supported by non-zero relaxation gap solutions to example cases created by radially connecting small test systems with non-zero relaxation gap solutions to IEEE test cases for which the semidefinite relaxation is tight. Non-convexity introduced in a small subsection of the network is sufficient to cause a non-zero relaxation gap solution. Further, for many cases where the semidefinite relaxation is not tight, heuristically-determined perturbations to small subsections of the network often result in problems with zero relaxation gap solutions.

Non-convexities that are isolated to small subsections of the network and the ability to obtain zero relaxation gap solutions to some perturbed OPF problems suggest directions for future research. One potential direction is development of a robust method for identifying non-convex subsections of the network before solving an OPF problem. A possible approach is to categorize common network structures that lead to non-convexity.

Another potential research direction is development of a systematic method for determining perturbations that result in zero relaxation gap solutions. Ideally, such a method would find the smallest perturbations necessary in order to obtain the "closest" OPF problem for which the semidefinite relaxation is tight. Perturbations within the uncertainty associated with power system data would be particularly useful in practice. Research on this topic may draw on such works as [71, 73, 74], which claim that zero relaxation gap solutions always result for OPF problems modified with a sufficient number of appropriately placed controllable phase shifting transformers along with allowing for load oversatisfaction (i.e., no upper bounds on load demands). These modifications may be viewed as method for perturbing the original OPF problem to a nearby problem that has zero relaxation gap solution. The substitution theorem [8] may allow for a more natural representation of the controllable phase shifting transformers as perturbations to bus power injections.

As an alternative to perturbing an OPF problem, it may be possible to add constraints that are redundant to the classical OPF problem but change the feasible space of the semidefinite relaxation in order to obtain a zero relaxation gap solution. Developing a proof-of-principle example and determining a systematic approach for determining appropriate constraints are questions for future research.

LIST OF REFERENCES

[1] National Academy of Engineering, "Greatest Engineering Achievements of the 20th Century." [Online]. Available: http://www.greatachievements.org/

[2] K. H. LaCommare and J. H. Eto, "Cost of Power Interruptions to Electricity Consumers in the United States (US)," *Energy*, vol. 31, no. 12, pp. 1845 – 1855, 2006.

[3] D. Ray, "Blackout of 2003: Description and Responses," November 7, 2003. [Online]. Available: http://www.pserc.wisc.edu/documents/publications/special_interest_publications/grid_reliability/ray_blackout_sep03.pdf

[4] Electric Consumer Research Council (ELCON), "The Economic Impacts of the August 2003 Blackout," February 2, 2004. [Online]. Available: http://www.elcon.org/Documents/EconomicImpactsOfAugust2003Blackout.pdf

[5] Energy Information Agency, "Summary Electricity Statistics 1999-2010." [Online]. Available: http://www.eia.gov/electricity/annual/pdf/tablees1.pdf

[6] X. Bai, H. Wei, K. Fujisawa, and Y. Wang, "Semidefinite Programming for Optimal Power Flow Problems," *International Journal of Electrical Power & Energy Systems*, vol. 30, no. 6-7, pp. 383–392, 2008.

[7] J. Lavaei and S. Low, "Zero Duality Gap in Optimal Power Flow Problem," *IEEE Transactions on Power Systems*, vol. 27, no. 1, pp. 92–107, February 2012.

[8] L. Chua, C. Desoer, and E. Kuh, *Linear and Nonlinear Circuits*. McGraw-Hill, New York, 1987.

[9] J. Glover, M. Sarma, and T. Overbye, *Power System Analysis and Design*. Thompson Learning, 2008.

[10] R. Klump and T. Overbye, "A New Method for Finding Low-Voltage Power Flow Solutions," in *Power Engineering Society Summer Meeting, 2000. IEEE*, vol. 1, 2000, pp. 593–597.

[11] H. Saadat, *Power System Analysis*. McGraw-Hill, 2005.

[12] W. Zangwill and C. Garcia, *Pathways to Solutions, Fixed Points, and Equilibria*. Prentice-Hall, 1981.

[13] J. Jarjis and F. D. Galiana, "Analysis and Characterization of Security Regions in Power Systems, Part I: Load Flow Feasibility Conditions in Power Systems," McGill University, Final Report, U.S. Department of Energy, Division of Electric Energy Systems, DOE/ET/29108–T1-Pt.1, March 1980.

[14] M. H. Banakar and F. D. Galiana, "Analysis and Characterization of Security Regions in Power Systems, Part II: Security Regions in Power Networks," McGill University, Final Report, U.S. Department of Energy, Division of Electric Energy Systems, DOE/ET/29108–T1-Pt.2, March 1980.

[15] M. Ilic, "Network Theoretic Conditions for Existence and Uniqueness of Steady State Solutions to Electric Power Circuits," in *Proceedings of 1992 IEEE International Symposium on Circuits and Systems (ISCAS)*, May 6, 1992, pp. 2821–2828.

[16] M. Ebrahimpour and J. Dorsey, "A Test for the Existence of Solutions in Ill-Conditioned Power Systems," in *IEEE Proceedings of Southeastcon '91.*, vol. 1, April 1991, pp. 444–448.

[17] S. Grijalva, "Individual Branch and Path Necessary Conditions for Saddle-Node Bifurcation Voltage Collapse," *IEEE Transactions on Power Systems*, vol. 27, no. 1, pp. 12–19, February 2012.

[18] I. Hiskens and R. Davy, "Exploring the Power Flow Solution Space Boundary," *IEEE Transactions on Power Systems*, vol. 16, no. 3, pp. 389–395, August 2001.

[19] S. Iwamoto and Y. Tamura, "A Load Flow Calculation Method for Ill-Conditioned Power Systems," *IEEE Transactions on Power Apparatus and Systems*, vol. PAS-100, no. 4, pp. 1736–1743, April 1981.

[20] T. Overbye, "A Power Flow Measure for Unsolvable Cases," *IEEE Transactions on Power Systems*, vol. 9, no. 3, pp. 1359–1365, August 1994.

[21] ——, "Computation of a Practical Method to Restore Power Flow Solvability," *IEEE Transactions on Power Systems*, vol. 10, no. 1, pp. 280–287, February 1995.

[22] I. Dobson and L. Lu, "New Methods for Computing a Closest Saddle Node Bifurcation and Worst Case Load Power Margin for Voltage Collapse," *IEEE Transactions on Power Systems*, vol. 8, no. 3, pp. 905–913, August 1993.

[23] F. Alvarado, I. Dobson, and Y. Hu, "Computation of Closest Bifurcations in Power Systems," *IEEE Transactions on Power Systems*, vol. 9, no. 2, pp. 918–928, May 1994.

[24] F. Echavarren, E. Lobato, and L. Rouco, "A Power Flow Solvability Identification and Calculation Algorithm," *Electric Power Systems Research*, vol. 76, no. 4, pp. 242–250, 2006.

[25] S. Granville, J. Mello, and A. Melo, "Application of Interior Point Methods to Power Flow Unsolvability," *IEEE Transactions on Power Systems*, vol. 11, no. 2, pp. 1096–1103, May 1996.

[26] V. Donde, V. Lopez, B. Lesieutre, A. Pinar, C. Yang, and J. Meza, "Severe Multiple Contingency Screening in Electric Power Systems," *IEEE Transactions on Power Systems*, vol. 23, no. 2, pp. 406–417, May 2008.

[27] Z. Feng, V. Ajjarapu, and D. Maratukulam, "A Practical Minimum Load Shedding Strategy to Mitigate Voltage Collapse," *IEEE Transactions on Power Systems*, vol. 13, no. 4, pp. 1285–1290, November 1998.

[28] J. Zhao, Y. Wang, and P. Ju, "Evaluation of Methods for Measuring the Insolvability of Power Flow," in *Third International Conference on Electric Utility Deregulation and Restructuring and Power Technologies, 2008 (DRPT 2008)*, April 2008, pp. 920–925.

[29] X. Yue and V. Venkatasubramanian, "Complementary Limit Induced Bifurcation Theorem and Analysis of Q Limits in Power-Flow Studies," in *Bulk Power System Dynamics and Control - VII. Revitalizing Operational Reliability, 2007 iREP Symposium*, August 2007, pp. 1–8.

[30] I. Dobson and L. Lu, "Voltage Collapse Precipitated by the Immediate Change in Stability When Generator Reactive Power Limits are Encountered," *IEEE Transactions on Circuits and Systems I: Fundamental Theory and Applications*, vol. 39, no. 9, pp. 762–766, September 1992.

[31] S.-H. Li and H.-D. Chiang, "Impact of Generator Reactive Reserve on Structure-Induced Bifurcation," in *IEEE Power Energy Society General Meeting, 2009. PES '09.*, July 2009, pp. 1–5.

[32] Reactive Reserve Working Group under the auspices of Technical Studies Subcommittee of the Western Electricity Coordinating Council, "Guide to WECC/NERC Planning Standards I.D: Voltage Support and Reactive Power," March 30, 2006.

[33] C. Taylor, *Power System Voltage Stability*. Electric Power Research Institute Series, McGraw-Hill, 1994.

[34] T. Van Cutsem and C. Vournas, *Voltage Stability of Electric Power Systems*. Springer-Verlag, New York, 2008.

[35] J. Baillieul and C. Byrnes, "Geometric Critical Point Analysis of Lossless Power System Models," *IEEE Transactions on Circuits and Systems*, vol. 29, no. 11, pp. 724–737, November 1982.

[36] T. Overbye and C. DeMarco, "Improved Techniques for Power System Voltage Stability Assessment Using Energy Methods," *IEEE Transactions on Power Systems*, vol. 6, no. 4, pp. 1446–1452, November 1991.

[37] Y. Tamura, H. Mori, and S. Iwamoto, "Relationship Between Voltage Instability and Multiple Load Flow Solutions in Electric Power Systems," *IEEE Transactions on Power Apparatus and Systems*, vol. PAS-102, no. 5, pp. 1115 –1125, May 1983.

[38] M. Ribbens-Pavella and F. Evans, "Direct Methods for Studying Dynamics of Large-Scale Electric Power Systems-A Survey," *Automatica*, vol. 21, no. 1, pp. 1 – 21, 1985.

[39] H.-D. Chiang, F. Wu, and P. Varaiya, "Foundations of Direct Methods for Power System Transient Stability Analysis," *IEEE Transactions on Circuits and Systems*, vol. 34, no. 2, pp. 160–173, February 1987.

[40] V. Venikov, V. Stroev, V. Idelchick, and V. Tarasov, "Estimation of Electrical Power System Steady-State Stability in Load Flow Calculations," *IEEE Transactions on Power Apparatus and Systems*, vol. 94, no. 3, pp. 1034–1041, May 1975.

[41] J. Thorp and S. Naqavi, "Load Flow Fractals," in *Proceedings of the 28th IEEE Conference on Decision and Control, 1989.*, vol. 2, December 1989, pp. 1822–1827.

[42] F. Salam, L. Ni, S. Guo, and X. Sun, "Parallel Processing for the Load Flow of Power Systems: The Approach and Applications," in *Proceedings of the 28th IEEE Conference on Decision and Control, 1989*, vol. 3, December 1989, pp. 2173–2178.

[43] S. Chow, J. Mallet-Paret, and J. Yorke, "Finding Zeros of Maps: Homotopy Methods that are Constructive With Probability One," *Math. Comp*, vol. 32, no. 143, pp. 887–899, 1978.

[44] W. Ma and S. Thorp, "An Efficient Algorithm to Locate All the Load Flow Solutions," *IEEE Transactions on Power Systems*, vol. 8, no. 3, p. 1077, 1993.

[45] W. Ma, "Dynamical Systems Analysis in Electric Power Systems," *Ph.D. Dissertation, Cornell University*, 1991.

[46] C.-W. Liu, C.-S. Chang, J.-A. Jiang, and G.-H. Yeh, "Toward a CPFLOW-based Algorithm to Compute All the Type-1 Load-Flow Solutions in Electric Power Systems," *IEEE Transactions on Circuits and Systems I: Regular Papers*, vol. 52, no. 3, pp. 625–630, March 2005.

[47] H.-D. Chiang, I. Dobson, R. Thomas, J. Thorp, and L. Fekih-Ahmed, "On Voltage Collapse in Electric Power Systems," *IEEE Transactions on Power Systems*, vol. 5, no. 2, pp. 601–611, May 1990.

[48] H. Chen, "Cascaded Stalling of Induction Motors in Fault-Induced Delayed Voltage Recovery (FIDVR)," *Masters Thesis, University of Wisconsin-Madison, Department of Electrical and Computer Engineering*, 2011. [Online]. Available: http://minds.wisconsin.edu/handle/1793/53749

[49] B. Lesieutre and I. Hiskens, "Convexity of the Set of Feasible Injections and Revenue Adequacy in FTR Markets," *IEEE Transactions on Power Systems*, vol. 20, no. 4, pp. 1790–1798, November 2005.

[50] J. Carpentier, "Contribution to the Economic Dispatch Problem," *Bull. Soc. Franc. Elect*, vol. 8, no. 3, pp. 431–447, 1962.

[51] M. Huneault and F. Galiana, "A Survey of the Optimal Power Flow Literature," *IEEE Transactions on Power Systems*, vol. 6, no. 2, pp. 762–770, May 1991.

[52] J. Momoh, R. Adapa, and M. El-Hawary, "A Review of Selected Optimal Power Flow Literature to 1993. I. Nonlinear and Quadratic Programming Approaches," *IEEE Transactions on Power Systems*, vol. 14, no. 1, pp. 96–104, February 1999.

[53] J. Momoh, M. El-Hawary, and R. Adapa, "A Review of Selected Optimal Power Flow Literature to 1993. II. Newton, Linear Programming and Interior Point Methods," *IEEE Transactions on Power Systems*, vol. 14, no. 1, pp. 105–111, February 1999.

[54] Z. Qiu, G. Deconinck, and R. Belmans, "A Literature Survey of Optimal Power Flow Problems in the Electricity Market Context," in *Power Systems Conference and Exposition, 2009. PSCE '09. IEEE/PES*, March 2009, pp. 1–6.

[55] R. Zimmerman, C. Murillo-Sánchez, and R. Thomas, "MATPOWER: Steady-State Operations, Planning, and Analysis Tools for Power Systems Research and Education," *IEEE Transactions on Power Systems*, vol. 26, no. 1, pp. 12–19, 2011.

[56] A. Nemirovski, "Lectures on Modern Convex Optimization," 2012. [Online]. Available: http://www2.isye.gatech.edu/~nemirovs/Lect_ModConvOpt.pdf

[57] L. Vandenberghe and S. Boyd, "Semidefinite Programming," *SIAM Review*, pp. 49–95, March 1996. [Online]. Available: http://stanford.edu/~boyd/papers/pdf/semidef_prog.pdf

[58] S. Boyd and L. Vandenberghe, *Convex Optimization*. Cambridge Univ Pr, 2004. [Online]. Available: http://www.stanford.edu/~boyd/cvxbook/bv_cvxbook.pdf

[59] J. Sturm, "Using SeDuMi 1.02, A MATLAB Toolbox for Optimization Over Symmetric Cones," *Optimization Methods and Software*, vol. 11, no. 1, pp. 625–653, 1999.

[60] B. Borchers and J. Young, "Implementation of a Primal–Dual Method for SDP on a Shared Memory Parallel Architecture," *Computational Optimization and Applications*, vol. 37, no. 3, pp. 355–369, 2007.

[61] M. Yamashita, K. Fujisawa, M. Fukuda, K. Kobayashi, K. Nakata, and M. Nakata, "Latest Developments in the SDPA Family for Solving Large-Scale SDPs," *Handbook on Semidefinite, Conic and Polynomial Optimization*, pp. 687–713, 2012.

[62] R. Tütüncü, K. Toh, and M. Todd, "Solving Semidefinite-Quadratic-Linear Programs using SDPT3," *Mathematical Programming*, vol. 95, no. 2, pp. 189–217, 2003.

[63] N. V. Sahinidis and M. Tawarmalani, *BARON 9.0.4: Global Optimization of Mixed-Integer Nonlinear Programs,* User's Manual, 2010.

[64] J. Lofberg, "YALMIP: A Toolbox for Modeling and Optimization in MATLAB," in *IEEE International Symposium on Computer Aided Control Systems Design*, 2004, pp. 284–289.

[65] C. Rowe and J. Maciejowski, "An Efficient Algorithm for Mixed Integer Semidefinite Optimisation," in *Proceedings of the American Control Conference, 2003*, vol. 6, June 2003, pp. 4730–4735.

[66] F. W. Kong, D. Kuhn, and B. Rustem, "A Cutting-Plane Method for Mixed-Logical Semidefinite Programs with an Application to Multi-Vehicle Robust Path Planning," in *49th IEEE Conference on Decision and Control (CDC), 2010*, December 2010, pp. 1360–1365.

[67] P. Parrilo, "Sum of Squares Programs and Polynomial Inequalities," in *SIAG/OPT Views-and-News: A Forum for the SIAM Activity Group on Optimization*, vol. 15, no. 2, 2004, pp. 7–15.

[68] Power Systems Test Case Archive. University of Washington Department of Electrical Engineering. [Online]. Available: http://www.ee.washington.edu/research/pstca/

[69] B. Zhang and D. Tse, "Geometry of Feasible Injection Region of Power Networks," in *49th Annual Allerton Conference on Communication, Control, and Computing, 2011*, September 28-30 2011.

[70] S. Bose, D. Gayme, S. Low, and K. Chandy, "Optimal Power Flow Over Tree Networks," in *49th Annual Allerton Conference on Communication, Control, and Computing, 2011*, September 28-30 2011.

[71] S. Sojoudi and J. Lavaei, "Physics of Power Networks Makes Hard Optimization Problems Easy To Solve," in *2012 IEEE Power & Energy Society General Meeting*, July 22-27 2012.

[72] J. Lavaei, D. Tse, and B. Zhang, "Geometry of Power Flows in Tree Networks," in *2012 IEEE Power & Energy Society General Meeting*, July 22-27 2012.

[73] M. Farivar and S. Low, "Branch Flow Model: Relaxations and Convexification–Part I," *IEEE Transactions on Power Systems*, vol. PP, no. 99, pp. 1–11, 2013.

[74] ——, "Branch Flow Model: Relaxations and Convexification–Part II," *IEEE Transactions on Power Systems*, vol. PP, no. 99, pp. 1–8, 2013.

[75] A. Lam, B. Zhang, A. Dominguez-Garcia, and D. Tse, "Optimal distributed voltage regulation in power distribution networks," *arXiv preprint arXiv:1204.5226*, 2012.

[76] W. A. Bukhsh, A. Grothey, K. I. McKinnon, and P. A. Trodden, "Local Solutions of Optimal Power Flow," University of Edinburgh School of Mathematics, Tech. Rep. ERGO 11-017, 2011, [Online]. Available: http://www.maths.ed.ac.uk/ERGO/pubs/ERGO-11-017.html.

[77] W. A. Bukhsh, A. Grothey, K. McKinnon, and P. Trodden, "Local Solutions of Optimal Power Flow Problem," To appear in *IEEE Transactions on Power Systems*, 2013.

[78] M. Fukuda, M. Kojima, K. Murota, K. Nakata *et al.*, "Exploiting Sparsity in Semidefinite Programming via Matrix Completion I: General Framework," *SIAM Journal on Optimization*, vol. 11, no. 3, pp. 647–674, 2001.

[79] K. Nakata, K. Fujisawa, M. Fukuda, M. Kojima, and K. Murota, "Exploiting Sparsity in Semidefinite Programming via Matrix Completion II: Implementation and Numerical Results," *Mathematical Programming*, vol. 95, no. 2, pp. 303–327, 2003.

[80] S. Kim, M. Kojima, M. Mevissen, and M. Yamashita, "Exploiting Sparsity in Linear and Nonlinear Matrix Inequalities via Positive Semidefinite Matrix Completion," *Mathematical Programming*, vol. 129, no. 1, pp. 33–68, 2011.

[81] X. Bai and H. Wei, "A semidefinite programming method with graph partitioning technique for optimal power flow problems," *International Journal of Electrical Power & Energy Systems*, vol. 33, no. 7, pp. 1309–1314, 2011.

[82] R. Jabr, "Exploiting Sparsity in SDP Relaxations of the OPF Problem," *IEEE Transactions on Power Systems*, vol. 27, no. 2, pp. 1138–1139, May 2012.

[83] B. C. Lesieutre, D. K. Molzahn, A. R. Borden, and C. L. DeMarco, "Examining the Limits of the Application of Semidefinite Programming to Power Flow Problems," in *49th Annual Allerton Conference on Communication, Control, and Computing, 2011*, September 28-30 2011.

[84] MidwestISO, "LMP Contour Map from 2:40 PM, June 22, 2011," [Online]. Available: http://www.midwestmarket.org/page/LMP+Contour+Map+%28EOR%29.

[85] J. Sun and L. Tesfatsion, "DC Optimal Power Flow Formulation and Solution using QuadProgJ," Iowa State University, ISU Economics Working Paper No. 06014, March 2010. [Online]. Available: http://www2.econ.iastate.edu/tesfatsi/dc-opf.jslt.pdf

[86] D. Kosterev, A. Meklin, J. Undrill, B. Lesieutre, W. Price, D. Chassin, R. Bravo, and S. Yang, "Load Modeling in Power System Studies: WECC Progress Update," in *Power and Energy Society General Meeting - Conversion and Delivery of Electrical Energy in the 21st Century, 2008 IEEE*, July 2008, pp. 1–8.

[87] F. Chassin, E. Mayhorn, M. Elizondo, and S. Lu, "Load Modeling and Calibration Techniques for Power System Studies," in *North American Power Symposium (NAPS), 2011*, August 2011, pp. 1–7.

[88] P. Kundur, N. Balu, and M. Lauby, *Power System Stability and Control*. McGraw-Hill Professional, 1994.

[89] Siemens PTI, "Volume II: Program Application Guide," *Power System Simulation for Engineering (PSS/E)*, vol. 31.0, December 2007.

[90] GE Energy, "User's Manual," *Positive Sequence Load Flow (PSLF)*, vol. 17.0_07, November 19, 2010.

[91] PowerWorld Corporation, "Help File," *PowerWorld Simulator 15*, June 11, 2011.

[92] A. Lam, B. Zhang, and D. Tse, "Distributed Algorithms for Optimal Power Flow Problem," *arXiv preprint arXiv:1109.5229*, 2011.

[93] H. Wolkowicz, R. Saigal, and L. Vandenberghe, *Handbook of Semidefinite Programming: Theory, Algorithms, and Applications*, ser. International Series in Operations Research & Management Science. Kluwer Academic Publishers, 2000.

[94] D. K. Molzahn, J. T. Holzer, B. C. Lesieutre, and C. L. DeMarco, "Implementation of a Large-Scale Optimal Power Flow Solver Based on Semidefinite Programming," To appear in *IEEE Transactions on Power Systems*.

[95] D. K. Molzahn, B. C. Lesieutre, and C. L. DeMarco, "Approximate Representation of ZIP Loads in a Semidefinite Relaxation of the OPF Problem," Submitted to *IEEE Transactions on Power Systems (Letters)*.

[96] ——, "A Sufficient Condition for Global Optimality of Solutions to the Optimal Power Flow Problem," To appear in *IEEE Transactions on Power Systems (Letters)*.

[97] R. Tarjan and M. Yannakakis, "Simple Linear-Time Algorithms to Test Chordality of Graphs, Test Acyclicity of Hypergraphs, and Selectively Reduce Acyclic Hypergraphs," *SIAM Journal on Computing*, vol. 13, p. 566, 1984.

[98] G. Valiente, *Algorithms on Trees and Graphs*. Springer Verlag, 2002.

[99] J. Gross and J. Yellen, *Graph Theory and its Applications*. CRC press, 2006.

[100] P. Amestoy, T. Davis, and I. Duff, "Algorithm 837: AMD, An Approximate Minimum Degree Ordering Algorithm," *ACM Transactions on Mathematical Software (TOMS)*, vol. 30, no. 3, pp. 381–388, 2004.

[101] D. K. Molzahn, B. C. Lesieutre, and C. L. DeMarco, "A Sufficient Condition for Power Flow Insolvability with Applications to Voltage Stability Margins," *IEEE Transactions on Power Systems*, vol. 28, no. 3, pp. 2592–2601, 2013.

[102] ——, "A Sufficient Condition for Power Flow Insolvability with Applications to Voltage Stability Margins," University of Wisconsin-Madison Department of Electrical and Computer Engineering, Tech. Rep. ECE-12-01, 2012, [Online]. Available: http://arxiv.org/abs/1204.6285.

[103] M. Hirsch and S. Smale, *Differential Equations, Dynamical Systems, and Linear Algebra*. Academic Press New York, 1974.

[104] R. Horn and C. Johnson, *Matrix Analysis*. Cambridge University Press, 1985.

[105] V. Ajjarapu and C. Christy, "The Continuation Power Flow: A Tool for Steady State Voltage Stability Analysis," *IEEE Transactions on Power Systems*, vol. 7, no. 1, pp. 416–423, February 1992.

[106] D. K. Molzahn, V. Dawar, B. C. Lesieutre, and C. L. DeMarco, "Sufficient Conditions for Power Flow Insolvability Considering Reactive Power Limited Generators with Applications to Voltage Stability Margins," in *Bulk Power System Dynamics and Control - IX. Optimization, Security and Control of the Emerging Power Grid, 2013 IREP Symposium*, August 25-30 2013.

[107] F. Rendl, "Semidefinite Relaxations for Integer Programming," *50 Years of Integer Programming 1958-2008*, pp. 687–726, 2010.

[108] D. Grigoriev and N. Vorobjov, "Complexity of Null- and Positivstellensatz Proofs," *Annals of Pure and Applied Logic*, vol. 113, no. 1, pp. 153–160, 2001.

[109] J. Löfberg, "Pre- and Post-Processing Sum-of-Squares Programs in Practice," *IEEE Transactions on Automatic Control*, vol. 54, no. 5, pp. 1007–1011, 2009.

[110] A. Klos and A. Kerner, "The Non-Uniqueness of Load Flow Solution," *Proc. PSCC-5*, p. 3.1/8, Cambridge, 1975.

[111] D. K. Molzahn, B. C. Lesieutre, and H. Chen, "Counterexample to a Continuation-Based Algorithm for Finding All Power Flow Solutions," *IEEE Transactions on Power Systems*, vol. 28, no. 1, pp. 564–565, 2013.

[112] R. Seydel, *Practical Bifurcation and Stability Analysis: From Equilibrium to Chaos*. Springer, 1994.

[113] D. K. Molzahn, B. C. Lesieutre, and C. L. DeMarco, "Investigation of Non-Zero Duality Gap Solutions to a Semidefinite Relaxation of the Power Flow Equations," Submitted to *47th Hawaii International Conference on System Sciences (HICSS), 2014*, 6-9 January 2014.

[114] S. Bruno, S. Lamonaca, G. Rotondo, U. Stecchi, and M. La Scala, "Unbalanced Three-Phase Optimal Power Flow for Smart Grids," *IEEE Transactions on Industrial Electronics*, vol. 58, no. 10, pp. 4504–4513, 2011.

[115] M. Abdel-Akher, K. Nor, and A. H. A. Rashid, "Improved Three-Phase Power-Flow Methods Using Sequence Components," *IEEE Transactions on Power Systems*, vol. 20, no. 3, pp. 1389–1397, 2005.

[116] C. Cheng and D. Shirmohammadi, "A Three-Phase Power Flow Method for Real-Time Distribution System Analysis," *IEEE Transactions on Power Systems*, vol. 10, no. 2, pp. 671–679, 1995.

[117] J.-H. Teng, "A Direct Approach for Distribution System Load Flow Solutions," *IEEE Transactions on Power Delivery*, vol. 18, no. 3, pp. 882–887, 2003.

[118] W. Xu, H. Dommel, and J. Marti, "A Generalised Three-Phase Power Flow Method for the Initialisation of EMTP Simulations," in *1998 International Conference on Power System Technology, 1998. Proceedings. POWERCON '98.*, vol. 2, 1998, pp. 875–879.

[119] Y.-Y. Hong and Y.-T. Chen, "Three-Phase Optimal Harmonic Power Flow," *IEE Proceedings-Generation, Transmission and Distribution*, vol. 143, no. 4, pp. 321–328, 1996.

[120] E. Dall'Anese, G. B. Giannakis, and B. F. Wollenberg, "Economic Dispatch in Unbalanced Distribution Networks via Semidefinite Relaxation," *arXiv preprint arXiv:1207.0048*, 2012.

[121] E. Dall'Anese, H. Zhu, and G. B. Giannakis, "Distributed Optimal Power Flow for Smart Microgrids," *arXiv preprint arXiv:1211.5856*, 2012.

[122] X.-P. Zhang, P. Ju, and E. Handschin, "Continuation Three-Phase Power Flow: A Tool for Voltage Stability Analysis of Unbalanced Three-Phase Power Systems," *IEEE Transactions on Power Systems*, vol. 20, no. 3, pp. 1320–1329, 2005.

[123] N. Laothumyingyong and P. Damrongkulkamjorn, "Security-Constrained Unit Commitment using Mixed-Integer Programming with Benders Decomposition," in *International Conference on Electrical Engineering/Electronics Computer Telecommunications and Information Technology (ECTI-CON), 2010*, May 2010, pp. 626–630.

[124] E. Fisher, R. O'Neill, and M. Ferris, "Optimal Transmission Switching," *IEEE Transactions on Power Systems*, vol. 23, no. 3, pp. 1346–1355, August 2008.

[125] J. Taylor and F. Hover, "Conic Relaxations for Transmission System Planning," in *North American Power Symposium (NAPS), 2011*, August 2011, pp. 1–4.

D.K. Molzahn Dissertation Errata

This list describes the changes and corrections made to the dissertation [A] after its initial publication.

1. **Error in the objective function of the dual form of the semidefinite relaxation of the OPF.**

   Corrected October 7, 2013

   There was an error in the objective function of the dual form of the semidefinite relaxation of the optimal power flow problem. In equation (2.8), the term $\sum_{k \in \mathcal{G}} \left(c_{k0} - \mathbf{R}_k^{22} \right)$ was incorrectly specified as $\sum_{k \in \mathcal{G}} \left(c_{k0} - \mathbf{R}_k^{12} \right)$. In equation (3.20), the term $\sum_{k \in \mathcal{G}_i^q} \left(\underline{\psi}_g P_{Gg}^{min} - \bar{\psi}_g P_{Gg}^{max} + c_{g0} - \mathbf{R}_g^{22} \right)$ was incorrectly specified as $\sum_{k \in \mathcal{G}_i^q} \left(\underline{\psi}_g P_{Gg}^{min} - \bar{\psi}_g P_{Gg}^{max} + c_{g0} - \mathbf{R}_g^{12} \right)$.

2. **Errors in the Seven-Bus System in Figure 6.4.**

   Corrected October 7, 2013

   There were several errors in the system diagram shown in Figure 6.4. The load demands at buses 3, 4, and 5 of $0.942 + j0.190$, $0.135 + j0.058$, and $0.183 + j0.127$ per unit, respectively, were incorrectly specified as $0.2 + j0.1$, $0.6 + j0.1$, and $0.2 + j0.1$ per unit, respectively. The impedance of the line connecting buses 3 and 4 of $0.024 + j0.100$ per unit was incorrectly specified as $0.04 + j0.12$ per unit. The impedance of the line connecting buses 4 and 5 of $0.024 + j0.100$ per unit was incorrectly specified as $0.04 + j0.12$ per unit.

References

[A] D.K. Molzahn, "Application of Semidefinite Optimization Techniques to Problems in Electric Power Systems," *Ph.D. Dissertation, University of Wisconsin–Madison Department of Electrical and Computer Engineering*, August 2013.